Membrane Permeability of HIV-1 Protease Inhibitors

by

Uraisha Ramlucken

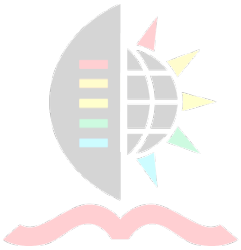

UNIVERSITY OF
KWAZULU-NATAL
INYUVESI
YAKWAZULU-NATALI

Dissertation presented for the degree of

Master of Science (Biochemistry)

at

University of KwaZulu-Natal

School of Life Sciences

College of Agriculture, Engineering and Science

January 2014

Supervisor: Dr. Patrick Govender

Co-Supervisor: Dr. Karen. Pillay

DECLARATIONS

Form EX1-5

COLLEGE OF AGRICULTURE, ENGINEERING AND SCIENCE

DECLARATION 1 - PLAGIARISM

I, Miss Uraisha Ramlucken declare that

1. The research reported in this thesis, except where otherwise indicated, and is my original research.

2. This thesis has not been submitted for any degree or examination at any other university.

3. This thesis does not contain other persons' data, pictures, graphs or other information, unless specifically acknowledged as being sourced from other persons.

4. This thesis does not contain other persons' writing, unless specifically acknowledged as being sourced from other researchers. Where other written sources have been quoted, then:

a. Their words have been re-written but the general information attributed to them has been referenced

b. Where their exact words have been used, then their writing has been placed in italics and inside quotation marks, and referenced.

5. This thesis does not contain text, graphics or tables copied and pasted from the Internet, unless specifically acknowledged, and the source being detailed in the thesis and in the References sections.

Signed

……

COLLEGE OF AGRICULTURE, ENGINEERING AND SCIENCE

DECLARATION 2 - PUBLICATIONS

DETAILS OF CONTRIBUTION TO PUBLICATIONS that form part and/or include research presented in this thesis (include publications in preparation, submitted, *in press* and published and give details of the contributions of each author to the experimental work and writing of each publication)

Not Applicable

Signed:…….. Date:……..

I, Dr Patrick Govender as supervisor of the MSc study hereby consent to the submission of this MSc Thesis.

Signed:…….. Date:……..

SUMMARY

According to the 2012 UNAIDS global report, sub-Saharan Africa hosts 69% of the world's total population living with HIV, South Africa being the most affected with a reported 24% incidence rate. To date, extensive research is being conducted globally, particularly involving anti-HIV treatment that targets the retroviral enzymes: reverse transcriptase, integrase and protease. The discovery of inhibitors to HIV protease which disrupts virion protein assembly has made this enzyme a prime target of anti-retroviral therapies, thus there exists a concerted research initiative to identify compounds with HIV protease inactivation potential. This study employs HIV protease that is isolated and purified from a genetically modified HIV protease overexpressing *Escherichia coli* strain to monitor the inhibitory capacity of new lead compounds. Optimized growth conditions for HIV protease production displayed that the use of chemically defined media resulted in higher yields of the enzyme. Recent research studies have shown that peptide-based cage and glycosylated compounds displayed HIV protease inhibitor activity in cell free enzymatic reactions that are comparable to commercially available HIV protease inhibitors. However, in contrast it has also been reported that these inhibitors are inactive in whole T-cell assays, when employing HIV infected CD4 cells.

It is a well-known fact that potential new chemical entities that do not possess oral bioavailability, in terms of their absorption properties, are not successful candidates within the drug discovery industry. Following this, the current study was designed to determine if inefficient membrane permeability of these promising anti-HIV protease lead compounds could result in their inactivity in whole T-cell assays. Two different methods were considered, a cell-based method using the Madin Darby Canine Kidney strain I (MDCKI) cell line and a non-cell based method, the parallel artificial membrane permeability assay (PAMPA). MDCKI cells have been extensively used to form monolayers that mimic human intestinal membranes whilst the PAMPA utilizes an artificial lipid membrane composition on a filter support. Data from permeability assays using the novel chemically synthesized inhibitors have been compared to commercially available drugs, antipyrine, metoprolol and caffeine, which displayed efficient membrane permeability characteristics, thereby validating the assay. The results indicated that novel cage-derived and glycosylated peptide inhibitors do not possess sufficient passive diffusion properties which may explain their inactivity in whole T-cell assays.

This thesis is dedicated to

My Dad, who always believed in me, there are no words to express how much I miss you.

BIOGRAPHICAL SKETCH

Uraisha Ramlucken was born on the 8th of June 1988 and brought up in the small suburb of Reservoir Hills. She matriculated in 2005 and achieved a distinction with merit and decided to further her studies in Science at the University of KwaZulu-Natal. She obtained her Bachelor of Science degree majoring in Biochemistry and Microbiology and her Bachelor of Science Honors degree in the field of Biochemistry. Uraisha has a very intriguing mind and a curious nature hence her interest in research. Her passion lies in the understanding of microbes and their infectious capacity as well as drugs that are used as therapeutic agents. She is intrigued by incurable diseases and hopes to one day work in the field of medical research.

Uraisha enjoys a myriad of activities. Her free time is spent doing anything from outdoor activities such as swimming and camping, to indoor activities such as reading, playing board games and watching television. She loves to socialize with people and has an enthusiastic interest in playing the piano.

ACKNOWLEDGEMENTS

I wish to express my sincere gratitude and appreciation to the following people and institutions:

- To **Sathya Sai Baba**, for giving me the perseverance but most of all the strength to get through this degree and for enabling a positive attitude in all my endeavors.

- My supervisor **Dr Patrick Govender**, for believing in me and motivating me to be the best that I can be, for his wisdom, understanding, encouragement and guidance throughout my degree and in all aspects of life.

- My co-supervisor and dear friend **Dr Karen Pillay**, for her mentorship and direction in this project, but most of all for always listening and being there for me especially in the trying times.

- My amazing mother, **Anthee Ramlucken**, for the sacrifices, endless support and being a pillar of strength that I needed to help me finish.

- My sister **Roxanne Ramlucken**, for always being willing to accompany me when I had lonely lab time, for always making me food when I was too lazy, and for being there for me in her own way.

- My lab colleagues, **Nick**, **Lethu**, **Sizwe**, **Amanda**, **Me**l, **Njabulo**, **Ramesh** and **Kamini**, for all the fun, laughter, joys, trials and tributes that we go through in this journey to obtain our degrees, most of all the companionship, some of you will forever remain in my heart.

- **Dinesh**, for going out of his way to offer assistance.

- **University of KwaZulu-Natal** for supporting my research study and for providing an environment conducive for me to attain my goals.

- The **National Research Foundation** (NRF) for the financial support.

- My beloved friends, **Meshkaya**, **Trisha**, **Sanesha**, **Dipti**, **Alicia**, **Vijay** and **Mahesh**, for providing a healthy distraction, without which I would have gone insane, and also for helping and supporting me in whatever I needed.

- **Leeven**, for unexpectedly entering my life and filling it with happiness.

- My late **Father**, who always encouraged me to further my education, I will forever be grateful to him and appreciate the time that I had with him. I wish you were here to witness this.

PREFACE

This dissertation is presented as a compilation of five chapters.

Chapter 1 **General Introduction and Project Aims**

Chapter 2 **Literature Review**

Chapter 3 **Research Results I**

Optimization of the Isolation, Purification and Enzyme Activity of HIV-1 Protease Subtype C

Chapter 4 **Research Results II**

Membrane Permeability of Novel Chemically Synthesized HIV-1 protease Inhibitors

Chapter 5 **General Discussion and Conclusion**

CONTENTS

ABBREVIATIONS

ABC	ATP-binding cassette
ADME/Tox	Absorption, distribution, metabolism, excretion or toxicity.
ADP	Adenosine diphosphosphate
ATCC	American type culture collection
ANOVA	One-way analysis of variance
ATP	Adenosine triphosphate
au	Arbitrary units
AZT	Azidothymidine
BBB	Blood brain barrier
BCRP	Breast cancer-resistance protein
BCS	Biopharmaceutical classification system
CM	Carrier mediated
cm	Centimeters
DEAE	Diethylaminoethyl
DMEM	Dulbecco's modified eagle medium
DTT	Dithiothreitol
EDTA	Ethylenediaminetetraacetic acid
Fa	Fraction absorbed
FDA	US Food and Drug Administration
FBS	Fetal bovine serum
GI	Gastrointestinal
GIT	Gastrointestinal tract
g	Grams
HBSS	Hanks balanced salt solution
HEPES	4-(2-hydroxyethyl)-1-piperazineethanesulfonic acid
HIV	Human immunodeficiency virus
HIV-PR	HIV protease
HIV-PR CSA	HIV protease subtype C
HTS	High throughput screening
h	Hours
IAM	Immobilized artificial membrane
IC_{50}	Half maximal inhibitory concentration
IN	Integrase

IPTG	Isopropyl β-D thiogalactoside
kDa	Kilodaltons
L	Litres
λ	Lambda
LB	Luria Broth
LogP	Octanol-water partition coefficient
$LogP_e$	Effective permeability
LY	Lucifer yellow
M	Molar
MDCK	Madin Darby canine kidney
MDCK1	Madin Darby canine kidney strain 1
MDR	Multi-drug resistance
mg	Milligrams
mL	Milliliters
mM	Millmolar
mΩ	Milliohm
Na_3-citrate.$2H_2O$	Tri-sodium citrate
NaCl	Sodium chloride
NCEs	New chemical entities
nm	Nanometers
nM-	Nanomolar
OD_{600}	Optical density at 600 nm
PAMPA	Parallel artificial membrane permeability assay
PBS	Phosphate buffered saline
PC	Phosphatidylcholine
PCU	Pentacycloundecane
P-gp	P-glycoprotein
PMSF	Phenylmethylsulfonylfluoride
PR	Protease
RFU	Relative fluorescence units
Rmp	Revolutions per minute
RT	Reverse transcriptase
SDS-PAGE	Sodium dodecyl sulfate polyacrylamide gel electrophoresis
TCA	Tricarboxylic acid
TEER	Transepithelial electrical resistance

TGX	Tris-glycine-extended
TJ	Tight junctions
µL	Micro litres
µg	Micro grams
UV	Ultraviolet
UWL	Unstirred water layer
V	Volts
V_A	Volume of acceptor compartment
V_D	Volume of donor compartment
WDI	World drug index
vol/vol	Volume/volume
wt/vol	Weight/ volume
Ω	Ohms
XTT	2,3-Bis-(2-Methoxy-4-Nitro-5-Sulfophenyl)-2*H*-Tetrazolium-5-Carboxanilide

LIST OF FIGURES

Figure 3.2 TGX-gel with purified protease product. Lanes 2 and 3 contains supernatant of different centrifugation steps during extraction; Lanes 4 to 8 contains filtrate from the concentration step of purification. Lanes 9 and 10 contain HIV-PR CSA grown in LB and chemically defined media respectively. Lane 11 contains molecular weight marker (PageRuler^{TM} Unstained Protein Ladder). Lanes 1 to 6 were required to establish if the protease was present at different steps of the protease extraction and purification technique.

Figure 3.3 Absorbance of each 5 ml column fraction at 280 nm

Figure 3.4 Purified protease using UV spectrophotometric analysis for monitoring fractions eluted by the column. Lane 1 contains the molecular weight marker (PageRuler^{TM} Unstained Protein Ladder). Lane 2 contains "peak" of the fraction curve. Lane 3 contains the "tail" of the peak. Lanes 4-7 contains filtrates of tails and peaks. Lanes 8 and 9 contains the supernatant of the centrifugation steps during the extraction of the protease.

Figure 3.5 Pure HIV-1 protease subtype C derived from different methods. Lane 1 contains the protein molecular weight marker (PageRuler^{TM} Unstained Protein Ladder). Lanes 2 and 3 contain the "peak" and "tail" fraction respectively of the curve after spectrophotometric analysis. Lane 4 contains the pure HIV-PR CSA obtained when the Bradford assay was used for analysis.

Figure 3.6 Absorption spectrum of HIV-1 South African subtype C protease. The experiment was carried out at 20 °C in 10 mM sodium acetate buffer, 0.1 M sodium chloride, pH 5.0. The spectrum illustrates the absorption of ultra-violet light by the aromatic amino acids' side chains of the protein at 280 nm wavelength

Figure 3.7 Enzyme specificity and catalytic activity using a standard reaction with a chromogenic peptide as the enzyme's substrate. The experiment was performed over 3 minutes and was done in triplicate. As time increased, the absorbance of the substrate decreased which indicates substrate hydrolysis.

Figure 4.1 The ratio obtained from the MycoAlert^{TM} assay after each subculture of MDCK1 cells in DMEM containing MycoZAP^{TM} plus-CL antibiotic. Assay buffer was used for the negative control and the MycoAlert^{TM} positive control was employed to validate the test. A ratio over three was obtained for all positive controls used for each test at each subculture, the use of three as minimum was depicted so a clear indication of a negative result for mycoplasma is noticed.

Figure 4.2 TEER values of low cell numbers 2 x 10^4, 4 x 10^4, 3 x 10^5, 4 x 10^5 and 5 x 10^5 cells/cm^2 was used in order to determine the optimal cell seeding density. TEER was observed over 21 days. Results are depicted as an average of three independent determinations and six resistance values were taken into account for each well. Each experiment was done with two cell-free wells that served as the control well (blank).

Figure 4.3 TEER values of high cell numbers 6 x 10^5, 1 x 10^6, 6 x 10^6 and 1 x 10^7 cells/cm^2 was used in order to determine the optimal cell seeding density. TEER was observed over 21 days. Results are depicted as an average of three independent determinations and six resistance values were taken into account for each well. Each experiment was done with two cell-free wells that served as the control well (blank).

Figure 4.4 Partial monolayer formations of MDCK1 cells after 21 days when using various cell densities. Wells 1- 3 contained 1 x 10^7 cells/cm^2, wells 4- 6 contained 6 x 10^6 cells/cm^2, wells 7- 10 contained 1 x 10^6 cells/cm^2. Wells 11 and 12 served as blanks as they did not contain cells.

Figure 4.5 Standard curves depicting concentration of the control drugs and absorbance at λ_{max}. The maximum wavelength of antipyrine, metoprolol and caffeine were 260, 230 and 270 nm respectively. Results are an average of three independent experiments and R^2 values only above 0.95 were taken into consideration.

Figure 4.6 Standard curve showing the relationship between Lucifer yellow concentration and fluorescence detected. Results displayed are an average of three independent experiments and R^2 values only over 0.95 were considered.

Figure 4.7 Standard curves showing the relationship between various concentrations of HIV protease inhibitors and UV absorbance. Results are an average of three independent experiments and R^2 values only over 0.95 were considered.

Figure 4.8 The effective permeability ($LogP_e$) of control drugs and inhibitors at different pH levels and at a concentration of 100 μM Results show an average of three independent experiments and the error bars represent standard deviations.

LIST OF TABLES

Chapter 1

INTRODUCTION AND PROJECT AIMS

1.1 Introduction

The field of drug discovery is one of the most interesting and complex fields of research. It employs a multidisciplinary scientific approach that encompasses medicine, chemistry, biotechnology and pharmacology. Developing new drugs utilises enormous resources in intellect, determination and patience for it is indeed a tedious process. Two major factors need to be considered when designing a new drug, firstly the effect it has on the established target -, in a process referred to as target validation, and more importantly will it be able to elicit that effect against the complexities the are encountered in the human system. "Lead compounds" are referred to as chemical entities that have the potential to become a drug candidate because it is able to exhibit pharmacological or biological activity against a set target. In essence, their chemical structure is used as a starting point for the development of a drug [1].

Human immunodeficiency virus, more commonly known as HIV, the causative agent of acquired immune deficiency syndrome (AIDS), gave rise to a multi-billion dollar drug research industry due to the disease being a major cause of death worldwide. According to the 2012 UNAIDS global report, sub-Saharan Africa is home to 69% of the world's total population living with HIV, of that South Africa being the most affected by the epidemic with a reported 24% incidence rate [2]. Due to the high genetic diversity of HIV, there are many subtypes of virus each having a unique genetic make-up, and more significantly, differ in drug resistance, catalytic activity and binding capacity to the active site [3, 4]. This study will thus focus on HIV-1 subtype C, which is the most prevalent in South Africa.

Currently, almost every aspect of HIV and its infection is being investigated, and a growing area of interest is in the aspartyl enzyme HIV protease. This protease is responsible for cleavage of the *gag* and *pol* poly-proteins, both of which are essential for the virion's assembly and function [5]. The inhibition/inactivation of this enzyme has thus piqued the attention of research institutes globally [6]. There are a multitude of chemically synthesised HIV protease inhibitors being produced worldwide as potential therapeutic agents in the treatment of AIDS, with each having their individual mechanism of action [7].

In keeping with the development process, a lead candidate must be able to be effective against the targeted component, in this case HIV protease. Much emphasis is placed on the synthesis, characterization and potency of the chemical inhibitors. However it should be noted that far less resources have been dedicated to the biotechnological production of specific HIV protease subtype enzymes. The exploration of this potential approach to anti-retroviral therapy necessitates the availability of enzyme in amounts sufficient to establish screening assays for inhibitors and additionally for studies involving the characterization of this enzyme. Thereby the role in the production of these enzymes is vital to the success of inhibitors. In view of the health hazards associated with handling live virus, isolation of adequate amounts of enzyme from native sources is problematic, and alternative approaches must be considered. A safer approach is to utilize genetically transformed bacteria as vehicles to express the enzyme, so it can be isolated and purified [8]. This strategy allows for the generation of sufficient yields of the protease in a safe and controlled environment. Furthermore and importantly this approach ensures reproducibility in that researchers can assess possible inhibitors against easily accessible common targets.

When developing a therapeutic candidate, numerous other biological parameters must be considered. It is said that for every 5000-10000 entities that flood the drug development industry, only approximately 250 make it into the clinical trial phase of testing, and of that only one candidate might actually enter the market [9]. The time period for a therapeutic agent to reach commercial status, i.e. from the time it is discovered to when it is available to treat patients, is approximately 10-15 years [10, 11]. A key reason for this poor success rate and long discovery time is the poor bioavailability potential of compounds. Bioavailability deals with the absorption and metabolism of a compound when it enters the human body. The most popular method of therapeutic agents entering the human system is via the oral route, although this comes with a host of problems that need to be addressed [12]. If the set compound can be efficiently absorbed and pass metabolism via the liver, it can be deemed as a promising lead candidate. Generally if an entity is efficiently absorbed into the human system, half the battle is won [13]. Currently one of the most popular *in vitro* techniques for screening of absorption is the cell-based transmembrane model utilizing the MDCK cell line [14]. However this biological system does have its drawbacks (reproducibility, precautions affiliated with cell culture, time-consuming) [15, 16]. As such a high-throughput, synthetic system referred to as the parallel artificial membrane assay (PAMPA) has been developed, which is rapidly becoming invaluable to drug screening studies. The combined use of these two methods makes for an efficient means of evaluating the absorption potential of a compound [17].

1.2 Aims of this study

The first part of this study involves optimization of a method to produce pure and active HIV protease subtype C, so that it can be readily utilized for the testing of the inhibitory potential of novel chemically synthesised compounds.

The second part of this study involves exploration of the absorption characteristics of novel HIV-1 protease inhibitors which have excelled in their functions independently, in that they were successful in inhibiting HIV-1 protease subtype C. However, when exposed to *in vitro* whole-cell testing, using HIV-1 infected MT4 cells, they were ineffective. A potential hypothesis is that the inhibitors' failure in a whole cell system is that the drug is not being absorbed efficiently through the cell membrane. As such, this study aims to predict the permeability capabilities of the chemically synthesised HIV-1 protease inhibitors with the use of cell-based and artificial membrane techniques.

1.3 References

1. Keserű, G.M. and G.M. Makara, Hit discovery and hit-to-lead approaches. *Drug discovery today*, 2006. **11**(15): p. 741-748.
2. UNAIDS. Global report on the AIDS epidemic 2012. Accessed on 11 Novenber 2013. Available from: http://www.unaids.org/en/media/unaids/contentassets/documents/epidemiology/2012/gr2012/20121120_unaids_global_report_2012_with_annexes_en.pdf.
3. Velazquez-Campoy, A., et al., Protease inhibition in African subtypes of HIV-1. *AIDS Rev*, 2003. **5**(3): p. 165-71.
4. Mosebi, S., *Kinetic and thermodynamic characterization of the South African subtype C HIV-1 protease: implications for drug resistance*, 2007, Faculty of Science, University of the Witwatersrand.
5. Brik, A. and C.H. Wong, HIV-1 protease: mechanism and drug discovery. *Organic & biomolecular chemistry*, 2003. **1**(1): p. 5-14.
6. Deeks, S.G., et al., HIV-1 protease inhibitors. *JAMA: the journal of the American Medical Association*, 1997. **277**(2): p. 145-153.
7. Martinez-Cajas, J.L. and M.A. Wainberg, Protease inhibitor resistance in HIV-infected patients: Molecular and clinical perspectives. *Antiviral Research*, 2007. **76**(3): p. 203-221.
8. Ido, E., et al., Kinetic studies of human immunodeficiency virus type 1 protease and its active-site hydrogen bond mutant A28S. *Journal of Biological Chemistry*, 1991. **266**(36): p. 24359-24366.
9. Innovation.org. Drug Discovery and Development understanding the R&D process. Accessed on 6 February 2013. Available from: http://www.innovation.org/drug_discovery/objects/pdf/RD_Brochure.pdf.
10. Lipsky, M.S. and L.K. Sharp, From idea to market: the drug approval process. *The Journal of the American Board of Family Practice*, 2001. **14**(5): p. 362-367.
11. Grass, G.M., Simulation models to predict oral drug absorption from in vitro data. *Advanced Drug Delivery Reviews*, 1997. **23**(1-3): p. 199-219.
12. van de Waterbeemd, H., et al., *Drug Bioavailability: Estimation of Solubility, Permeability, Absorption and Bioavailability*. 2008: John Wiley & Sons.
13. Chaturvedi, P.R., C.J. Decker, and A. Odinecs, Prediction of pharmacokinetic properties using experimental approaches during early drug discovery. *Current Opinion in Chemical Biology*, 2001. **5**(4): p. 452-463.
14. Irvine, J.D., et al., MDCK (Madin-Darby canine kidney) cells: A tool for membrane permeability screening. *Journal of pharmaceutical sciences*, 1999. **88**(1): p. 28-33.
15. Cho, M.J., et al., the Madin Darby canine kidney (mdck) epithelial-cell monolayer as a model cellular-transport barrier. *pharmaceutical research*, 1989. **6**(1): p. 71-77.
16. Braun, A., et al., Cell cultures as tools in biopharmacy. *European Journal of Pharmaceutical Sciences*, 2000. **11**: p. S51-S60.
17. Song, C.M., S.J. Lim, and J.C. Tong, Recent advances in computer-aided drug design. *Briefings in bioinformatics*, 2009. **10**(5): p. 579-591.

CHAPTER 2

LITERATURE REVIEW

2.1 Introduction

Previously, in the field of drug discovery, there was a common misconception that identification of the active molecule for a particular target was the most important factor when designing a new chemical compound. Once identified, this molecule also known as the lead compound would enter a development program that results in a long period of time before it reaches the market [1]. This strategy had a major flaw in its design, solely because these so called "lead compounds" are not compatible in both physicochemical (solubility, dissolution rate, chemical stability) and biological (membrane permeability and enzyme stability) properties that contributes to its potential as a therapeutic agent thereby resulting in wastage of valid time and resources to increase its bioavailability [2]. Therefore equal importance must be placed to both target validation and bioavailability requirements in order to achieve a positive outcome for a therapeutic agent.

Bioavailability is defined as the fraction of an administered dose of a drug that reaches the systemic circulation. Therefore, by definition, if a drug is administered intravenously its bioavailability is 100%, but unfortunately the most convenient and thus favoured route for drug administration is via the oral route. However, although this is the preferred route, more work needs to be performed to design drugs that are suitable for oral administration [1]. Drug discovery is an exceedingly complex and demanding enterprise which relies on diverse disciplines, often with conflicting goals, to integrate their knowledge to achieve a balanced clinical candidate. Bioavailability is the key factor in all drug design procedures, and it is achieved by five main properties which are known as ADME/Tox, namely absorption, distribution, metabolism, excretion and toxicity.

When a drug is released into the system orally it has to overcome numerous barriers in order for it to elicit its pharmaceutical response. The first is absorption of the active compound into the systemic circulation from the gut lumen. This requires crossing the physical and selective barrier of the small and large intestines as well as surviving enterocyte metabolism including first phase metabolism in the liver. If this formidable task is achieved, once in the systemic circulation, the candidate has to be distributed throughout the body to elicit the response to the intended target tissue. In addition, this must be achieved whilst trying to protect itself from the body's defence system since the human body is prone to destroy xenobiotics i.e. drugs that are used for medicinal purposes. This is usually done via metabolism in the liver and intestine, as well as through excretion of the parent compound and their metabolites into bile, the intestinal lumen, and urine (Figure 2.1).

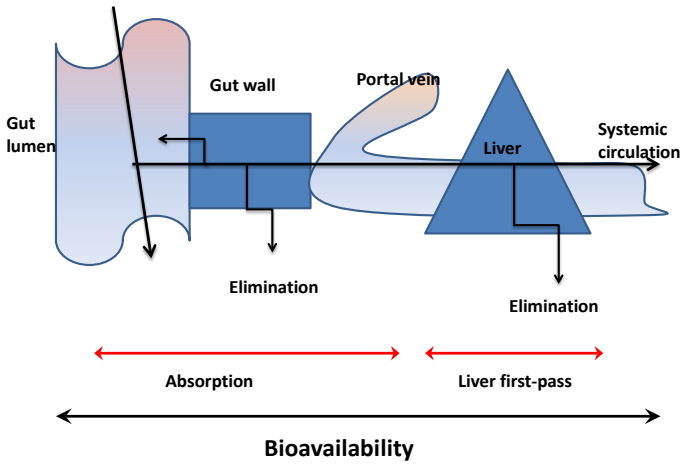

Figure 2 1 Absorption and bioavailability route of orally administered drugs. Adapted from Logan *et al*. [3].

Adsorption is probably the most imperative of the ADME/tox variables and will be covered in this review. If the compound possesses reasonable physicochemical properties, has low to intermediate clearance properties, satisfactory metabolic stability and efficient absorbance; adequate oral bioavailability can be achieved [1]. In order to understand absorption, the compounds permeability capacity is thoroughly investigated due to its critical role in oral absorption. Permeability has significant impact on metabolism and transporter effects, drug disposition and pharmacokinetics–pharmacodynamics relationships. Furthermore it plays a vital role along with solubility in the Biopharmaceutical Classification System (BCS) which is used extensively in the drug development community [4].

There are numerous procedures that attempt to study the permeability characteristics of novel potential candidates, with the market being saturated by *in vitro*, *in vivo, in situ*, *ex vivo* etc. methods. However, whilst there are many arguments for the efficiency of the different methods, *in vitro* methodology for the investigation of drug permeability has recently been proven to be the preferred method [5-7]. It is also important to examine the cost involved in development of a new drug and especially the impact of product failure on the overall development expense. In addition, the time taken for a drug to enter the market should not be too long. Therefore *in vitro* technologies provide a platform for drugs to be screened rapidly whilst keeping costs to a minimum [7]. The utilization of cells has become an innovative and successful means to predict drug permeability. Whist it does have disadvantages, the benefits of cell mediated screening outweigh their drawbacks. One of the main advantages of a cell-based system is that it has the ability to represent the human intestinal barrier more efficiently than any other means of *in vitro* screening. Therefore candidates can be screened and the result will give you the best possible indication of its permeability without the tediousness and difficulties associated with *in vivo* assays.

2.2 The intestinal plasma membrane

The intestinal membrane is said to be the "gatekeeper" of the body. It is a system of continuous renewal and controls the entry of nutrients as well as xenobiotics. The intestinal plasma membrane is composed of a tightly packed array of columnar epithelial cells arranged in single (simple epithelium) or multiple (stratified epithelium) cell layers [8]. These cells are more commonly referred to as enterocytes, are covered with a glycocalyx surface coat which contains digestive enzymes, and consist of an apical and basolateral plasma membrane. Passage through both membranes is necessary if a substance is to enter the blood capillary and subsequent systemic circulation [9].

On the apical side of the membrane there are long protrusions referred to as microvilli or commonly called the "brush border". The intestinal plasma membrane is also accompanied by a clear film of mucus called intestinal mucosa. This layer is constantly exposed to the external environment and plays a fundamental role in the absorption and metabolism of nutrients, drugs and other materials passing through the intestinal lumen. In order to maximize their absorptive and secretory functions, the intestines are structured in such a way that it has maximum surface area [8]. Along the length of the intestinal lumen are folds that are in a wave like structure along the inner surface. Villi add to the surface area by projecting 1 mm into the intestinal lumen (Figure2.2).

The epithelial cells of the gastrointestinal (GI) tract is the interface that separates the outside from the inside world. Therefore it has a major "support system" to aid in its function. The membrane is supported by a complex and well organized connective tissue (Laminar Propria) consisting of fibroblasts, blood vessels, lymph vessels, nerves, and smooth muscle cells [10]. Furthermore, components of the immune system are also found in close contact with the intestinal epithelium. It has been reported that about one third of the lymphocytes present in the human body are found in the intestine [8].

Between the enterocytes are tight junctions (TJ) which can be defined as highly complex protein structures that form size and charge selective barriers [11, 12]. Five distinct protein subunits have been identified, two of which are highly phosphorylated thus suggesting a role of phosphorylation in tight junction regulation. Tight junctions are also intimately associated with actin filaments and the phosphorylation of the actin cytoskeleton is associated with changes in permeability of tight junctions [12]. Therefore the extent of resistance to transport posed by tight junctions is not only defined by the structure of the tight junctions which is a function of the cell type, but is also subject to regulation by physiological stimuli. Tight junctions are the main barrier for substances especially hydrophilic molecules when it comes to paracellular passive diffusion due to the fact that these structures keep the membrane intact.

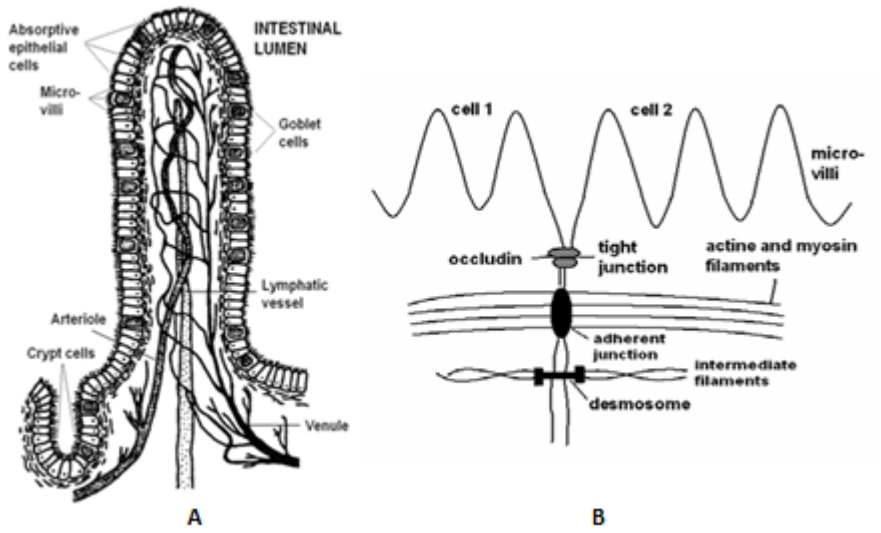

Figure 2.2 Schematic structure of an intestinal villus covered by a monolayer of absorptive epithelial cells (enterocytes) and mucus producing cells (goblet cells) (A), and the epithelial cell junctional complex with a tight junction, an adherent junction and a desmosome (B). Reproduced from Laitinen *et al*. [13].

2.3 The transport of drugs through the human body

The most frequent way of drug delivery to the systemic circulation for its complete pharmacological response, is the oral route. Administering drugs orally is considered to be safe, efficient, cost effective and easily accessible with minimal discomfort to the patient as compared to other methods of drug administration [14]. Furthermore it requires the least amount of sterility while still affording flexibility in the design of the dosage form [14]. In order for a drug to reach the systematic circulation and its site of action, it must contain the chemical and physical properties that are able to withstand the pathways of the digestive system. There are many barriers that the drug has to overcome before it can perform its therapeutic effect. Among these is the hostile environment of the gut [15]. The gut is where food is digested and the acidic atmosphere of the gut must be taken into consideration when designing a drug. Furthermore, the gut is designed to eliminate any xenobiotics that enter the body orally. An effective drug must be able to overcome this physiological environment as well as survive the action of the plethora of digestive and metabolic enzymes found within the stomach, pancreas, and small intestine. These enzymes include proteases, lipases and nucleases, and there is also the aspect of bile secretion (bile salts).

It has been reported that very few drugs are actually absorbed in the stomach. Most of them are retained there temporarily, largely in solution and are progressively delivered to the small intestine where it is absorbed. This concept is commonly known as gastric emptying and is a critical factor in drug absorption [16]. Generally, liquids are emptied faster than solids. All these considerations must be analysed when designing a drug. For instance when a drug is given in a solid dosage form it does not disintegrate in the gastric medium, it may remain in the stomach for a variable length of time until it gets emptied into the small intestine. The dosage and the form (liquid, solid, powder) varies with the action and the time that the response must be elicited.

2.3.1 Intestinal transport of drugs

Understanding the passage of compounds through the intestine is one of the most important aspects needed when creating any novel drug. Of note, absorption in the stomach is limited for most molecules since the surface area of the stomach is low especially when compared to the large surface area of the intestine [16]. Thus most drugs are absorbed in the duodenum followed by the jejunum and ileum; and as a result, the enterocytes of the intestine is said to be the main barrier during drug absorption [17]. Although drug transport is yet to be completely understood, there has been some headway in understanding the mechanisms involved. The two main pathways of drug passage are passive transport and active transport, and will be discussed in detail in the following sections.

2.3.1.1 Passive transport

Passive transport can occur by two means with compounds passing the epithelial layer either by paracellular or transcellular routes. Paracellular passive diffusion occurs between the small spaces or “gaps” between the lined enterocytes and the transcellular route is the transport of drugs through the actual enterocyte (Figure 2.3). It has been reported that the most common means for drug transport is through the transcellular route, due to the surface area of the intestinal epithelium being 1000-fold larger than the paracellular spaces [18]. The paracellular pathway is an aqueous, extracellular route across the epithelium. The driving forces for passive paracellular diffusion are the electrochemical potential gradients derived from the difference in concentration, electric potential and the hydrostatic pressure between the two sides of the cells. This route transports mostly hydrophilic compounds through the water pores [19, 20]. The negatively charged tight junctions (TJ) are the primary rate-limiting obstacle to drug transport through the paracellular route [11, 12]. However there are many studies [12, 21-23], including one presented by Hayashi and Tomita [24], where it was found that there are numerous enhancers within the cell that aid in drug transport across the membrane. These enhancers work on both paracellular and transcellular routes, and also open up the TJs thus increasing the permeability of the drug (Figure 2.3).

As most drugs are fairly lipophilic, the transcellular passive mode of diffusion is the most frequently used for absorption, with the apical membrane imposing the rate limiting step. The requirement for transcellular permeability is that the drug molecule must be able to partition between the aqueous contents of intestinal lumen, the phospholipid bilayer of the apical cell membranes, the aqueous contents of the enterocytes, and again, the phospholipid bilayer of the basolateral cell membranes. In addition the drug molecule has to be hydrophilic enough to be able to leave the cell membrane when entering the circulation and very lipophilic molecules run the risk of remaining solubilized in the cell membrane [25].

2.3.1.2 Active transport

Active transport is the transport through membranes against the concentration gradient and which require energy. The three different types of active transport via the intestinal membrane are facilitated diffusion, primary active transport and secondary active transport. Facilitated diffusion theoretically falls under the mode of passive transport since it is transportation of substances down the concentration gradient. However it can also be regarded as a type of active transport since it makes use of carrier mediated (CM) proteins (Figure 2.3). Primary active transport includes adenosine triphosphate (ATP) powered protein pumps (F-type and P-type ATPases) that derive their energy from the high-energy phosphate bond when ATP is hydrolyzed to form adenosine diphosphosphate (ADP). Secondary active transporters consist of ion pumps (symporters and uniporters) and their energy is derived from ion gradients (mostly Na^+, Ca_2^+ and H^+ gradients) [26].

The majority of nutrient absorption takes place in the proximal jejunum, thus there are large numbers of carrier proteins, channels and enzymes expressed in this highly absorptive part of the GI tract [14]. Researchers therefore modify their compounds based on this mode of transport, allowing them to mimic substrates of the CM proteins thus increasing their oral bioavailability. Generally, poorly absorbed drugs (commonly hydrophilic) are modified in such a way that the receptors recognise these molecules and pass them through the membrane. Nutrients and micronutrients can also aid in permeation when dealing with the nutrient transport system [27]. The two most important transport systems that are employed for drug transport are the oligopeptide carrier and the amino acid transport family [14]. Even though most commercially available drugs are delivered by the transcellular passive route; future research is leaning towards synthesizing entities that can be transported actively using CM proteins.

Another form of active transport is transcytosis (Figure 2.3). This process is a derivative of endocytosis, involving the capture of substances on the surface of the enterocyte layer and transportation of them across a membrane while bound within a vesicle. However this method for drug transport is very rare and not as effective as the other routes of permeability, because cellular vesicles contain large amounts of proteolytic enzymes which degrade most exogenous proteins [28]. This route of transport is generally used by highly potent drugs such as peptide antigens due to their large size.

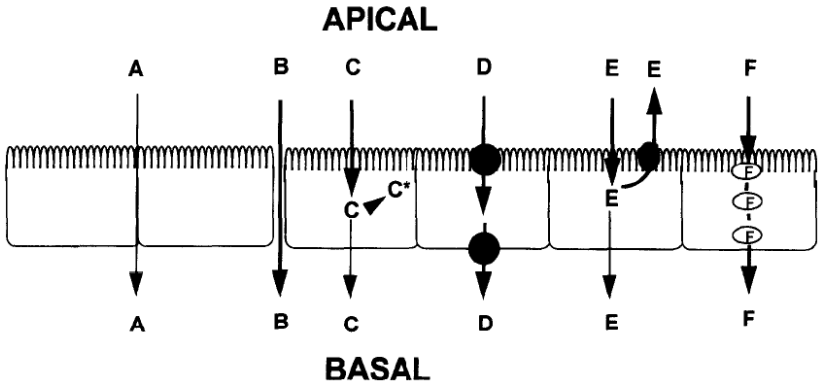

Figure 2.3 Pathways of intestinal absorption. (A) paracellular diffusion; (B) paracellular diffusion enhanced by a modulator of tight junctions; (C) transcellular passive diffusion, (C *, intracellular metabolism); (D) carrier-mediated transcellular transport; (E) transcellular diffusion modified by an apically polarized efflux mechanism; (F) transcellular vesicular transcytosis. Figure reproduced from Hunter and Hirst [29].

2.3.2 Hepatic clearance

Once the drug has escaped metabolism in the intestine, it would have passed the basolateral membrane of the enterocyte. It will then be transported, via the portal vein to the liver, which is the major site of metabolism in the human body [15]. However, this is beyond the scope of this review so it will not be discussed.

2.4 Multi-drug resistance

Clinical resistance to therapeutic agents is a major problem in the treatment of many diseases. Multi-drug resistance (MDR) is defined as the ability of the cells exposed to a single drug to develop resistance to a broad range of structurally and functionally unrelated drugs (cross-resistance), due to enhanced outward transport (efflux) of drugs, mediated by a membrane, energy dependant glycoprotein “drug transport pump” [29]. The intestinal epithelium also has a carrier mediated efflux system that limits the uptake of xenobiotics. This system includes

the expression of a high molecular weight, surface glycoprotein called the P-glycoprotein (P-gp) which is encoded by the multi-drug resistance transporter gene *MDR1*. Additional MDR protein efflux pumps found in the enterocytes include the breast cancer-resistance protein (BCRP) and the multi-drug resistance family (MDRP 1-6). The P-gp pump is the most well understood and most extensively studied [14] and is found in abundance in the intestine as well as in the liver, kidney, testes, placenta and the blood brain barrier (BBB). The P-gp is recognized as a member of the ATP-binding cassette (ABC) super family of membrane transport proteins. The current model of the mechanism of action of P-glycoprotein is that drugs can be detected and expelled as they enter the plasma membrane in the manner of a "hydrophobic vacuum cleaner" [30]. It has been reported that the energy to drive this ATPase activity comes from the drug itself. P-gp has a "flippase" characteristic that detects drugs in the inner leaflet of the membrane and "flips" it into the outer leaflet or directly into the extracellular space [29]. A major goal in clinical as well as experimental research is to try and inhibit the effects of this protein pump in an attempt to increase absorption.

2.5 Unstirred water layer (UWL)

Besides the epithelial barrier, drugs must pass the unstirred water layer as well. This is a mucous layer that is adjacent to the enterocyte cells on either side of the cell membrane. This undisturbed solution is made of mucin molecules (large glycoproteins with a net negative charge that forms the gel structure in mucus) secreted from goblet cells, and water. This layer contains lipids, cellular proteins, secreted immunoglobulins, as well as cell debris [31, 32]. The UWL is often surpassed when referring to intestinal permeation but it can act as a form of pre-epithelial diffusion barrier for rapidly permeating compounds and plays a critical role in balancing and maintaining the pH of the surface of the enterocytes.

2.6 Properties of potential drugs for optimum absorption

In the drug discovery industry there are thousands of chemical compounds entering the market. However most of these compounds prove to be unsuccessful and only a handful of drugs move on to the next phase of testing. Of this, less than half the amount enters the human clinical trial phase of testing. Upcoming drugs are referred to as new chemical entities (NCEs). There are many problems that NCEs have to overcome before it is considered to be an efficient drug. One of the major complications is the bioavailability of the drug. A pharmaceutically accepted compound undergoes tedious screening until it has favourable absorption and clearance properties as well as metabolic stability to carry out the specific response.

The general protocol, used by the world drug index (WDI) when developing drugs, is to follow "Lipinski's rule of 5", which was developed in 1997 by Christopher Lipinski using computational methods [33]. The name of this concept came about because the cut offs for each of the parameters are 5 and multiples of 5. It states that the drug compound must not have more than 5 hydrogen bond donors, these are expressed as the sum of hydroxyl (OH) and primary amine groups (NH), the molecular weight of the compound must be less than 500 daltons, the octanol-water partition coefficient (LogP) must not exceed 5 and finally that there must not be more than 10 hydrogen bond acceptors which are expressed as the sum of nitrogen and oxygen molecules [33]. There are exceptions to this rule; which include antifungal agents, antibiotics, vitamins and cardiac glycosides. However, their success in bioavailability stems from the fact that these agents have structural characteristics that allow the drugs to have substrates that bind to naturally occurring transporters within the membrane [33].

2.6.1 Solubility and dissolution

Before absorption can take place, the first and most important properties to consider are the dissolution rate and solubility. These properties need to be addressed during the early stages of drug discovery. Dissolution rate refers to the time taken for the compound to completely disintegrate from a solid form into the solvent, and solubility refers to the ability of the compound to go into aqueous solution. When a drug is ingested it resides in the intestinal fluid of the body, and must be presented to the permeable barrier in an aqueous state therefore the success of NCEs depends on its ability to be soluble. Hence solubility is regarded as a limiting factor in the absorption process. More than 40% of NCEs developed in the pharmaceutical industry are practically insoluble in water, which leads to inadequate bioavailability as well as mucosal toxicity. Solubility and dissolution thus play key roles in the dosage required.

In the pharmaceutical industry, many companies strive to achieve maximum permeability of drugs thereby attaining maximum absorption. This is the reason that many drugs are designed to be lipophilic, thus enabling easy passive diffusion across the membrane. However, this is a common misconception, as the more lipophilic the drug is the less soluble it is. Therefore it is imperative to have adequate solubility as well as lipophilic properties.

In the mid 1990's the Biopharmaceutical classification system (BCS) was introduced which depicts the direct relationship between aqueous solubility and membrane permeability of drugs. This system shows the *in vivo/in vitro* correlation of the different classes of drugs. According to this system drugs are classified into one of four categories (Figure 2.4) [34]. Class I drugs are said to be the most prosperous when it comes to bioavailability. Statistically, 85% of these drugs are dissolved within 30 minutes at physiological pH and has an expectancy of 100% intestinal absorption with the rate limiting step being gastric emptying. Class II drugs are absorbed easily but are limited by solubility. In class III drugs, dissolution occurs rapidly, however permeability is a rate limiting step, and finally class IV drugs, which unless the required dose is very low, are generally very poor drug candidates [35]. The BCS also shows that highly permeable molecules (classes I and II) exhibit a high *in vivo/in vitro* correlation, whereas poorly permeable molecules (classes III and IV) show a low *in vivo/in vitro* correlation [9].

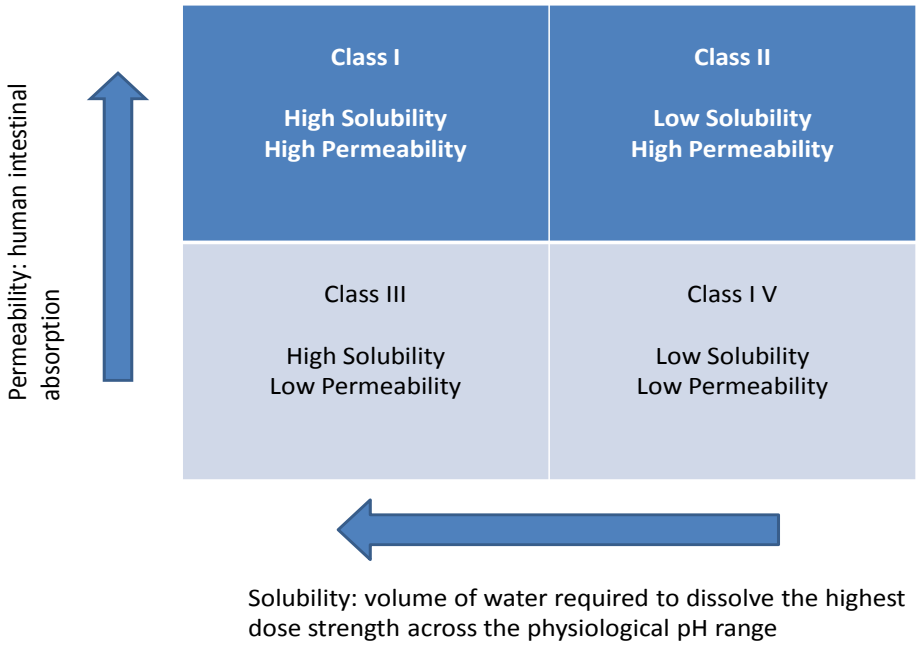

Figure 2.4 The Biopharmaceutics classification system. Drug substances according to their solubility and permeability properties, representing a fundamental view of the drug intestinal absorption process following oral administration. Adapted from Amidon *et al*. [34].

Permeability tends to vary over a more narrow range than solubility. The difference between a high-permeability and a low-permeability compound can be 50-fold whereas the difference between a high-solubility and low-solubility compound can be one million–fold. Therefore, if a structural modification improves solubility by 1,000 fold while it reduces permeability by 10-fold, then there will still be a100-fold improvement in absorption [36-38]. From this observation it seems practical to alter the solubility of a drug to make it more compatible with rules of bioavailability, rather than permeability. There are many properties, such as ionization, particle size and lipophilicity, which need to be considered that directly affect the solubility of drugs and hence its absorption.

2.6.2 Ionization (pK_a)

In the past, the pH partitioning theory presumed that neutral species crossed the membrane optimally. However this theory has been challenged [39] and it has been discovered that ionized species have a greater affinity for the aqueous phase and passes through the membrane in an ionized form. Currently, the majority of the drugs on the market contain ionizable groups [39]. There are 75% of basic drugs, 20% of acidic drugs and only 5% are not ionizable (neutral) [40].The degree of ionization is measured by pK_a and it is an important property to consider with regards to solubility and permeability, especially with passive diffusion. Ionized molecules are more soluble in aqueous media than neutral molecules because they are more polar, conversely ionized species are less permeable than neutral molecules and as a result this is the predominant form that uses the passive route for permeation. Since there are varying pH levels through the intestine, acidic and basic drugs will permeate at different levels. For an acid (pK_a=5), passive diffusion is enhanced in the direction of higher pH and it is vice versa for a base (pK_a=10). Therefore there is a trade-off between solubility and permeability because of the effects of ionization. Medical chemists can modify compounds using sub-structures (Table 2.1) to increase or decrease the pK_a thus affecting its solubility or permeability. For example, the strength of an acid can be increased by adding halogens or other electron withdrawing groups (carboxy, cyano, nitro) whilst attachment of an aromatic group (aniline) increases the strength of the base [40]. Further increase of the basicity of aniline can be achieved by adding electron donors such as methoxy [40]. There are many methods in which pK_a can be measured and there are several databases available to aid in the drug discovery process.

Table: 2.1 Examples of acid and base sub-structures and their respective pK_a that commonly appear in drug molecules. Adapted from Kerns and Di [40].

Acids	pK_a	Bases	pK_a
CF_3COOH	0.23	Guanidine	13.6
CCl_3COOH	0.9	Acetamide	12.4
CCl_2HCOOH	1.3	Pyrrolidine	11.3
$CClH_2COOH$	2.9	Piperidine	11.1
HCOOH	3.8	Methyl amine	10.6
C_6H_5COOH	4.2	Piperazine	9.8,5.3
Succinic acid	4.2,5.6	Trimethyl amine	9.8
CH_3COOH	4.8	Glycine	9.8
Thiophenol	6.5	Morpholine	8.4
p-Nitrophenol	7.2	Imidazole	6.8
m-Nitrophenol	9.3	Pyridine	5.2
C_6H_5OH	10.0	Quinoline	4.9
		Aniline	4.9
		Triazole	2.5
		Purine	2.4
		Pyrimide	1.2
		Diphenylamine	0.8

2.6.3 Particle size

The solubility of a drug is often intrinsically related to its particle size. Generally, the smaller the particle or drug the greater the surface area to volume ratio. This in turn allows for a larger interaction with the intestinal fluid thereby resulting in an increase in solubility.

Particle size also affects the dissolution of the drug, the smaller the entity the faster the dissolution rate. In terms of class II drugs where dissolution is the rate limiting step, one of the improvements could be the alteration of the particle size so that the surface area is increased [35].

2.6.4 Lipophilicity

Lipophilicity is defined as the tendency of a compound to partition into a non-polar lipid matrix instead of an aqueous matrix, and is measured by Log P and Log D. The fundamental difference between the two measurements is that Log P measures the partition of neutral species and Log D measures the partition of species that are ionized (pk_a). As previously noted, ionized compounds have a greater affinity for the polar aqueous phase than the non-polar organic phase. This property plays a vital role in the solubility, permeability, metabolism and toxicity of a drug, therefore making it an important determinant of an effective drug entity. The general consensus is that the more lipophilic a compound is the more permeable it is across the membrane. However lipophilicity does not act as a separate entity and it is affected by other attributes of the drug, for example a very lipophilic compound will not be easily soluble, thus affecting its bioavailability. Furthermore, pH plays an equal and vital role in the compound's lipophilic ability. For acidic compounds, the neutral ratio of molecules in solution decreases with increasing pH therefore log D decreases with an increase in pH [37]. Conversely for basic compounds, the neutral ratio of molecules increases in solution with increasing pH, therefore Log D increases with increasing pH [37]. Studies conducted by Abraham *et al*. [41, 42] have shown that lipophilicity is affected by several fundamental structural properties of the compound such as molecular weight, dipolarity, as well as hydrogen bond donors and acceptors (hydrogen bond acidity and hydrogen bond basicity respectively). Although Lipinski has stated that the Log P value of a compound should be less than 5, the ideal range is 0-3. In this range a good balance of permeability and solubility exists.

All physicochemical properties of NCEs are inter-correlated therefore changing one property affects several others. The two main concerns when designing a compound with regards to absorption are solubility and permeability which as discussed have an indirectly proportional relationship with each other. Medicinal chemists must amend the different structural features (Table 2.2) to find a balance between solubility and permeability for the clinical candidate in order to achieve optimal absorption (Figure2.5).

Table: 2.2 Structural modification strategies for improving solubility and permeability, and thereby adsorption. Adapted from Kerns and Di [36, 38].

Solubility Improvement	Permeability improvement
Add ionizable group	Ionizable group to non-ionizable group
Reduce lipophilicity	Esterify carboxylic acid
Add hydrogen bonding	Reduce hydrogen bonding and polarity
Add polar group	Reduce size
Reduce molecular weight	Add non-polar side chain
Construct a prodrug*	Construct a pro-drug*
	Isosteric replacement of polar groups
	Add lipophilicity

*Pro-drugs (precursor of a drug) are drugs that are modified with an inactive component so that it can aid in the adsorption process. However this topic is beyond the scope of this review.

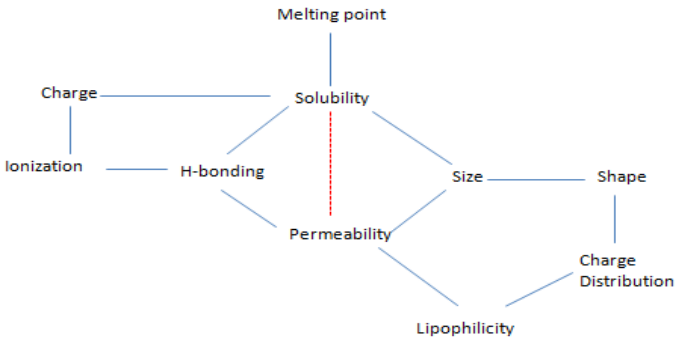

Figure 2.5 Effects of structural properties on solubility and permeability. Adapted from Kerns and Di [36].

Besides using the fundamental Lipinski's rule of 5, there are other criteria that need to be considered to render a compound more "drug-like". The concept of drug likeness simply means molecules which contain functional groups and/or have physical properties consistent with the majority of known drugs. This way there can be some "rules" or "filters" that can help chemists to identify "drug like" molecules [43]. Furthermore these databases can also distinguish from different types of drugs, for example drug moieties that are used for the central nervous system (CNS) will have different properties (more lipophilic) that that used to

permeate the intestinal barrier. Whilst Lipinski's rules are very helpful in eliminating non-drug like molecules, it is important to consider other factors. Functional groups of a NCE are essential, and Andrews *et al.*[44] identified that the functional groups that should be used are those that impart biological activity. A more recent approach to identifying drug-like molecules is the work of Muegge *et al.* [45]. This study used a scoring system based on the number of pharmacophoric elements found in drugs and it was noted that many drugs affecting the CNS are relatively small and contain one pharmacophoric group [45]. There is a second filter that does not classify these compounds as non-drugs. A study done by Oprea [46] who analysed compounds from major drug databases such as MARCCS-II drug data report (MDDR) [47], comprehensive medicinal chemistry (CMC) [48] and the available chemicals database (ACD) [49], discovered that NCEs should consist of ring bonds, rigid bonds and rotational bonds.

Another aspect for determining "drug-like" moieties is the frame work of the specific drug. When comparing the scaffolding of drugs, it turns out there are only about 32 frame works that are commonly used in drugs. This was revealed by a study conducted by Bemis and Murcko [50], who also showed that there are "shape themes" reused in widely divergent drug design situations. In another study conducted by the same authors, it was determined that the mean number of side chains is four and the number of heavy atoms per side chain was two [51]. There have also been studies which eliminated drugs by their structure because they were toxic [52].

It must be noted that even though these structural filters are successful in weaning out poor drug like molecules, one must avoid the temptation of being overzealous. It is important not to eliminate some "interesting" molecules.

2.7 *In vitro* tools for predicting drug permeability

Since drug absorption is an important selection criterion in drug discovery and development, there is a need for reliable and appropriate screening methods to assess intestinal permeability. The validity of these assays should reflect their ability to predict the behaviour of a drug at the *in vivo* intestinal barrier [5]. To produce high quality, useful predictions of the transport processes, highly standardized *in vitro* models are used to screen a large number of drug candidates and *in vitro* applications have far surpassed the use of *in vivo* applications.

There are several advantages of implementing *in vitro* techniques over *in vivo* methods, which include a requirement of fewer test compounds for evaluation, it is easier to conduct (excludes the work of live animals), quicker turn-around time, allows for evaluation of specific mechanisms involved in membrane transport, provides information on the metabolism of compounds which occur during transport, aid in formulation design and development of structure-transport relationships, and also provides samples that are free from contaminating plasma proteins for analysis, thus allowing more efficient analysis [53].

2.7.1 Cell-based methods

The first practical method for *in vitro* screening came in the form of cell monolayers. This system utilizes specific cell types that are grown on porous membranes, and which mimic the intestinal epithelial cell layer once differentiated. Cells are plated on a specialized two chamber insert which has an apical (A) side and a basolateral (B) side (Figure 2.6) between the porous membranes containing the monolayer. Test compounds are placed in buffer at the apical side whilst the basolateral side is exposed to buffer only. As time progresses, passive diffusion is verified by the transfer of the compound from the apical to the basolateral side through the cell monolayer. Analysis is done via HPLC or liquid chromatography/mass spectrometry (LC/MS) techniques using aliquots from both the compartments. This apical to basolateral (A>B) experiment quantifies permeability in the absorptive direction, which models absorption in the GI tract. This permeability assessment has been correlated by several research groups to absorption in the small intestine or to fraction of dose absorbed. When such a correlation is established, it can assist medicinal chemists with predicting *in vivo* absorption of their compounds [54].

One important consideration when growing the cell monolayer is that the monolayer is kept intact (with no “spaces”). If this is not maintained, the compound could diffuse through the porous membrane, resulting in a false positive. Evaluation of the monolayer integrity is tested using trans-epithelial electrical resistance (TEER). The TEER value indicates if the cell layer is forming a continuous network of tight junctions and low TEER values represent a high level of paracellular permeation. Many devices to measure the TEER value are commercially available [54].

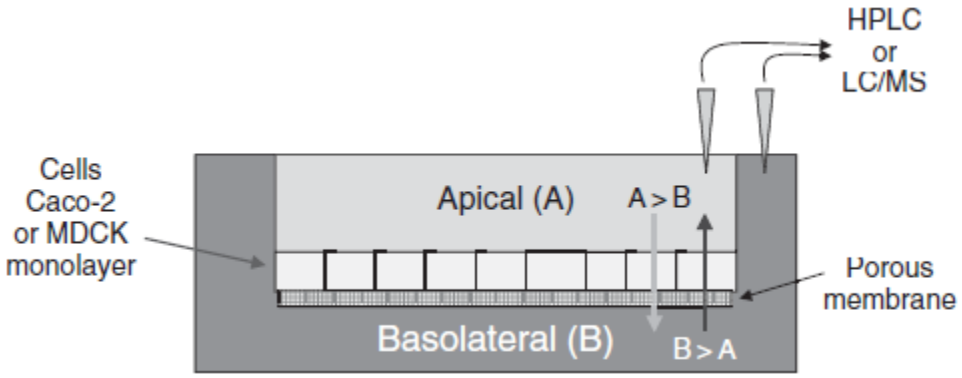

Figure 2.6 Cell permeability cell culture assay. Reproduced from Kerns and Di [54].

2.7.1.1 The Caco-2 cell line

The Caco-2 cell line was first established from a moderately well differentiated colon adenocarcinoma and was isolated from a 72-year old patient [55]. Caco-2 cell lines are said to be the gold standard when it comes to *in vitro* cell culture screening for permeability of new chemical entities. It is a polyclonal cell line, that is it consists of a heterogeneous population of cells, which means that the properties of the cells may change with time in culture [14]. They differentiate spontaneously in culture and remarkably mimic the functional and structural characteristics of mature human enterocytes [56]. The cells differentiate into a uniform monolayer with polarization, apical brush border microvilli, villi expression and dome formation [55, 56]. Furthermore the electrical properties (TEER values) and the ionic conductivity characteristics of these monolayers are similar to colonic crypt cells [55]. The time for these cells to reach full differentiation is approximately 10 days with confluency being reached at around 21 days [57]. The differentiated cells exhibit high levels of enzymes that are usually present in the brush border microvilli of human enterocytes (alkaline phosphatase, sucrose, amino peptidase etc.) [56]. Caco-2 cells produce tight junctions between their cells and contain many of the transporters that are found within the intestinal barrier. In addition, a distinctive property of this cell line is the expression of the P-gp protein. Although with certain research outputs, concentrating only on permeability, this does not represent a positive attribute of the cell line. However, its expression does open up research opportunities regarding this protein.

Numerous researchers have made use of this cell line due to its qualitative relationship with cellular transport and *in vivo* drug permeability [58]. There are extensive applications of Caco-2 cells which include studies regarding the transport mechanisms and analysing the permeability attributes of many amino acids, protein peptides, inhibitors and a series of drugs. Extensive research using this cell line was done by Artusson and co-workers as well as Karlsson and co-workers who exploited the passive and active transport of these cells [19, 59-62]. The transport of drugs across the intestinal epithelium may occur by one or more of four different routes, namely the passive transcellular and paracellular routes, the carrier mediated route and by transcytosis. Caco-2 monolayers have been used to study drug transport by all four routes.

It has been reported however that the Caco-2 cell line does exhibit some characteristics of the colonic region of humans such as poor paracellular permeability and the high TEER values resemble colonic region properties which differs from the intestinal epithelium thus creating a disadvantage for this model [19, 20]. Other disadvantages are the extended time period that these cells take to differentiate (21 days) and the fact that many laboratories have reported diverse results when testing the same compounds. The heterogeneous nature of these cells explains the difference in morphology, paracellular permeability, and expression of enzymes and transporters reported by researchers [28, 63].

2.7.1.2 The MDCK cell line

Madin Darby canine kidney (MDCK) cells were derived from dog kidney by Madin and Darby in the 1950's, and is thought to represent a distal tubular phenotype. They form monolayers that represent columnar epithelial cells with tight junctions when cultured on semi-permeable membranes. Ion channels and pumps are arranged on the membrane in a polarized fashion [64]. The MDCK cell line is amongst the best studied epithelial cell lines with respect to genetics, lipid composition, expression of proteins and other parameters. More recently, MDCK cells have also been used for transport studies [65, 66]. Although similar to Caco-2 cells in terms of morphology, MDCK cells have been proven more advantageous in high throughput screening (HTS) of a compound's passive diffusion ability across the intestinal barrier. This is due to the fact that MDCK cells take a shorter time (2-7 days) to differentiate as well as display lower TEER values when compared to the Caco-2 cells. There are two distinct sub-clones of MDCK cells, MDCK strain I (MDCKI) that exhibit tight monolayers with high TEER values and MDCK strain II (MDCKII) that form monolayers with more "leaky" tight junctions with lower TEER values [67, 68]. The latter is preferred when dealing with drug transport studies because the "leakiness" resembles the human intestine more closely [69].

An attractive characteristic of MDCK cells is that they have a low expression of P-gp; therefore the passive diffusion of drug transport can be studied without the hindering effects of P-gp. However they do express endogenous canine transporters due to the species difference, which is likely to be different from the transporters found in the human intestine, therefore it is not applicable to use these cells for active drug transport predicting active uptake or efflux mechanisms. However, there is still vast application using this cell line. One of the most studied applications apart from prediction of passive permeability is the genetic engineering of these cells to produce cells that overexpress P-gp (MDR1-MDCK). Additionally these cells grow with more tight junctions and are generally used to predict permeability in blood brain barrier studies (BBB) [70].

2.7.1.3 The HT29 cell line

HT29 cells are also another well studied human colon carcinoma cell line. The wild type of this cell line when cultured under standard conditions (glucose containing media) grows in an unpolarised, undifferentiated multilayer which does not resemble enterocytes thus proving irrelevant in intestinal permeability studies. However when these cells are grown in a galactose supplemented medium they grow as differentiated polarized monolayers of absorptive and/or mucus secreting goblet cells [68]. Several mucus producing sub-lines have been established from human HT29 cells [71].The most popular clones are the HT29-H and the H29-MTX (methotrexate-induced cells), which produce mucus producing monolayers with enterocyte characteristics (highly polarized cells, which express microvilli, hydrolases and resemble goblet cells). These mucus-layer producing variants have attracted some interest for two main reasons; the mucus layer covering the intestinal epithelium *in vivo* may limit the absorption of some drugs and Caco-2 and MDCK cell lines do not secrete this barrier [68].With the exception of a few studies, the role of mucus on drug transport has been largely ignored. To remedy this issue, co-cultures of Caco-2 and H29-H and H29-MTX have been investigated, however these are not found in wide application in drug discovery [72-74].

2.7.2 Methods utilizing artificial membranes

Although cell models are being used extensively in the drug development industry, their limitations must be considered. For example cell models lack some of the physiological factors that influence the passage of drugs (mucus, bile salts, cholesterol) [9]. Furthermore, standardizing procedures with these models could be time consuming and reproducibility may be problematic. Cells differ in their growth depending on factors such as passage

number, culture medium composition, nutrients available, cell density, etc. Moreover, with a biological system different laboratories may encounter trouble optimizing the system. There are other methods that can be used to determine the permeability of NCEs, however these methods may not give you a full depiction of the bioavailability of the drug and the other parameters that need to be assessed, but merely focus on the permeability aspect, which is important.

2.7.2.1 Immobilized Artificial Membrane (IAM) Columns

Immobilized artificial membrane (IAM) columns are reverse phase liquid chromatographic columns (HPLC), where the common octadecyl groups that coat the solid support is replaced by phospholipids. The major phospholipid that is found in membranes is phosphatidylcholine (PC), thus the IAM column is manufactured using PC analogues. IAM columns closely mimic the surface of biological membranes; therefore they have a high affinity for membrane proteins [75]. The longer retention time in the column means that the more permeable a drug is across the intestinal membrane. This is due to the fact that it is interacting with the stationary lipid phase of the column. The advantages of using these columns is that it offers HTS, only a small amount of compound is needed, automation is straight forward, and because of the absence of a biological system it is rapid as well as cost effective [76]. It has been found that IAM columns have a good correlation to results yielded by traditional cell-based methods [77-79].Whilst it is an attractive method for determining permeability, IAM columns have some obvious limitations, such as that it does not consider the potential role of paracellular transport, carrier-mediated transport, drug metabolism, intestinal enzymes, and efflux transporters on permeability. This results in a very limited view of the true intestinal absorption of a potential compound. Beside IAM there are a variety of commercially available columns specifically designed to screen compounds, and the historical concerns for column stability have been overcome [76].

2.7.2.2 Parallel Artificial Membrane Permeability Assay (PAMPA)

In contrast to cell-based assays the development of artificial membranes supported by filters renders a faster, flexible, cheap and fully automated system for HTS of potential therapeutic candidates [76]. One of the most popular systems and probably the most successful is a system that was created by Kansy *et al*. in 1998 [80]. The parallel artificial membrane permeability assay (PAMPA) is predominantly used to screen moieties that are transported passively through the intestinal barrier. It is an excellent alternative to cellular models for the

earliest ADME primary screening of research compounds [81]. This system represents a "sandwich" which is formed from two plates (donor and receiver). The base of the receiver plate which is a 96-well microfilter plate is always immersed in buffer. Between this "sandwich" are filters, which are generally 125µm thick with 0.45µm pores and 0.3 cm^2 cross-sectional area with 70% porosity, onto which a solution of the artificial lipid membrane is placed (Figure 2.7) [76]. There are many different commercially available PAMPA systems that have different materials coating their filters in accordance to their different applications (Table 2.3).These coats mimic the lipids of the cell membrane. The system works similarly to the cell-based permeability assays (Caco-2 and MDCK) where the samples are added to the donor wells and are diluted with buffer. The receiver plate is placed on top of the donor wells, the lipid solution is added carefully ensuring that there is complete coverage of the filter support and then the buffer solution for the receiver system is added. The resulting sandwich is covered to avoid evaporation. After the samples have been incubated for a set amount of time the plates are separated and aliquots of the samples are analysed. The concentration of samples in both receiver and donor wells are determined and quantified using HPLC, LC/MS or UV detection [76]. Although seemingly a gold standard when it comes to measuring drug permeability, its disadvantages are the same as IAM in that it does not contain the enzymes present in a biological system. Furthermore if detection is done by UV analysis it is limited to compounds that exhibit UV absorbance. Another limitation is that experimental times could exceed 15 hours.

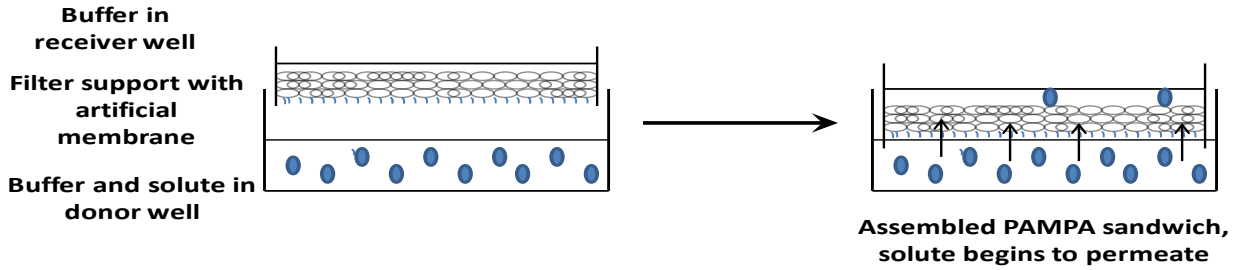

Figure 2.7 Schematic representation of the PAMPA system. Adapted from Manson [75].

Table 2.3: The different PAMPA assays available and their characteristics .Adapted from Faller *et al.*[82].

PAMPA type	Target barrier	Filter	Solvent	Membrane composition	pH	Incubation time (h)
Egg-PAMPA	GI-tract	Hydrophobic PVDF (125µm)	*n*-dodecane	10% egg lecithin	6.5 and 7.4	15
HDM-PAMPA	GI-tract	10µm PC	1.7 octadiene	n-hexadecane	4.0,6.8-8.0	4
BM-PAMPA	GI-tract	Hydrophobic PVDF (125µm)	*n*-dodecane	3% of a phospholipid mixture[a]	6.5	15
	GI-tract	Hydrophillic PVDF (125µm)	*n*-dodecane	1% egg lecithin	5.5 and 7.4	2
DOPC-PAMPA	GI-tract	Hydrophobic PVDF (125µm)	*n*-dodecane	2% DOPC		15
DS-PAMPA	GI-tract	Hydrophobic PVDF (125µm)	*n*-dodecane	20% phospholipid mixture	Gradient 6-7.4	15
BBB-PAMPA	BBB	Hydrophobic PVDF (125µm)	*n*-dodecane	2% PBL	7.4	18
PAMPA skin	skin	Hydrophobic PVDF (125µm)	70% silicon oil 30%IMP	70% silicon oil 30%IMP	variable	7

[a] lipid mixture made of 33% cholesterol, 27% phosphatidylcholine, 27% phosphatidylethanolamine, 7% phosphatidylserine and 7%phosphatidylinositol

2.8 HIV Protease (HIV-PR)

One of the leading fields in drug discovery is with acquired immune deficiency syndrome (AIDS), more specifically the human immunodeficiency virus (HIV). HIV is a well-known disease that attacks the immune system of humans, disarming its defence system. Initially influenza-like symptoms is demonstrated which is followed by a prolonged period of dormancy, eventually resulting in a fully compromised immune system results in death. Generally common illnesses such as influenza and chest infections cause death in patients. At the onset of the epidemic in the early 1980s, no existing drug was known to be useful against AIDS and completely new pharmaceutical agents had to be created. Although azidothymidine (AZT), the first drug shown to counteract the effects of HIV-1 infection, which was previously known as a potential anticancer agent, the rapid progress in the understanding of the structure and life cycle of the virus led to unprecedented development of other drugs targeted to a variety of viral proteins. The retroviral enzymes, reverse transcriptase (RT), integrase (IN), and protease (PR) were the obvious targets for drug discovery [83].

HIV-PR is commonly known as the "protein cutting" enzyme as it is responsible for the cutting of *gag* and *gag-pol* polyproteins into their functional constituent proteins [84]. Their role is therefore to prepare proteins for subsequent manufacturing of new virions (or even enzymes) thus the function of this enzyme is essential for proper virion assembly and maturation. Inactivation of HIV-1 PR by either mutation or chemical inhibition leads to the production of immature, non-infectious viral particles [85-87].The introduction of HIV-1 PR inhibitors that reduce the virus proliferation and subsequent infection made this enzyme a prime target for AIDS therapy [88].

It is well established that HIV-PR shares the similar catalytic activity as most eukaryotic aspartic enzymes. This statement is supported by many researchers that have acknowledged a highly conserved amino acid sequence amongst HIV-PR and other aspartic enzymes [83, 89, 90] this is further correlated by crystal structures of their actives sites revealing them to be nearly identical. In addition it has been reported that HIV-PR is inhibited by pepstatin A which is a well-known aspartic protease inhibitor [90]. However it must be noted that although they have similar catalytic activity HIV-PR is unique, as its optimum function resides at a higher pH level then other aspartic proteases [91].

2.8.1 HIV protease structure

HIV-PR is a retroviral aspartyl protease homo-dimer which consists of 99 amino acids and one active site which is C_2-symetric in the free form [92]. Like all aspartic proteases it has a highly conserved active site, Asp-Thr-Gly. What separates this enzyme from the family is that it is the only aspartic protease that is dimeric [93]. Each monomer contains an extended β-sheet region which is a glycine-rich loop. This section is known as the flap, which contains one of the two essential aspartyl residues (Asp-25 and Asp-25'). This "flap" plays an integral role in substrate binding as a part of the substrate binding site lies within this structure (Figure 2.8).

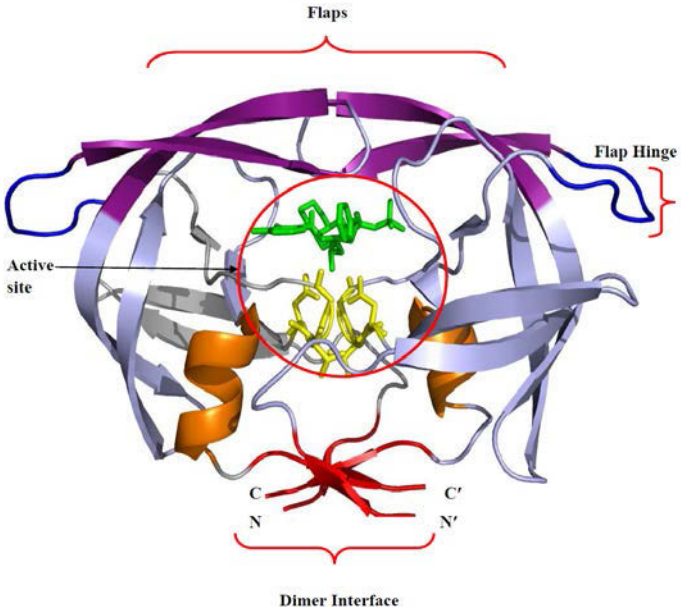

Figure 2.8 Ribbon structure of HIV-1 protease (HIV-1 PR).Reproduced from Maputsoe *et al*. [94].

2.8.2 Mechanism of action

There have been many reports of the mechanism of action of HIV-1 protease, however most correlate to the protease having an acid-base mechanism of action (similar to most enzymes in the aspartic protease family). The most widely accepted mechanism for aspartic protease has been described by Suguna *et al.* [95] and involves the reaction of one of the aspartyl residues with a water molecule which acts as a nucleophile that resides between the two residues. After the activation of the nucleophile by the negative aspartic side chain, the water molecule attacks the carbon of the carbonyl group of the substrate to generate an oxianion tetrahedral intermediate. Protonation of the substrate amide N atom results in the breakdown of the tetrahedral intermediate to hydrolytic products (Figure2.9). The two aspartyl residues contribute to the hydrophobic nature of this enzyme [92].

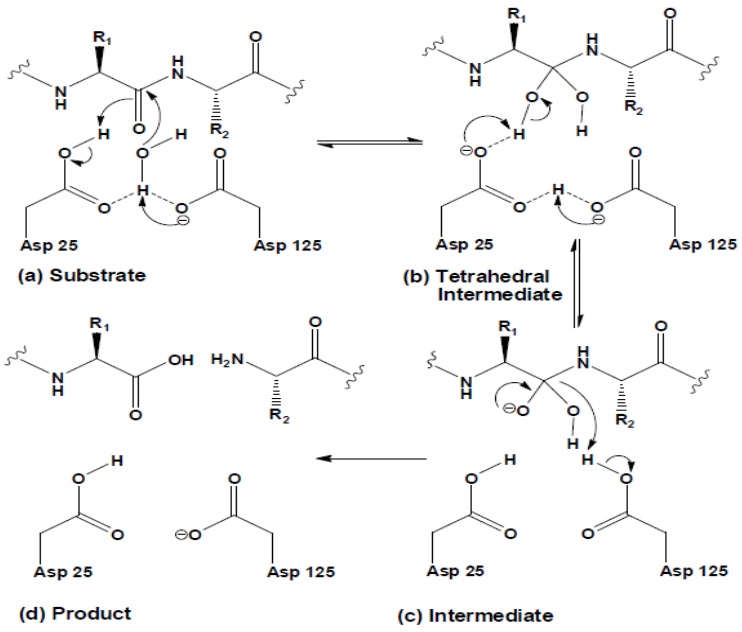

Figure 2.9 Mechanism of HIV-1 protease cleavage. Reproduced from Makatini *et al.* [96]

2.8.3 Substrate binding

Amidst the aspartic residues lies a well-designed active site consisting of a triad of amino acids, Asp25-Thr26-Gly27 [93, 97]. These amino acids are joined by a network of hydrogen bonds referred to as the "fireman's grip" and this contributes to its highly selective nature. The enzyme catalyses the hydrolysis of a specific peptide bond known as the scissile bond. The substrate binding site has a number of well-defined binding pockets referred to as S_1 to S_n. These sites accommodate specific side chains of the substrate commonly known as P_1 to P_n.(Figure2.10) [83, 98].There are specific sequences that this enzyme cleaves, as shown in table 2.4 and figure 2.11.

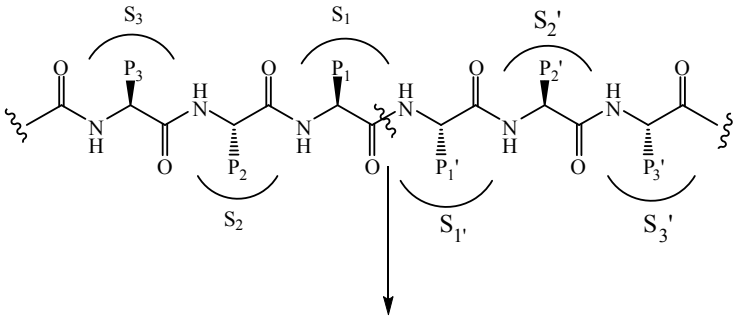

Figure 2.10 The binding of substrate to active site pockets. S_1....S_n are the standard nomenclature for the sub-sites of the active site. P_1....P_n are the amino acid residues of the substrate. Due to the symmetric property of the enzyme, the corresponding substrate pockets and substrate side chains are termed S_1'....S_n' and P_1'....P_n' respectively. Adapted from Brik and Wong [92].

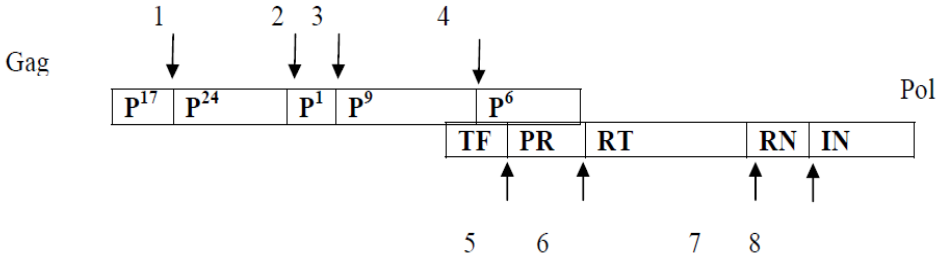

Figure 2.11 Cleavage sites within the *gag* and *gag-pol* precursor proteins. Reproduced from Abdel-Rahman *et al*. [99].

Table 2.4: Amino acid sequence by sites cleaved by HIV protease. Adapted from Makatini *et al.* [96]

Site	Sequence
1	-Ser-Gln-Asn-Tyr*Pro-Ile-Val-Gln-
2	-Ala-Arg-Val-Leu*Ala-Glu-Ala-Met-
3	-Ala-Thr-Ile-Met*Met-Gln-Arg-Gly-
4	-Pro-Gly-Asn-Phe*Leu-Gln-Ser-Arg-
5	-Ser-Phe-Asn-Phe*Pro-Gln-Ile-Thr-
6	-Thr-Leu-Asn-Phe*Pro-Ile-Ser-Pro-
7	-Ala-Glu-Thr-Tyr*Phe-Val-Asp-Gly-
8	-Arg-Lys-Ile-Leu*Phe-Leu-Asp-Gly-

* indicates the position of the scissile bond

2.8.4 HIV Protease inhibitors

Extensive research of HIV-protease inhibitors (PIs) in the mid-1990s changed the dynamics of AIDS research. The basic rationale amongst the design of inhibitors was to create a molecule that mimics the transition state of the enzyme's substrate. Generally it is in the form of a peptide linkage of which the protease is unable to cleave. PIs are programmed to attack the active site of the aspartic protease and are designed utilizing the knowledge of the aspartyl protease's mode of action. The most promising transition state mimic was hydroxyethylamine which led to the discovery of the first protease inhibitor, Saquinavir. Following this discovery, other HIV protease inhibitors were designed using the same principle (Figure 2.12) [100].

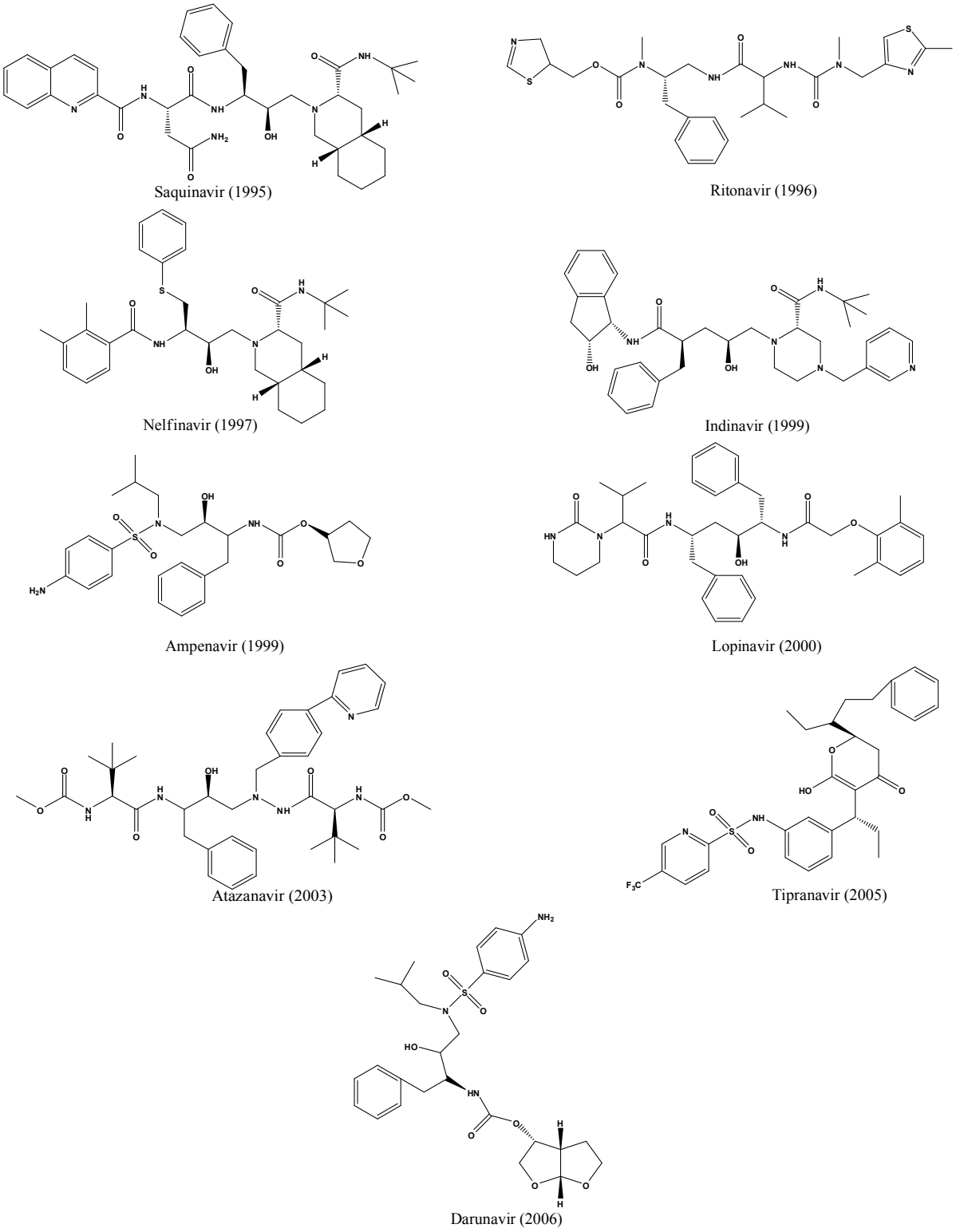

Figure 2.12 FDA approved HIV-1 protease inhibitors. Adapted from Makatini *et al.* [96].

However, with deletions and mutations of this enzyme, resistant species appeared to evolve. This poses a serious problem as resistant species deny commercial drugs of their potential inhibition. This is mainly attributed to the vast genetic variability among species. There are reports of different subtypes of HIV-1 appearing in different parts of the world [88]. Genetic variation between subtypes usually ranges between 25 and 35% at nucleotide level and variation within subtypes can range from 15 to 20%[101]. One of them is the HIV-1 subtype C which displays significant genetic variability from its parent subtype (HIV-1 subtype B). This mutant is predominate in sub-Saharan Africa (mainly found in South Africa) and shows rapid development of resistance to common drugs [88]. Awareness of this has induced a niche for fundamental research of inhibitors that target specific mutations of this enzyme.

2.8.5 Novel chemically designed protease inhibitors

There is a vast area of research that indicated that the attachment of a polycyclic cage moiety to a drug can add numerous benefits to the drug itself. It has been reported that these compounds increase the antiviral and antibacterial resistance to a broad range of infection [102, 103]. One of the most remarkable features of the addition of cage moieties is that it is able to confer greater membrane permeability properties to the drug. The cage compound induces receptor site specificity for the lipophilic regions on the receptor molecule.

A study done by Makatini *et al.* [104] used this interesting concept of polycyclic cage derived compounds as scaffolds for chemically synthesized HIV-1 protease subtype C inhibitors (Figure 2.13). In this study a peptide based inhibitor was synthesized with an attached polycyclic cage derivative to yield the first account of a pentacycloundecane (PCU) lactam-peptide inhibitor that targeted the mutated South African subtype C protease.

The natural HIV-protease substrate FEAIS [105] was chemically altered to replace the F with the cage moiety to ensure the high specificity of the proposed inhibitor to the active site. The PCU that was selected contained a hydroxyl carbonyl functional group and a very stable amide bond strategically positioned so that it is able to interact with the catalytic residues of the active site (Figure 2.13). Various peptide chains were then added to the cage to evaluate its inhibitory potential. These peptides contained the amino acid residues that bound to the hydrophobic substrate binding sub-sites. However it was proven that the original natural substrate that contained the cage displayed the greatest inhibition of the enzyme with the highest specificity and binding to the enzyme's catalytic site.

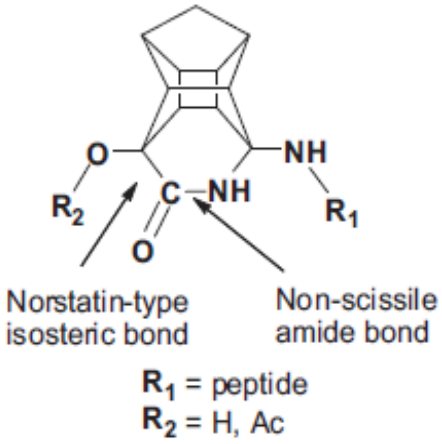

Figure 2.13 Pentacycloundecane scaffold representing the PCU lactam-peptide derivatives as novel potential transition-state analogues for HIV-PR inhibition. R_1 is indicative of the position of different peptide inhibitors. Reproduced from Makatini *et al*. [106].

Using the same peptide synthesis approach Pawar *et al.* [107] attempted a study using carbapeptide analogues for the inhibition of HIV-1 protease (Figure 2.14). This study exploited the use of glycopeptides as a source of potency to the enzyme. The basis of this comes from the research done on the application of glycopeptides used in medicine. There is a vast number of effective inhibitors such as farnesyltransferase (PFT) [108], proteasome [109], glycosidase [110], and glycoamidase [111] in the drug discovery field. The rationale of this work is on account of majority of US Food and Drug Administration (FDA) peptide based protease inhibitors and drug molecules undergo classic problems such as proteolysis and poor bioavailability. The incorporation of glycosylation of these peptides proposes an interesting means of protection against degradation and improved aqueous solubility [112].Using a known peptide protease inhibitor, darunavir, a sequence embedded in a sugar moiety was created. Glycopeptides in this manner was used as a means to enhance pharmokinetic properties such as enzyme binding efficiency and membrane permeability of these peptide protease inhibitors to generate more effective analogues.

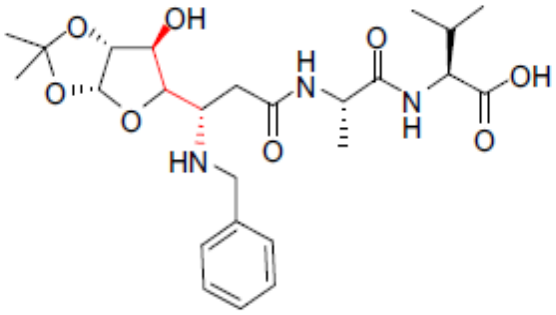

Figure 2.14 Glycopeptide HIV protease inhibitor. This inhibitor was used as the basis for the synthesis of the glycopeptide analogues. Reproduced from Pawar *et al.* [107].

From the above studies it was presented that cage moieties and glycosylated analogues do confer a greater binding capacity and inhibitory potential to the protease than their unaltered derivatives. There was a remarkable IC_{50} potential in both cases when subjected to the HIV-1 protease subtype C in a chemical reaction, which was comparable to commercially available HIV-1 protease inhibitors. Substantial decrease in the activity of the protease was noted thereby making these novel chemically synthesized peptide inhibitors very attractive as lead compounds in drug discovery. However the major drawback to both types of protease inhibitors, were that they were not effective in eliciting their toxic effect to HIV infected cells *in vitro*.

2.9 Conclusion

In drug design and drug development, adequate model systems have to be introduced in the early stages to avoid loss of promising compounds due to insufficient absorption. For permeation studies, model systems have been established at various levels of complexity from animal models to lipophilic membranes [57]. When choosing a test system there is always a struggle between high throughput with low predictive potential and low throughput with high predictive potential. Cell culture takes an intermediate position within the pyramid complexity of permeation studies. They produce medium to low throughput results but depict prediction reasonably accurately. If an optimized cell based system can be established it will prove to be a vital tool to researchers that are interested in synthesizing new chemical compounds.

However, before screening for absorption properties of a molecule, NCEs have to be able to be fit as "lead candidates". The above mentioned, chemically synthesised HIV inhibitors proved to be effective against the enzyme. In order for this to be established there was a need for a substantial amount of HIV protease to be available to screen the inhibitory potential. As the HI virus is difficult to handle alternate means of isolation is required. Techniques that employ the use of recombinant protein expression using expression vectors in a heterologous system seems to be the most convenient, well understood, reproducible manner that this vital goal is achieved.

The content of this review highlights two key aspects that are critical to the drug development process. The success of newly synthesised HIV protease inhibitors is dependent on its ability to be deemed as lead candidates and if so, its capacity to permeate the GI membrane.
Therefore a need exists for a reproducible technique that measures permeability and also for an optimised method for isolating HIV protease that has good purity.

2.10 References

1. Chaturvedi, P.R., C.J. Decker, and A. Odinecs, Prediction of pharmacokinetic properties using experimental approaches during early drug discovery. *Current Opinion in Chemical Biology*, 2001. **5**(4): p. 452-463.
2. Gibaldi, M., *Phamacokinetics, edn 2. Edited by Gilbaldi M, Perrier D*, 1982, New York: Marcel Dekker, Inc.
3. Logan, C., *Use of Animals for the Determination of Absorption and Bioavailability*, in *Drug Bioavailability*. 2004, Wiley-VCH Verlag GmbH & Co. KGaA. p. 132-154.
4. Wu, C.-Y. and L.Z. Benet, Predicting drug disposition via application of BCS: transport/absorption/elimination interplay and development of a biopharmaceutics drug disposition classification system. *Pharmaceutical research*, 2005. **22**(1): p. 11-23.
5. Volpe, D.A., Application of Method Suitability for Drug Permeability Classification. *Aaps Journal*, 2010. **12**(4): p. 670-678.
6. Stewart, B.H. and Y. Wang, .< i> Ex vivo</i> approaches to predicting oral pharmacokinetics in humans. *Annual Reports in Medicinal Chemistry*, 2000. **35**: p. 299-307.
7. Grass, G.M., Simulation models to predict oral drug absorption from in vitro data. *Advanced Drug Delivery Reviews*, 1997. **23**(1-3): p. 199-219.
8. Quaroni, A. and J. Hochman, Development of intestinal cell culture models for drug transport and metabolism studies. *Advanced Drug Delivery Reviews*, 1996. **22**(1-2): p. 3-52.
9. Le Ferrec, E., et al., In vitro models of the intestinal barrier - The report and recommendations of ECVAM Workshop 46. *Atla-Alternatives to Laboratory Animals*, 2001. **29**(6): p. 649-668.
10. Madara, J.L., *Functional Morphology of Epithelium of the Small Intestine*, in *Comprehensive Physiology*. 2010, John Wiley & Sons, Inc.
11. Madara, J.L., et al., Functional coupling of tight junctions and microfilaments in T84 monolayers. *Am J Physiol*, 1988. **254**(3 Pt 1): p. G416-23.
12. Madara, J.L., D. Barenberg, and S. Carlson, Effects of cytochalasin D on occluding junctions of intestinal absorptive cells: further evidence that the cytoskeleton may influence paracellular permeability and junctional charge selectivity. *J Cell Biol*, 1986. **102**(6): p. 2125-36.
13. Laitinen, L., Caco-2 cell cultures in the assessment of intestinal absorption: Effects of some co-administered drugs and natural compounds in biological matrices. 2006.
14. van de Waterbeemd, H., et al., *Drug Bioavailability: Estimation of Solubility, Permeability, Absorption and Bioavailability*. 2008: John Wiley & Sons.
15. Fearn, R.A. and B.H. Hirst, Predicting oral drug absorption and hepatobiliary clearance: Human intestinal and hepatic in vitro cell models. *Environmental Toxicology and Pharmacology*, 2006. **21**(2): p. 168-178.
16. Hirtz, J., The gastrointestinal absorption of drugs in man: a review of current concepts and methods of investigation. *Br J Clin Pharmacol*, 1985. **19**(2): p. 77S-83S.
17. Hidalgo, I.J., Assessing the absorption of new pharmaceuticals. *Current topics in medicinal chemistry*, 2001. **1**(5): p. 385-401.
18. Pappenheimer, J.R. and K.Z. Reiss, Contribution of solvent drag through intercellular junctions to absorption of nutrients by the small intestine of the rat. *J Membr Biol*, 1987. **100**(2): p. 123-36.
19. Artursson, P., Epithelial transport of drugs in cell culture. I: A model for studying the passive diffusion of drugs over intestinal absorptive (Caco-2) cells. *Journal of pharmaceutical sciences*, 1990. **79**(6): p. 476-82.
20. Artursson, P., A.L. Ungell, and J.E. Lofroth, Selective paracellular permeability in two models of intestinal absorption: cultured monolayers of human intestinal epithelial cells and rat intestinal segments. *Pharmaceutical research*, 1993. **10**(8): p. 1123-9.
21. Ward, P.D., T.K. Tippin, and D.R. Thakker, Enhancing paracellular permeability by modulating epithelial tight junctions. *Pharmaceutical science & technology today*, 2000. **3**(10): p. 346-358.
22. Madara, J.L., Loosening tight junctions. Lessons from the intestine. *Journal of Clinical Investigation*, 1989. **83**(4): p. 1089.
23. Anderberg, E.K., T. Lindmark, and P. Artursson, Sodium caprate elicits dilatations in human intestinal tight junctions and enhances drug absorption by the paracellular route. *Pharmaceutical research*, 1993. **10**(6): p. 857-864.
24. Hayashi, M. and M. Tomita, Mechanistic analysis for drug permeation through intestinal membrane. *Drug Metabolism and Pharmacokinetics*, 2007. **22**(2): p. 67-77.
25. Karlsson, J. and P. Artursson, A new diffusion chamber system for the determination of drug permeability coefficients across the human intestinal epithelium that are independent of the unstirred water layer. *Biochimica Et Biophysica Acta*, 1992. **9**(2): p. 204-10.

26. Anderle, P., Y. Huang, and W. Sadee, Intestinal membrane transport of drugs and nutrients: genomics of membrane transporters using expression microarrays. *European Journal of Pharmaceutical Sciences*, 2004. **21**(1): p. 17-24.
27. Zhang, Y. and L.Z. Benet, The Gut as a Barrier to Drug Absorption: Combined Role of Cytochrome P450 3A and P-Glycoprotein. *Clinical Pharmacokinetics*, 2001. **40**(3): p. 159-168.
28. Artursson, P., K. Palm, and K. Luthman, Caco-2 monolayers in experimental and theoretical predictions of drug transport. *Advanced Drug Delivery Reviews*, 1996. **22**(1–2): p. 67-84.
29. Hunter, J. and B.H. Hirst, Intestinal secretion of drugs. The role of P-glycoprotein and related drug efflux systems in limiting oral drug absorption. *Advanced Drug Delivery Reviews*, 1997. **25**(2-3): p. 129-157.
30. Raviv, Y., et al., Photosensitized labeling of a functional multidrug transporter in living drug-resistant tumor cells. *The Journal of biological chemistry*, 1990. **265**(7): p. 3975-80.
31. Specian, R.D. and M.G. Oliver, Functional biology of intestinal goblet cells. *Am J Physiol*, 1991. **260**(2 Pt 1): p. C183-93.
32. Larhed, A.W., P. Artursson, and E. Bjork, The influence of intestinal mucus components on the diffusion of drugs. *Pharmaceutical research*, 1998. **15**(1): p. 66-71.
33. Lipinski, C.A., et al., Experimental and computational approaches to estimate solubility and permeability in drug discovery and development settings. *Advanced Drug Delivery Reviews*, 1997. **23**(1-3): p. 3-25.
34. Amidon, G.L., et al., A theoretical basis for a biopharmaceutic drug classification: the correlation of in vitro drug product dissolution and in vivo bioavailability. *Pharmaceutical research*, 1995. **12**(3): p. 413-20.
35. Dahan, A.S. and G.L. Amidon, *Gastrointestinal Dissolution and Absorption of Class II Drugs*, in *Drug Bioavailability*. 2009, Wiley-VCH Verlag GmbH & Co. KGaA. p. 33-51.
36. Kerns, E.H. and L. Di, *Permeability*. Drug-Like Properties: Concepts, Structure Design and Methods:from adme to toxicity optimization. 2008. 86-99.
37. Kerns, E.H. and L. Di, *Lipophilicity*. Drug-Like Properties: Concepts, Structure Design and Methods:from adme to toxicity optimization. 2008. 43-47.
38. Kerns, E.H. and L. Di, *Solubility*. Drug-Like Properties: Concepts, Structure Design and Methods:from adme to toxicity optimization. 2008. 56-85.
39. Pagliara, A., et al., Evaluation and prediction of drug permeation. *J Pharm Pharmacol*, 1999. **51**(12): p. 1339-57.
40. Kerns, E.H. and L. Di, *pK(a)*. Drug-Like Properties: Concepts, Structure Design and Methods:from adme to toxicity optimization. 2008. 48-55.
41. Abraham, M.H., et al., Determination of solute lipophilicity, as log P(octanol) and log P(alkane) using poly(styrene-divinylbenzene) and immobilised artificial membrane stationary phases in reversed-phase high-performance liquid chromatography. *Journal of Chromatography A*, 1997. **766**(1): p. 35-47.
42. Abraham, M.H., et al., Connection between chromatographic data and biological data. *J Chromatogr B Biomed Sci Appl*, 2000. **745**(1): p. 103-15.
43. Walters, W.P. and M.A. Murcko, Prediction of 'drug-likeness'. *Advanced Drug Delivery Reviews*, 2002. **54**(3): p. 255-271.
44. Andrews, P.R., D.J. Craik, and J.L. Martin, Functional group contributions to drug-receptor interactions. *Journal of medicinal chemistry*, 1984. **27**(12): p. 1648-57.
45. Muegge, I., S.L. Heald, and D. Brittelli, Simple selection criteria for drug-like chemical matter. *Journal of medicinal chemistry*, 2001. **44**(12): p. 1841-6.
46. Oprea, T.I., Property distribution of drug-related chemical databases. *J Comput Aided Mol Des*, 2000. **14**(3): p. 251-64.
47. MDDR. Accessed on 14/01/2013. Available from: http: / /www.mdli.com.
48. CMC. . Accessed on 16/01/2013. Available from: http: / /www.mdli.com.
49. ACD. Accessed on Available from: http: / /www.mdli.com.
50. Bemis, G.W. and M.A. Murcko, The properties of known drugs. 1. Molecular frameworks. *Journal of medicinal chemistry*, 1996. **39**(15): p. 2887-93.
51. Bemis, G.W. and M.A. Murcko, Properties of known drugs. 2. Side chains. *Journal of medicinal chemistry*, 1999. **42**(25): p. 5095-5099.
52. Wang, J.S., L.H. Lai, and Y.Q. Tang, Structural features of toxic chemicals for specific toxicity. *Journal of Chemical Information and Computer Sciences*, 1999. **39**(6): p. 1173-1189.
53. Lee, C.P., R.L.A. deVrueh, and P.L. Smith, Selection of development candidates based on in vitro permeability measurements. *Advanced Drug Delivery Reviews*, 1997. **23**(1-3): p. 47-62.
54. Kerns, E.H. and L. Di, *Barriers to Drug Exposure in Living Systems*. Drug-Like Properties: Concepts, Structure Design and Methods:from adme to toxicity optimization. 2008. 17-33.
55. Fogh, J., J.M. Fogh, and T. Orfeo, One hundred and twenty-seven cultured human tumor cell lines producing tumors in nude mice. *J Natl Cancer Inst*, 1977. **59**(1): p. 221-6.

56. Pinto, M., et al., enterocyte-like differentiation and polarization of the human-colon carcinoma cell-line caco-2 in culture. *Biology of the Cell*, 1983. **47**(3): p. 323-330.
57. Braun, A., et al., Cell cultures as tools in biopharmacy. *European Journal of Pharmaceutical Sciences*, 2000. **11**: p. S51-S60.
58. Volpe, D.A., Variability in Caco-2 and MDCK cell-based intestinal permeability assays. *Journal of pharmaceutical sciences*, 2008. **97**(2): p. 712-25.
59. Artursson, P. and J. Karlsson, Correlation between oral drug absorption in humans and apparent drug permeability coefficients in human intestinal epithelial (Caco-2) cells. *Biochemical and biophysical research communications*, 1991. **175**(3): p. 880-885.
60. Artursson, P. and R.T. Borchardt, Intestinal drug absorption and metabolism in cell cultures: Caco-2 and beyond. *Pharmaceutical research*, 1997. **14**(12): p. 1655-8.
61. Artursson, P., K. Palm, and K. Luthman, Caco-2 monolayers in experimental and theoretical predictions of drug transport. *Advanced Drug Delivery Reviews*, 2001. **46**(1–3): p. 27-43.
62. Karlsson, J., et al., Paracellular drug transport across intestinal epithelia: influence of charge and induced water flux. *European Journal of Pharmaceutical Sciences*, 1999. **9**(1): p. 47-56.
63. Hidalgo, I.J., T.J. Raub, and R.T. Borchardt, Characterization of the human colon carcinoma cell line (Caco-2) as a model system for intestinal epithelial permeability. *Gastroenterology*, 1989. **96**(3): p. 736-49.
64. Arthur, J.M., The MDCK cell line is made up of populations of cells with diverse resistive and transport properties. *Tissue & Cell*, 2000. **32**(5): p. 446-450.
65. Cho, M.J., et al., the madin darby canine kidney (mdck) epithelial-cell monolayer as a model cellular-transport barrier. *Pharmaceutical research*, 1989. **6**(1): p. 71-77.
66. Irvine, J.D., et al., MDCK (Madin-Darby canine kidney) cells: A tool for membrane permeability screening. *Journal of pharmaceutical sciences*, 1999. **88**(1): p. 28-33.
67. Richardson, J.C.W., V. Scalera, and N.L. Simmons, Identification of 2 strains of mdck cells which resemble separate nephron tubule segments. *Biochimica Et Biophysica Acta*, 1981. **673**(1): p. 26-36.
68. Ungell, A.-L. and P. Artursson, *An Overview of Caco-2 and Alternatives for Prediction of Intestinal Drug Transport and Absorption*, in *Drug Bioavailability*. 2009, Wiley-VCH Verlag GmbH & Co. KGaA. p. 133-159.
69. Rothen-Rutishauser, B., et al., MDCK cell cultures as an epithelial in vitro model: Cytoskeleton and tight junctions as indicators for the definition of age-related stages by confocal microscopy. *Pharmaceutical research*, 1998. **15**(7): p. 964-971.
70. Wang, Q., et al., Evaluation of the MDR-MDCK cell line as a permeability screen for the blood-brain barrier. *International journal of pharmaceutics*, 2005. **288**(2): p. 349-359.
71. Huet, C., et al., Absorptive and mucus-secreting subclones isolated from a multipotent intestinal cell line (HT-29) provide new models for cell polarity and terminal differentiation. *J Cell Biol*, 1987. **105**(1): p. 345-57.
72. Wikman, A., et al., A Drug Absorption Model Based on the Mucus Layer Producing Human Intestinal Goblet Cell Line HT29-H. *Pharmaceutical research*, 1993. **10**(6): p. 843-852.
73. Wikmanlarhed, A. and P. Artursson, cocultures of human intestinal goblet (ht29-h) and absorptive (caco-2) cells for studies of drug and peptide absorption. *European Journal of Pharmaceutical Sciences*, 1995. **3**(3): p. 171-183.
74. Hilgendorf, C., et al., Caco-2 versus Caco-2/HT29-MTX co-cultured cell lines: permeabilities via diffusion, inside- and outside-directed carrier-mediated transport. *Journal of pharmaceutical sciences*, 2000. **89**(1): p. 63-75.
75. Pidgeon, C. and U.V. Venkataram, Immobilized artificial membrane chromatography: supports composed of membrane lipids. *Anal Biochem*, 1989. **176**(1): p. 36-47.
76. Mason, B.P., *High-Throughput Measurement of Physicochemical Properties*, in *Drug Bioavailability*. 2009, Wiley-VCH Verlag GmbH & Co. KGaA. p. 101-132.
77. Lundahl, P. and F. Beigi, Immobilized liposome chromatography of drugs for model analysis of drug-membrane interactions. *Advanced Drug Delivery Reviews*, 1997. **23**(1-3): p. 221-227.
78. Yang, C.Y., et al., Immobilized artificial membranes - Screens for drug membrane interactions. *Advanced Drug Delivery Reviews*, 1997. **23**(1-3): p. 229-256.
79. Zhu, C.Y., et al., A comparative study of artificial membrane permeability assay for high throughput profiling of drug absorption potential. *European Journal of Medicinal Chemistry*, 2002. **37**(5): p. 399-407.
80. Kansy, M., F. Senner, and K. Gubernator, Physicochemical high throughput screening: parallel artificial membrane permeation assay in the description of passive absorption processes. *Journal of medicinal chemistry*, 1998. **41**(7): p. 1007-10.
81. Ruell, J.A. and A. Avdeef, *Absorption Screening Using the PAMPA Approach*. 2004. p. 37-64.
82. Faller, B., Artificial Membrane Assays to Assess Permeability. *Current Drug Metabolism*, 2008. **9**(9): p. 886-892.

83. Wlodawer, A. and J. Vondrasek, Inhibitors of HIV-1 protease: a major success of structure-assisted drug design. *Annu Rev Biophys Biomol Struct*, 1998. **27**: p. 249-84.
84. Sijbesma, R., et al., Synthesis of a fullerene derivative for the inhibition of HIV enzymes. *Journal of the American Chemical Society*, 1993. **115**(15): p. 6510-6512.
85. Kohl, N.E., et al., active human immunodeficiency virus protease is required for viral infectivity. *Proceedings of the National Academy of Sciences of the United States of America*, 1988. **85**(13): p. 4686-4690.
86. McQuade, T.J., et al., a synthetic hiv-1 protease inhibitor with antiviral activity arrests hiv-like particle maturation. *Science*, 1990. **247**(4941): p. 454-456.
87. Seelmeier, S., et al., human immunodeficiency virus has an aspartic-type protease that can be inhibited by pepstatin-a. *Proceedings of the National Academy of Sciences of the United States of America*, 1988. **85**(18): p. 6612-6616.
88. Velazquez-Campoy, A., et al., Protease inhibition in African subtypes of HIV-1. *AIDS Rev*, 2003. **5**(3): p. 165-71.
89. Darke, P.L., et al., Human Immunodeficiency Virus Protease - Bacterial Expression and Characterization of the Purified Aspartic Protease. *Journal of Biological Chemistry*, 1989. **264**(4): p. 2307-2312.
90. Seelmeier, S., et al., Human immunodeficiency virus has an aspartic-type protease that can be inhibited by pepstatin A. *Proceedings of the National Academy of Sciences*, 1988. **85**(18): p. 6612-6616.
91. Hyland, L.J., T.A. Tomaszek Jr, and T.D. Meek, Human immunodeficiency virus-1 protease. 2. Use of pH rate studies and solvent kinetic isotope effects to elucidate details of chemical mechanism. *Biochemistry*, 1991. **30**(34): p. 8454-8463.
92. Brik, A. and C.H. Wong, HIV-1 protease: mechanism and drug discovery. *Organic & biomolecular chemistry*, 2003. **1**(1): p. 5-14.
93. Toh, H., M. Ono, and T. Miyata, Retroviral gag and DNA endonuclease coding sequences in IgE-binding factor gene. 1985.
94. Maputsoe, X., *Impact of L38↑ N↑ L insertions on structure and function of HIV-1 South African subtype C Protease*, 2012.
95. Suguna, K., et al., binding of a reduced peptide inhibitor to the aspartic proteinase from rhizopus-chinensis - implications for a mechanism of action. *Proceedings of the National Academy of Sciences of the United States of America*, 1987. **84**(20): p. 7009-7013.
96. Makatini, M.M., *Design, Synthesis and Screening of Novel PCU-peptide/peptoid Derived HIV Protease Inhibitors*, 2011, University of KwaZulu-Natal, Westville.
97. Navia, M.A., et al., Three-dimensional structure of aspartyl protease from human immunodeficiency virus HIV-1. 1989.
98. Reetz, M., Preparation of novel HIV-protease inhibitors. *Chemical Communications*, 1998(19): p. 2075-2076.
99. Abdel-Rahman, H.M., et al., HIV protease inhibitors: peptidomimetic drugs and future perspectives. *Current medicinal chemistry*, 2002. **9**(21): p. 1905-1922.
100. De Clercq, E., The history of antiretrovirals: key discoveries over the past 25 years. *Reviews in medical virology*, 2009. **19**(5): p. 287-299.
101. Hemelaar, J., et al., Global and regional distribution of HIV-1 genetic subtypes and recombinants in 2004. *Aids*, 2006. **20**(16): p. W13-W23.
102. Wüthrich, K., *NMR in Structural Biology: A Collection of Papers by Kurt Wüthrich*. 1995: World Scientific River Edge, NJ.
103. Bothnerby, A.A., et al., structure determination of a tetrasaccharide - transient nuclear overhauser effects in the rotating frame. *Journal of the American Chemical Society*, 1984. **106**(3): p. 811-813.
104. Makatini, M.M., et al., Pentacycloundecane-based inhibitors of wild-type C-South African HIV-protease. *Bioorganic & medicinal chemistry letters*, 2011. **21**(8): p. 2274-2277.
105. Lee, J., et al., Lignan, sesquilignans and dilignans, novel HIV-1 protease and cytopathic effect inhibitors purified from the rhizomes of< i> Saururus chinensis</i>. *Antiviral research*, 2010. **85**(2): p. 425-428.
106. Makatini, M.M., et al., Synthesis and structural studies of pentacycloundecane-based HIV-1 PR inhibitors: A hybrid 2D NMR and docking/QM/MM/MD approach. *European journal of medicinal chemistry*, 2011. **46**(9): p. 3976-3985.
107. Pawar, S.A., et al., Synthesis and molecular modelling studies of novel carbapeptide analogs for inhibition of HIV-1 protease. *European journal of medicinal chemistry*, 2012. **53**: p. 13-21.
108. Overkleeft, H.S., et al., Design and synthesis of a protein: farnesyltransferase inhibitor based on sugar amino acids. *Tetrahedron letters*, 1999. **40**(21): p. 4103-4106.
109. Risseeuw, M.D., et al., Sugar amino acid based peptide epoxyketones as potential proteasome inhibitors. *Bioorganic Chemistry*, 2010. **38**(5): p. 202-209.

110. Lohse, A., K.B. Jensen, and M. Bols, The first combinatorial library of azasugar glycosidase inhibitors. *Tetrahedron letters*, 1999. **40**(15): p. 3033-3036.
111. Wang, L.-X., et al., Combined chemical and enzymatic synthesis of a C-glycopeptide and its inhibitory activity toward glycoamidases. *Journal of the American Chemical Society*, 1997. **119**(46): p. 11137-11146.
112. Jensen, K.J. and J. Brask, Carbohydrates in peptide and protein design. *Peptide Science*, 2005. **80**(6): p. 747-761.

Chapter 3

RESEARCH RESULTS I

Optimization of the isolation, purification and enzyme activity of HIV-1 protease subtype C

Optimization of the Isolation, Purification and Enzyme Activity of HIV Protease Subtype C

Uraisha Ramlucken[a], Karen Pillay [a] and Patrick Govender [a]
[a] School of Life Sciences, Biochemistry, University of KwaZulu Natal, South Africa

3.1 Abstract

The Human immunodeficiency virus 1 (HIV-1) subtype C is responsible for the majority of infections of patients in Southern Africa. The HIV protease enzyme is one of the targets for anti-retroviral treatment of AIDS because of its pivotal role in the maturation of the virus in the host cell. For target validation of novel HIV protease inhibitors there is a need for the availability of an abundance of this protease. This study reports on an optimized method for the isolation and purification of HIV-1 protease derived from HIV-1 subtype C. It involves the use of a transgenic *E. coli* strain that was engineered to overexpress the native form of the enzyme via inclusion bodies. A stringent method for the isolation, purification and renaturation resulted in the production of highly pure active HIV-1 protease. In an attempt to increase protease yields, an optimised growth strategy was employed. A chemically defined medium with lower glucose content and devoid of essential amino acids of the TCA cycle was used as an alternative to the widely used nutrient rich Luria Bertani (LB) medium. Results indicated an increase of protease yield up to twice the amount thereby making this medium an attractive alternative for increasing biomass and HIV protease production for future research.

3.2 Introduction

The genetic variability of HIV is extensive and because of this it is classified to many types, sub-types and recombinant forms [1, 2]. HIV is divided into two types, the more virulent and easily transmitted, HIV-1 and the less widespread HIV-2, which has a slower transmission and infection rate [3, 4]. HIV-1 is further categorised into nine sub-types: A-D, F-H, J and K. HIV-1 subtype B being well understood and the most prevalent in North America and Western Europe [5]. HIV-1 subtype C (CSA) is responsible for the majority of infections in the sub-Saharan region of Africa with a few cases of subtype A and G being reported [5]. In South Africa HIV-1 subtype C accounts for approximately 95% of infections [6]. It has been widely reported that the structure of these subtypes vary quite considerably and as a result anti-HIV drugs are ineffective due to their genetic diversity.

Research regarding HIV-1 protease is mainly with the enzymes that are isolated from HIV-1 subtype B, but little information is known about HIV protease that is isolated from the subtype C. It has been reported that, although structurally similar these enzymes isolated from different subtypes differ in their catalytic ability and binding capacity to the active site [5, 7, 8]. Furthermore mutations of the subtypes create independent drug resistance [9]. Thereby there is a need for crucial information of the protease that is derived from subtype C to be examined if any progress of its activation is to be made. For this there is a need for an abundance of this enzyme to be available for inhibitor testing and enzymology. Previously HIV protease has been synthesised chemically [10], but a more common method for isolation includes heterologous protease production in a vector system. Generally genetically engineered bacteria are used as vehicles to produce these enzymes as inclusion bodies, so that it can be easily isolated.

Due to the complex nature of HIV and its dangerous infectious capacity, it is one of the most difficult organisms to work with. Thus alternative methods for the study of this specific enzyme need to be considered. *Escherichia coli* (*E. coli*) has been used extensively in the past and currently as vehicles for the expression of heterologous proteins from wild-type organisms that are not easily accessible [11]. Due to the lack of natural selection, the relationship between *E. coli* and the protein produced is directly proportional [12] therefore there is a vast area of interest in creating an environment that enables increased cell density cultures thereby allowing maximum production of recombinant proteins [13-16]. Studies have shown that manipulation of the nutrient content and feeding strategy of *E. coli* can result in an increase of target proteins.

A study by Ido *et al.* [17] created an accessible platform to study HIV-PR using an *E. coli* vector system for easy isolation of the protease. PCR-based methods incorporated with multiple restriction enzyme reactions were used to create a plasmid that expresses the HIV-PR enzyme when transformed into the *E. coli* bacterium [17]. This strategy to clone the HIV-PR gene of the virus was employed taking two vital factors into consideration, namely the codons that favoured highly abundant *E. coli* proteins and more importantly the highly specific restriction sites of the actual gene. The cassette included the 99-residue HIV protease gene, followed by a stop codon with 10 upstream residues. This was then ligated to a plasmid to give rise to a pUC12-HIV-PR plasmid which contains the entire synthetic HIV-1 protease gene. Following this, an expression vector pET-HIV-PR was created to synthesize a 14-kDa precursor which is the fusion of 16 amino acid residues from the expression vector to 109 residues of the HIV sequence [18]. The bacterium was transformed with this vector and the enzyme was expressed.

Using this strategy a plasmid encoding for HIV-1 protease isolated from HIV-1 subtype C (CSA) specifically was generated by Mosebi *et al.* [7] employing a site directed mutagenesis approach to generate the plasmid which was transformed into *E. coli* BL21 (DE3) pLysS cells. The coding region of the protease in the transgenic strain was confirmed by DNA sequencing. Protease was overexpressed as inclusion bodies and purified to yield a product that had a monomeric size of 11 kDa when resolved by sodium dodecyl sulphate-polyacrylamide gel electrophoresis (SDS-PAGE) and an apparent oligomeric molecular mass of 22 kDa [19]. In this study it was shown that the protease isolated from HIV-1 subtype C catalytic activity did not differ from its subtype B wild type, however, it was established that it was more resistant to commercially available anti-protease drugs such as Saquinavir, Ritonavir, Indinavir and Nelfinavir. This confirmed that mutations in the different subtypes created multi-drug resistance. It is therefore imperative that further drug discovery be designed on the subtype specific basis.

This communication describes the optimisation of the above method which was originally derived by the Protein Structure-Function Research Unit (University of the Witwatersrand, Johannesburg, South Africa). To this end we investigated growth medium composition for sustenance of the transgenic *E. coli* strain as an option for increasing HIV protease enzyme production.

3.3 Materials and methods

Chemicals, solvents and media used in this study were of molecular biology grade and purchased from Merck (Pty) Ltd, South Africa unless otherwise stated. Antibiotics were purchased from Melford Laboratories Ltd, South Africa and filter sterilized prior to use.

3.3.1 Strains

Glycerol stocks of transformed *E. coli* BL21 (DE3) pLysS cells containing the plasmid encoding the HIV-1 protease from HIV-1 subtype C (HIV-1 CSA) (containing the mutation Q7K designed to reduce the hypersensitive autolytic site) were a kind gift from Dr Y. Sayed of the Protein Structure-Function Research Unit (University of the Witwatersrand, Johannesburg, South Africa).

3.3.2 Media culturing conditions

Plasmid encoding HIV-1 subtype C protease is expressed as inclusion bodies in *E. coli* BL21 (DE3) pLysS cells. Cells are stored as glycerol stocks with 100 µL of 30% (vol/vol) glycerol (Sigma Aldrich, Germany) and 100 µL of mid-log cultures.

Cells were grown in two different types of media during expression in order to evaluate which medium results in quicker culturing time and higher protein yields. The first medium used was Luria Bertani broth (LB) containing 1% (wt/vol) Trypton, 0.5% (wt/vol) yeast extract and 0.5% (wt/vol) NaCl, supplemented with 100 µg/mL of ampicillin and 35 µg/mL of chloramphenicol. The second medium used was a chemically defined medium (Table 3.1) supplemented with 100 µg/mL of ampicillin,35 µg/mL of chloramphenicol [12].

Table 3.1: Chemically defined media composition with the inclusion of yeast extract (1L)*

Component	Quantity
ATM4S solution	
Ammonium sulphate $(NH_4)_2SO_4$	4 g
Sodium dihydrogen phosphate ($NaH_2PO_4.H_20$)	5.2 g
Di-potassium hydrogen phosphate (K_2HPO_4)	12.5 g
Tri-sodium citrate (Na_3-citrate.$2H_2O$)	0.66 g
Make up with deionised water (18 mΩ) to	295 mL
Glucose solution	
Glucose Monohydrate	1 g
Magnesium sulphate heptahydrate	0.050 g
Make up with deionised water (18 mΩ) to	250 mL
Yeast extract solution	
Yeast Extract	10 g
Make up with deionised water (18 mΩ) to	150 mL
Trace metal stock solution	
Na-EDTA	20.1 g/L
$FeCl_3.6H_2O$	16.7 g/L
$ZnCl_2$	0.13 g/L
$CoCl_2.6H_2O$	0.18 g/L
$NaMoO_4.2H_2O$	0.13 g/L
$CaCl_2$	0.50 g/L
$CuSO_4.5H_2O$	0.16 g/L
H_3BO_3	0.28 g/L
$MnCl_2.2H_2O$	0.11 g/L
Remove from stock solution	2 ml

*Combine 295,250, 150 and 2 ml of respective solutions and bring up to 1 L with deionised water (18 mΩ).

3.3.3 Overexpression and extraction of HIV-PR

3.3.3.1 Overexpression of protease using recombinant *E .coli*

E. coli cells harbouring the plasmid DNA were retrieved from glycerol stocks (100 µL cells in 100 mL media) and cultivated in LB broth medium supplemented with 100 µg/mL of ampicillin and 35 µg/mL of chloramphenicol. Cells were incubated at 37 °C with shaking at 250 rpm in an Infors HT Multitron environmental shaker (United Scientific, South Africa). The overnight culture was diluted 100-fold by adding 10 mL to 990 mL to fresh LB broth or chemically defined media, both supplemented with ampicillin (100 µg/mL) and chloramphenicol (35 µg/mL) in 5 L Erlenmeyer flasks. Cultures were incubated at 37 °C with shaking at 180 rpm until an optical density of the mid-log phase of growth was obtained. Optical density was monitored using an AnalytikJena Specord 210 spectrophotometer at 600 nm (OD_{600}). Induction of the overexpression of the HIV-PR CSA was achieved by adding isopropyl β-D thiogalactoside (IPTG) (Sigma Aldrich, Germany) to a final concentration of 0.4 mM and induction was allowed to proceed for a further 4 hours.

Once the incubation period for overexpression of the protease was complete, the cells were collected in pre-sterilized centrifuge tubes and pelleted via centrifugation at 5000 x g for 12 minutes using an Avanti centrifuge J-26XPI (Beckman Coulter, USA) at 4 °C. The pellet was re-suspended in 50 mL of cold extraction buffer [10 mM Tris, 2 mM EDTA and 1 mM PMSF (Sigma Aldrich, Germany) (added fresh) pH 8.0]. Both pellet and supernatant was analysed by SDS-PAGE even though the protease was within inclusion bodies that was present in the pellet.

3.3.3.2 Protease extraction from recombinant *E. coli*

Cells were retrieved from -20 °C storage by thawing to 4 °C with ice. The volume was brought up to 100 mL with extraction buffer and treated with 10 mM magnesium chloride followed by homogenization with a Bio-Gen PRO200 homogenizer (ProScientific, USA) until a uniform solution was obtained. Maintaining a 4 °C environment, DNAse1 (Thermo Scientific, South Africa) at a concentration of 5 µg/mL was added whilst stirring to remove all traces of DNA. Once the viscosity of the mixture was decreased, 20 mL aliquots of the solution was transferred to sterile Falcon tubes and exposed to vigorous sonication at 4 °C (5x 1 minute cycles) using a Qsonica (Q125) probe sonicator (USA). This was essential for the disruption of cells. Cells were

then pelleted by centrifugation at 25000 x *g* for 30 minutes at 4 °C, and were re-suspended in extraction buffer containing 1% (v/v) Triton X-100. This homogenization and centrifugation steps were performed twice and the pellet was re-suspended first in ice cold extraction buffer and then in solubilisation buffer (10 mM Tris-HCL, 8 M urea, 2 mM DTT; pH 8) at room temperature. The supernatant was then collected after final centrifugation for further purification. Due to the highly concentrated amount of urea present in the solubilisation buffer, the protease conforms to its unfolded form which is needed for column purification [17].

3.3.4 HIV Protease Purification

3.3.4.1 Column purification

The solution containing the HIV-PR was loaded onto a diethylaminoethyl (DEAE) anion exchange column (BIO-RAD laboratories, USA) that was initially regenerated with ten volumes of NaCl and then equilibrated with an equal volume of solubilisation buffer at room temperature. Fractions (5 mL) were collected and subjected to the Bradford assay (Sigma Aldrich, Germany) in order to determine presence of the protease. Fractions containing the protease were pooled and formic acid (Sigma Aldrich, Germany) was added to a final concentration of 25 mM, resulting in the reduction of the pH to approximately 3.0. The acidic environment created resulted in exclusion of all non-aspartyl protein contaminants as they are not acidic in nature, and also aided in the refolding of the protease.

In conjunction with the Bradford method, ultraviolet (UV) spectrophotometric analysis at a wavelength of 280 nm using an automated microplate reader (Synergy HT) from BioTek Instruments was used to elucidate the fractions that contained the protease. The wells that contained the peak of the curve were pooled for further purification. In addition to the Bradford assay, all fractions were further calorimetrically analysed by determining the intensity of the colour formed using a wavelength of 595 nm [20]. The highest intensity fractions were pooled for further protein purification. Final pooled fractions were stored at 4 °C in order to precipitate protein contaminants. Following an overnight incubation period, the precipitated contaminants were removed by centrifugation at 15 000 x g for 30 minutes at 4 °C.

3.3.4.2 Protein folding

HIV-1 protease refolding was conducted by extensive dialysis (~18 hours, fresh buffer was introduced every 6 hours) into 10 mM formic acid at 4 °C using Slide-A-Lyzer dialysis cassettes G2 (Thermo Scientific, South Africa) with a 10 kDa cut off, and then against the storage buffer (10 mM sodium acetate, 1 mM NaCl and 1 mM DTT, pH 5.0).The dialysis buffers were hundred times the volume of the sample and dialysis yielded a 11 kDa protein precursor [17]. The folded protease was concentrated to a final volume of ~5 mL using Vivaspin 20 concentration tubes (Sartorius stedim biotech, USA) and stored at -20 °C.

3.3.5 Confirmation of HIV protease expression

3.3.5.1 Sodium dodecyl sulphate-polyacrylamide gel electrophoresis (SDS-PAGE)

Confirmation of gene expression and subsequent purification of the protease enzyme was performed using SDS-PAGE. This technique uses electrophoresis to separate proteins by molecular weight and samples can be visually analysed by the size of the bands produced on the gel [21].

Mini-Protean TGX™ Any kD (2-250) precast gels were purchased from BIO-RAD laboratories (USA) and were employed for this study. These precast tris-glycine-extended (TGX) gels that are a novel modified version of the Laemmli system for separation of proteins [21], with advantages such as a more stable matrix, much higher resolution, and a time-saving ease of application. Laemmli sample buffer, tris-glycine-SDS (10x) running buffer and the PAGE electrophoresis system were also purchased from BIO-RAD (USA). PageBlue™ protein staining solution containing Coomassie brilliant blue G-250 dye was purchased from Thermo Scientific (South Africa). PageRuler™ unstained protein ladder (Thermo Scientific, South Africa) ranging in size from 10 kDa to 200 kDa, and was used as the reference molecular weight ladder.

Buffers and samples were prepared as shown in Table 3.2 as per manufacturer's instructions. Sample (20 µL) and protein ladder (10 µL) were loaded to the gel which was set up in the PAGE system. Electrophoreses was conducted in 1x running buffer (tris-glycine-SDS) at a constant voltage of 120 V until the bands ran to approximately 1 cm away from the bottom of the gel (approximately 1 hour). Gels were then stained overnight with PageBlue™ staining solution with continuous shaking at 20 rpm at room temperature. Gels were then washed three times using 18 mΩ deionised water with submergence intervals of 10 minutes, to remove all traces of the stain.

The gels were then viewed using Syngene G:box gel documentation system (Vacutec, South Africa).

Table 3.2: Preparation of buffers and samples for SDS-PAGE

	SDS PAGE components		
	Sample(µl)	**Running Buffer(mL)**	**Protein Ladder(µl)**
Sample	10	-	-
Laemmli sample buffer	10	-	-
Tris-glycine-SDS (10X)	-	100	-
Deionized water (18 mΩ)	-	900	-
PageRuler^{TM} Unstained Protein Ladder	-	-	10
Total volume	20	1000	10

3.3.5.2 Determination of protein concentration

To determine the concentration of the purified HIV-PR CSA, UV spectrophotometric analysis was conducted at the standard protein absorbance wavelength of 280 nm using an AnalytikJena Specord 210 spectrophotometer. Final concentration of protein was calculated by implementation of the Beer-Lamberts law:

$$A = \varepsilon cl$$

Equation 1

where A represents the absorbance of the solution at a wavelength of 280 nm (λ_{280}), ε is the molar extinction coefficient ($M^{-1}cm^{-1}$) at λ_{280}, c is the molar concentration of the absorbing solution, and l is the path length of the light passing through the solution (cm). A value of $11800M^{-1}cm^{-1}$ was used for molar extinction coefficient [22].

The protein concentration was determined by diluting the protein sample four times with 10 mM sodium acetate buffer. The absorbance reading was taken at λ_{280} and λ_{340}. The protein was diluted progressively until a ten times dilution was obtained, and the absorbance read after each dilution. The 10 mM sodium acetate buffer was used as the blank. The λ_{340} for each dilution was subtracted from the 280 nm absorbance for each dilution. This value was then corrected for the

buffer. A plot of protein fraction against absorbance was generated and the slope was divided by the extinction coefficient to obtain the protein concentration.

3.3.6 Determination of HIV-PR CSA Protease Activity

The catalytic potential of the HIV-PR CSA was evaluated by its specific activity which is regarded as one of the most effective means to determine the enzyme's purity [23]. This study monitored the catalytic hydrolysis of a chromogenic peptide substrate Lys-Ala-Val-Nle-p-nitro-Phe-Glu-AlaNle-NH_2 which mimics the conserved KARVL/AEAM cleavage site between the capsid protein and nucleocapsid (CA-p2) within the Gag poly-protein precursor [24, 25]. The chromogenic peptide was a kind gift from Dr M. Makatini (School of Chemistry, University of KwaZulu-Natal, Durban, South Africa).

The hydrolysis of this substrate was monitored at 300 nm, using an AnalytikJena Specord210 spectrophotometer. The reaction mixture contained 50 μM of both substrate and protein (within range of 100-200nM) and 50 mM sodium acetate buffer (pH 5, with 0.1 M sodium chloride), at a final volume of 120 μL. Protease hydrolytic activity was measured by monitoring the relative decrease in absorbance at 300 nm over a time period of 3 minutes at room temperature.

3.4 Results

3.4.1 Optimization using different media

3.4.1.1 Growth curve analysis of media

In this study two different types of media for the overexpression of the protease were evaluated. LB and a specialized chemically defined media (Table 3.1), both supplemented with antibiotics, were used to determine which media resulted in higher cell density thus potentially leading to a greater yield of overexpressed protein product [12]. A standard growth curve of the bacteria was analysed using the optical density as a measurement of cell density. Optical density at 600 nm measures the turbidity of the media and hence provides an indication of the concentration of cells in the media at a specific point. Growth curve analysis was also required for the time of induction for protein expression.

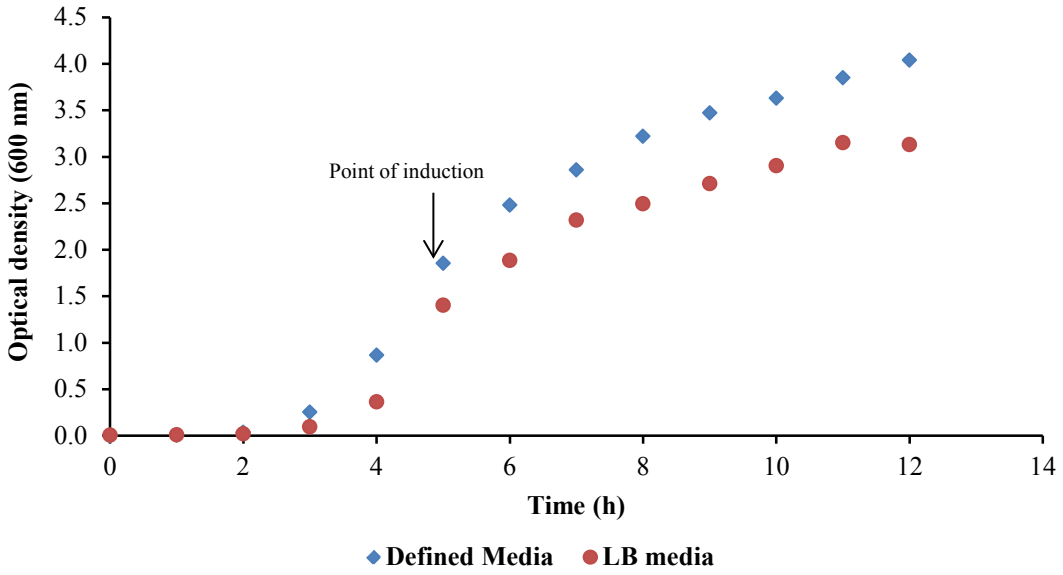

Figure 3.1 *E. coli* BL21 (DE3) growth patterns in chemically defined and LB media monitored for 12 hours. OD_{600} of samples were evaluated every hour. Samples were done in duplicate Growth curves were done concurrently with starter cultures being inoculated from an overnight culture (18 hours of growth). Point of induction of expression occurred at 5 hours.

3.4.1.2 Purification using different media

Recombinant *E. coli* was grown in the two different types of media and subsequent protein expression, extraction and purification was performed. Protein determination using SDS-PAGE (Figure 3.2) and protein concentration were evaluated using spectrophotometric analysis (Table 3.3). Supernatant was collected during centrifugation steps in the extraction phase of the protease so that the loss of enzyme could be traced to a specific part of the method in the event of unsuccessful protease purification. Filtrate during the concentration steps in the above method was also analysed for traces of lost protease.

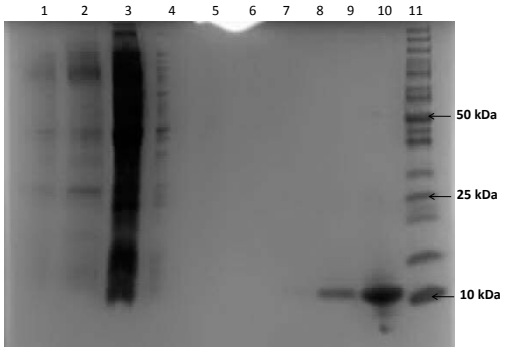

Figure 3.2 TGX-gel with purified protease product. Lanes 2 and 3 contains supernatant of different centrifugation steps during extraction; Lanes 4 to 8 contains filtrate from the concentration step of purification. Lanes 9 and 10 contain HIV-PR CSA grown in LB and chemically defined media respectively. Lane 11 contains molecular weight marker (PageRuler^{TM} Unstained Protein Ladder). Lanes 1 to 6 were required to establish if the protease was present at different steps of the protease extraction and purification technique.

As can be seen in Figure 3.2, expected results were achieved. Protease was evident by a band size confirmation of 11 kDa and the absence of protease in the filtrate and supernatant confirms that protease purification was successful. The abundance of protein present in lanes 2 and 3 is evidence of cell proteins extracted during extraction of the inclusion body. Filtrate analysis indicated that the concentration of the protease was achieved. Protease purified from *E. coli* grown in chemically defined medium (Lane 10) resulted in twice the amount of protease produced compared to *E. coli* grown in LB medium (Lane 9);which was further confirmed by protein determination using Beer Lamberts law (Table 3.3).

Table 3.3: Protein determination using different growth media

Medium	Protein concentration (µM)
Luria Bertani (LB)	22.1
Chemically defined	44.2

3.4.2 Optimization of the HIV-PR isolation and Purification method using methods other than the Bradford assay

Purification of the protease was optimized by methods described above, where analysis omitted the Bradford assay. All fractions collected from the DEAE column were analysed spectrophotometrically at 280nm to determine which eluted fractions contained the protease (Figure 3.3).

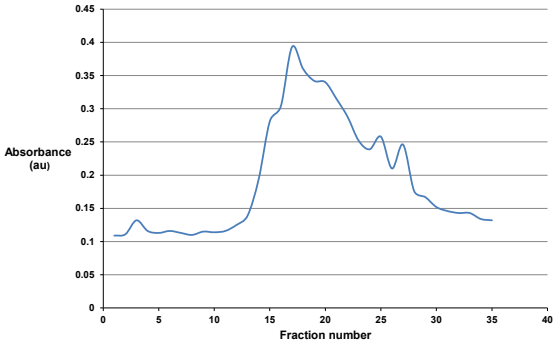

Figure 3.3 Absorbance of each 5 ml column fraction at 280 nm. Fractions 15-25 was considered for further purification, this was further divided into two groups, namely "tail" which utilized fractions 15-18 and 21-25, and "peak", which contained fractions 18-21.

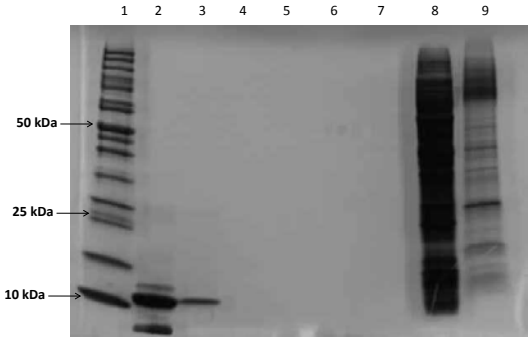

Figure 3.4 Purified protease using UV spectrophotometric analysis for monitoring fractions eluted by the column. Lane 1 contains the molecular weight marker (PageRuler^{TM} Unstained Protein Ladder). Lane 2 contains "peak" of the fraction curve. Lane 3 contains the "tail" of the peak. Lanes 4-7 contains filtrates of tails and peaks. Lanes 8 and 9 contains the supernatant of the centrifugation steps during the extraction of the protease.

Table 3.4: Concentration of protease in the different pooled fractions

Sample	Concentration (µM)
"peak"	44.2
"tail"	10.5

Results in Figure 3.4 show an impure protease with multiple bands present in the "Peak" fraction. This did not concur with results obtained from purification using the Bradford assay.

3.4.3 Final HIV-PR CSA purification

Optimized methods were finally used to isolate and purify HIV-1 protease subtype C. Comparison of the results (Figure 3.5) show that the UV spectrophotometric analysis of the pooled fractions eluted by the column was not reliable due to multiple band formation and loss of protease due to their presence in the "tail" fraction. The Bradford assay deemed a more suitable method for detection as it resulted in one band indicating a pure protease.

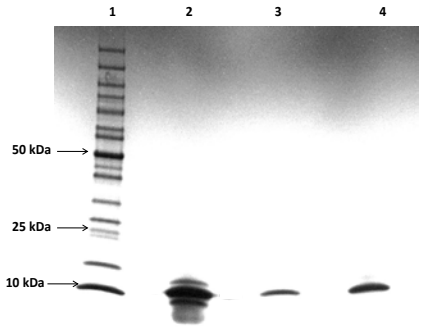

Figure 3.5 Pure HIV-1 protease subtype C derived from different methods. Lane 1 contains the protein molecular weight marker (PageRuler^{TM} Unstained Protein Ladder). Lanes 2 and 3 contain the "peak" and "tail" fraction respectively of the curve after spectrophotometric analysis. Lane 4 contains the pure HIV-PR CSA obtained when the Bradford assay was used for analysis.

Table 3.5: Concentration of protease present in the samples used to generate Figure 3.5

Sample	Concentration (µM)
Lane 2	68.2
Lane 3	8.4
Lane 4	62.8

Table 3.5 confirmed the above conclusion that using the Bradford assay is more suited then spectrophotometric analysis as maximum protease yield occurs from all pooled fractions. Therefore the final method for optimisation includes use of the chemically defined media but fraction testing using the Bradford assay from the original method.

3.4.3.1 Protease conformation

Besides size confirmation, further verification of the purified product was performed by UV spectrum analysis of the purified product. This resulted in the expected spectral data (Figure 3.6). The amino acids that make up proteins absorb ultra violet light very strongly and are commonly identified at 280 nm. Mostly the aromatic residues, tryptophan, tyrosine and cysteine, are responsible for absorbance at this wavelength and these are found in abundance in the 99 amino acid HIV-1 protease [10, 26]. The spectral data revealed a peak at 280 nm confirming the presence of a protein. For reasons unexplained, the HIV protease spectral scan has a characteristic “shoulder” approximately at 290 nm as seen in Figure 3.6, this can be an additional confirmation for a pure protease. This result correlates to data represented in studies of this nature [27].

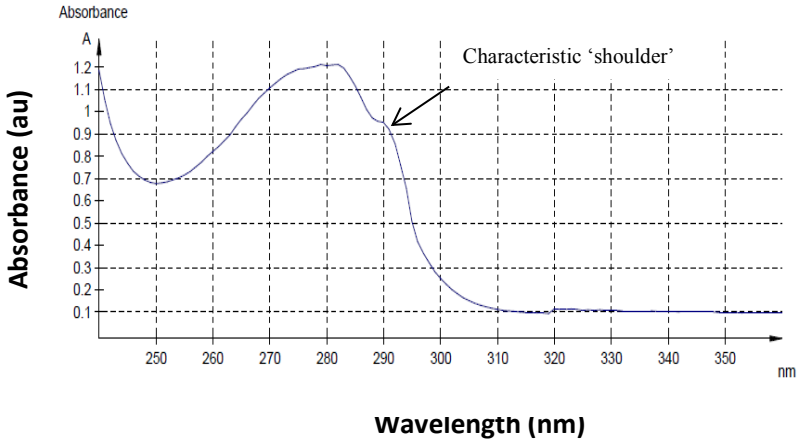

Figure 3.6 Absorption spectrum of HIV-1 South African subtype C protease. The experiment was carried out at 20 °C in 10 mM sodium acetate buffer, 0.1 M sodium chloride, pH 5.0. The spectrum illustrates the absorption of ultra-violet light by the aromatic amino acids' side chains of the protein at 280 nm wavelength

3.4.3.2 Enzyme specificity

The purified protease catalytic activity was tested by the use of a chromogenic substrate. As stated in the Materials and Methods section above, this substrate mimics the cleavage site of the peptide substrate of HIV-1 protease. The hydrolysis of this substrate is an indication of the HIV-PR CSA's ability to specifically bind to the substrate as well as cleave it appropriately. The protease hydrolytic activity was monitored be the break-down of the chromogenic substrate resulting in the decrease of absorbance.

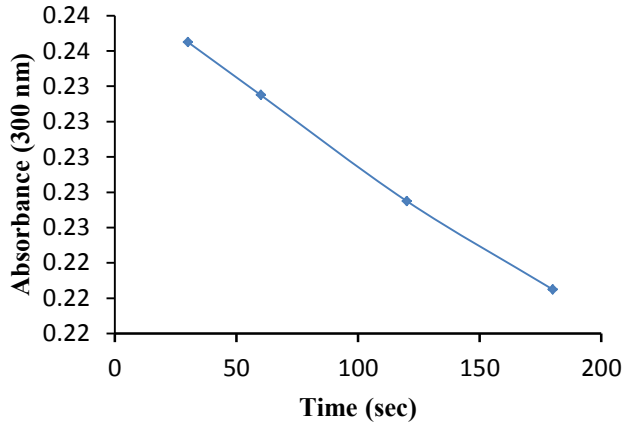

Figure 3.7 Enzyme specificity and catalytic activity using a standard reaction with a chromogenic peptide as the enzyme's substrate. The experiment was performed over 3 minutes and was done in triplicate. As time increased, the absorbance of the substrate decreased which indicates substrate hydrolysis.

3.5 Discussion

Growth potential of *E. coli* harbouring transgenes for the expression of recombinant proteins is an area of interest for many reasons, particularly the impact of high cell density cultivation on recombinant proteins [28-30]. Manipulating the feeding strategy of these organisms alters their protein output in various ways. The general consensus of the nutrient control is that a decrease in glucose content eliminates the probability of over-feeding and excessive by-product formation which may inhibit growth. It has been previously established that the depletion of certain key amino acids encourages increased recombinant protein expression, this is due to the fact that these proteins are not composed of the essential amino acids that are required by the indigenous *E. coli* proteins [12, 31-33].

Studies indicate that recombinant bacteria undergo metabolic stress when expressing transgenes thereby leading to low cell density and low protein concentration. However, it has been proven that using a chemically defined media that contains certain additives of the tricarboxylic acid (TCA) cycle, relieves the burden of metabolic stress caused on the bacterium therefore enhancing optimal heterologous protein synthesis [12, 32, 33].

In a study conducted by Ramcahran *et al.* [12], recombinant *E. coli* was used to express the protease xylanase using additives from the TCA cycle to recreate the effects of metabolic stress. This study applies the same principle by adding TCA intermediates such as citrate to the growth medium (Table 3.1) in order to enhance the generation of HIV-PR CSA. From the results, it can be seen that using a similar chemically defined medium promoted greater cell biomass which generated a higher protease concentration (Figures 3.1, 3.2 and Table 3.3). The growth curve employed in this study was also used to determine the point in the growth phase where induction of expression is required. The point of induction of expression is of great importance because the inducer if used untimeously would significantly contribute to metabolic stress of the bacterium and ultimately low heterologous protein expression. The best time for induction is the mid-log phase which was established to be after 5 hours (Figure 3.1). The optimization strategy employing chemically defined medium clearly indicates a higher protease yield.

The Bradford assay has been used for decades for the detection of the concentration of proteins. It is a colorimetric reaction that presents as a blue chromophore upon binding of proteins. Although specific for proteins, the major drawback of this assay is that it does not discriminate between different types of proteins, thus contaminating proteins can be included when using this assay [20]. Spectrophotometric analysis at 280 nm is a also another means for detecting proteins in a sample [34].

In an attempt to optimize HIV protease yield all fractions eluted from the anion exchange column was monitored using both the Bradford and spectrophotometric methods. However, pooling of selected eluted fractions using spectrophotometric analysis yielded an impure protease as the end product (Figure 3.4 and 3.5). Although the expected protease band size was evident, multiple band formation was also evident (Figure 3.4 and 3.5). Furthermore the fractions consisted of the "tail" generated small quantities of protease. Conversely when the monitoring of fractions was performed using the Bradford assay, a pure protease product was achieved (Figure 3.5). Based on the above results, it is proposed that the Bradford method be employed as a preferred method to pool fractions so as to ensure greater and more purified protease preparations.

These findings are supported by the proposed method by Mosebi *et al.* [7], and correlate with data obtained from Naicker *et al.* and Maputsoe *et al*.[35, 36]. HIV-1 PR was clearly evident by the visualization of a single 11 kDa band upon SDS-PAGE analysis (Figure 3.5). Ultra-violet spectrophotometric analysis of the renaturated and purified protease (Figure 3.6) confirmed the presence of the protease since the unique finger print "shoulder" between 285 and 295 nm is a characteristic that is indicative of the HIV-1 protease [36, 37].

HIV-1 protease catalyses the hydrolysis of peptide bonds with high sequence selectivity and catalytic proficiency. The protease sequence selectivity ranges from a select few amino acid sequences each with the characteristic scissile bond (Chapter 2, section 2.8.3). The substrate was designed to accommodate these specific amino acids and is therefore a suitable candidate for selective binding. Therefore, further evidence of a pure and active HIV-PR CSA was exhibited in an enzyme specific reaction and it was revealed that the specific activity of the enzyme was a positive enzyme reaction. Since HIV protease cleaves the specific sequence of the chromogenic peptide [24, 25, 38] thus decreasing its absorbance, it is safe to assume that the enzyme has the efficient ability to selectively cleave the substrate (Figure 3.7).

3.6 Conclusion:

As discussed above, an optimised method for HIV-1 protease derived from HIV-1 subtype C production was established. This was achieved using a known method to isolate and purify the enzyme, and with the use of a specialized feeding strategy. Combination of these optimisation strategies yielded an 11 kDa pure protein precursor from the overexpressed gene of interest. The protease generated also displayed expected catalytic activity. It was established that growth of the transgenic strain in a chemically defined media yielded a 100% increase in HIV-1 PR production.

The HIV-1 protease produced in this study was subsequently used to chemically test the enzyme inhibition capabilities of novel cage and sugar-based peptide HIV protease inhibitors that were synthesised at this institute. Further work on the structure, dynamics, and modification, etc., of HIV-1 protease isolated from HIV-1 subtype C can now be possible due to the optimization strategy for HIV-1 protease production.

3.7 Acknowledgements

This study was made possible through financial support from the National Research Foundation and the research facilities were provided by the University of KwaZulu-Natal.

3.8 References

1. Charneau, P., et al., Isolation and envelope sequence of a highly divergent HIV-1 isolate: definition of a new HIV-1 group. *Virology*, 1994. **205**(1): p. 247-253.
2. Subbarao, S. and G. Schochetman, Genetic variability of HIV-1. *Aids*, 1996. **10**: p. S13-24.
3. Reeves, J.D. and R.W. Doms, Human immunodeficiency virus type 2. *Journal of General Virology*, 2002. **83**(6): p. 1253-1265.
4. Parkin, N.T. and J.M. Schapiro, Editorial review Antiretroviral drug resistance in non-subtype B HIV-1, HIV-2 and SIV. *Antiviral therapy*, 2004. **9**: p. 3-12.
5. Velazquez-Campoy, A., et al., Protease inhibition in African subtypes of HIV-1. *AIDS Rev*, 2003. **5**(3): p. 165-71.
6. Foulkes, J.E., et al., Role of invariant Thr80 in human immunodeficiency virus type 1 protease structure, function, and viral infectivity. *Journal of virology*, 2006. **80**(14): p. 6906-6916.
7. Mosebi, S., et al., Active-site mutations in the South african human immunodeficiency virus type 1 subtype C protease have a significant impact on clinical inhibitor binding: kinetic and thermodynamic study. *J Virol*, 2008. **82**(22): p. 11476-9.
8. Mosebi, S., *Kinetic and thermodynamic characterization of the South African subtype C HIV-1 protease: implications for drug resistance*, 2007, Faculty of Science, University of the Witwatersrand.
9. Velazquez-Campoy, A., et al., Catalytic efficiency and vitality of HIV-1 proteases from African viral subtypes. *Proceedings of the National Academy of Sciences*, 2001. **98**(11): p. 6062-6067.
10. Nutt, R.F., et al., Chemical synthesis and enzymatic activity of a 99-residue peptide with a sequence proposed for the human immunodeficiency virus protease. *Proceedings of the National Academy of Sciences*, 1988. **85**(19): p. 7129-7133.
11. Balbas, P. and F. Bolivar, *[3] Design and construction of expression plasmid vectors in escherichia coli*, in *Methods in Enzymology*, V.G. David, Editor. 1990, Academic Press. p. 14-37.
12. Ramchuran, S.O., O. Holst, and E.N. Karlsson, Effect of postinduction nutrient feed composition and use of lactose as inducer during production of thermostable xylanase in Escherichia coli glucose-limited fed-batch cultivations. *Journal of Bioscience and Bioengineering*, 2005. **99**(5): p. 477-484.
13. Karlsson, E.N., O. Holst, and A. Tocaj, Efficient production of truncated thermostable xylanases from Rhodothermus marinus in Escherichia coli fed-batch cultures. *Journal of Bioscience and Bioengineering*, 1999. **87**(5): p. 598-606.
14. Gombert, A.K. and B.V. Kilikian, Recombinant gene expression in Escherichia coli cultivation using lactose as inducer. *Journal of Biotechnology*, 1998. **60**(1–2): p. 47-54.
15. O'Connor, G.M., F. Sanchez-Riera, and C.L. Cooney, Design and evalution of control strategies for high cell density fermentations. *Biotechnology and Bioengineering*, 1992. **39**(3): p. 293-304.
16. Ramírez, D.M. and W.E. Bentley, Fed-batch feeding and induction policies that improve foreign protein synthesis and stability by avoiding stress responses. *Biotechnology and Bioengineering*, 1995. **47**(5): p. 596-608.
17. Ido, E., et al., Kinetic studies of human immunodeficiency virus type 1 protease and its active-site hydrogen bond mutant A28S. *Journal of Biological Chemistry*, 1991. **266**(36): p. 24359-24366.
18. Ido, E., et al., kinetic-studies of human-immunodeficiency-virus type-1 protease and its active-site hydrogen-bond mutant A28S. *Journal of Biological Chemistry*, 1991. **266**(36): p. 24359-24366.
19. Mosebi, S., et al., Active-site mutations in the South African human immunodeficiency virus type 1 subtype C protease have a significant impact on clinical inhibitor binding: Kinetic and thermodynamic study. *Journal of virology*, 2008. **82**(22): p. 11476-11479.
20. Bradford, M.M., A rapid and sensitive method for the quantitation of microgram quantities of protein utilizing the principle of protein-dye binding. *Analytical Biochemistry*, 1976. **72**(1–2): p. 248-254.
21. Laemmli, U.K., Cleavage of structural proteins during assembly of head of bacteriophage-t4. *Nature*, 1970. **227**(5259): p. 680-&.
22. Polgar, L., Z. Szeltner, and I. Boros, Substrate-Dependent Mechanisms in the Catalysis of Human Immunodeficiency Virus Protease. *Biochemistry*, 1994. **33**(31): p. 9351-9357.
23. Wharton, C.W. and R. Eisenthal, *Molecular enzymology*. 1981: Blackie.
24. Makatini, M.M., et al., Pentacycloundecane-based inhibitors of wild-type C-South African HIV-protease. *Bioorganic & medicinal chemistry letters*, 2011. **21**(8): p. 2274-2277.

25. Pawar, S.A., et al., Synthesis and molecular modelling studies of novel carbapeptide analogs for inhibition of HIV-1 protease. *European journal of medicinal chemistry*, 2012. **53**: p. 13-21.
26. Darke, P.L., et al., Human Immunodeficiency Virus Protease - Bacterial Expression and Characterization of the Purified Aspartic Protease. *Journal of Biological Chemistry*, 1989. **264**(4): p. 2307-2312.
27. Mpye, K.L., *Structural and functional effects of an I36TT insertion in the South African HIV-1 subtype C protease*, 2010.
28. Lee, S.Y., High cell-density culture of< i> Escherichia coli</i>. *Trends in biotechnology*, 1996. **14**(3): p. 98-105.
29. Choi, J.H., K.C. Keum, and S.Y. Lee, Production of recombinant proteins by high cell density culture of< i> Escherichia coli</i>. *Chemical Engineering Science*, 2006. **61**(3): p. 876-885.
30. Shiloach, J. and R. Fass, Growing< i> E. coli</i> to high cell density—A historical perspective on method development. *Biotechnology advances*, 2005. **23**(5): p. 345-357.
31. Ramérez, D.M. and W.E. Bentley, Enhancement of recombinant protein synthesis and stability via coordinated amino acid addition. *Biotechnology and bioengineering*, 1993. **41**(5): p. 557-565.
32. Harcum, S.W. and W.E. Bentley, Heat-shock and stringent responses have overlapping protease activity in Escherichia coli. *Applied biochemistry and biotechnology*, 1999. **80**(1): p. 23-37.
33. Ramchuran, S., et al., Production of heterologous thermostable glycoside hydrolases and the presence of host-cell proteases in substrate limited fed-batch cultures of Escherichia coli BL21 (DE3). *Applied microbiology and biotechnology*, 2002. **60**(4): p. 408-416.
34. Aitken, A. and M. Learmonth, *Protein determination by UV absorption*, in *The protein protocols handbook*. 1996, Springer. p. 3-6.
35. Naicker, P., et al., Structural insights into the South African HIV-1 subtype C protease: impact of hinge region dynamics and flap flexibility in drug resistance. *Journal of Biomolecular Structure and Dynamics*, 2012(ahead-of-print): p. 1-11.
36. Maputsoe, X., *Impact of L38↑ N↑ L insertions on structure and function of HIV-1 South African subtype C Protease*, 2012.
37. Todd, M.J., N. Semo, and E. Freire, The structural stability of the HIV-1 protease. *Journal of Molecular Biology*, 1998. **283**(2): p. 475-488.
38. Makatini, M.M., et al., Synthesis and structural studies of pentacycloundecane-based HIV-1 PR inhibitors: A hybrid 2D NMR and docking/QM/MM/MD approach. *European journal of medicinal chemistry*, 2011. **46**(9): p. 3976-3985.

Chapter 4

RESEARCH RESULTS II

Membrane permeability of chemically synthesized novel HIV-1 protease inhibitors

Membrane Permeability of Chemically Synthesized Novel HIV-1 Protease Inhibitors

Uraisha Ramlucken[a], Karen Pillay [a] and Patrick Govender [a]
[a] School of Life Sciences, Biochemistry, University of KwaZulu Natal, South Africa

4.1 Abstract

Potential lead compounds must comprise of good biopharmaceutical properties to avoid becoming an additional failed statistic in the multi-billion dollar drug discovery industry. The intestinal permeability of a lead compound is one such property which is particularly important and needs to be established early in drug development. Two individually designed chemically synthesized HIV-1 protease peptide inhibitors, the first, attached to a sugar sequence and the second, a cage moiety, were presented as lead anti-retroviral candidates. These were reported to have excellent inhibitory activity against the enzyme as well as increased binding capacity to the substrate-binding site. However, their failure to be effective against HIV positive T-cells prompted the bioavailability hypothesis in that the newly designed inhibitors were incapable of permeating the cellular membrane. In this study the passive permeability potential of these HIV-1 protease inhibitors were determined employing two globally accepted models. The first was a cell-based method using Madin Darby canine kidney cells strain 1 (MDCK1) that differentiate into a membrane that mimics the human gastrointestinal tract (GIT) and the second a cell-free system, parallel artificial membrane permeability assay (PAMPA) that utilized specialised lipid membranes that serve as the intestinal barrier. Results from the first model were inconclusive as growth of an intact membrane was not reliably achieved. However, results obtained from PAMPA analysis suggest that these inhibitors possessed poor passive permeability properties. Data from the permeability assays of the peptide inhibitors were compared to three drugs (antipyrine, metoprolol and caffiene) that belong to the list suggested by the FDA for validation of *in vitro* permeability methods. A comparison of the passive permeation profile of the inhibitors versus Saquinavir a commercially available HIV-1 protease inhibitor was established which confirmed our hypothesis. In addition, Lucifer yellow, a dye that is impermeable via passive diffusion was used as a negative control to verify permeability properties of these novel peptide inhibitors.

4.2 Introduction

In the words of Steve Jobs; *"Ideas are worth nothing unless executed. They are just a multiplier. Execution is worth millions."* This can be said for many new upcoming drugs that are flooding the pharmaceutical industry at present. Good lead candidates that have efficient potency against their targets are failing to elicit their response in the human system. This can be attributed to very low bioavailability after oral administration because of poor biopharmaceutical properties such as the in ability to be absorbed by the gastrointestinal tract, thus making it a poor candidate as a potential therapeutic agent.

This seems to be the case for two types of novel chemically synthesized HIV-1 protease subtype C inhibitors. As described in chapter 2 section 2.9.5, the first inhibitor was presented as a peptide attached to a polycyclic cage compound, more specifically a pentacycloundecane (PCU) moiety; and the second inhibitor as sugar moieties attached to potent peptide inhibitors i.e. a glycopeptide. It was predicted that both of these modifications would increase inhibition of the protease as well as the binding capacity to the enzyme. When tested against the pure enzyme that was generated in chapter 3, these inhibitors were effective in inhibiting activity of the enzyme in test tube based reactions. The highest IC_{50} value for the cage moiety was reported to be 0.078 ± 0.0035 μM [1]. For the glycopeptide, the highest IC_{50} value reported was 1090 ± 0.02 nM [2]. Furthermore both these inhibitors were able to increase the binding affinity of the inhibitor to the target enzyme. These characteristics thus made them promising candidates as novel HIV protease inhibitors.

However, when exposed to a whole-cell system using HIV-1 infected MT4 cells, both these peptide inhibitors were found to be ineffective [2, 3]. In an attempt to determine the degree of potency, these inhibitors were tested via the in vitro assay referred to as the XTT assay. In this assay the cytotoxic effects of the inhibitor are tested by means of cell proliferation, which is indicative of the potency of the inhibitors. The basic principle of the assay is to detect cell viability with the use of a reduction reaction of the tetrazolium dye, XTT, which turns orange in colour, when reduced by mitochondrial oxidoreductases of the cell [4]. Thereby a decrease in colour would be indicative of a decrease in cell proliferation that may be the result of cellular necrosis or apoptosis. With the use of HIV-1 infected cells, a positive result using the HIV protease inhibitors would be a colourless end-product i.e. cell death representing effective inhibitors as they would be able to prevent virus proliferation. Unfortunately these in vitro tests gave a negative result as none of the tested inhibitors, from both studies, indicated any cell death and/or a decrease in cell proliferation.

These contradicting results gave rise to several questions. One immediate concern was the assessment of the compound's intestinal permeability properties which, as stated previously, is a critical factor used to establish if a compound can be considered as a potential therapeutic agent or not. The aim of this chapter is thus to assess the permeation ability of these novel chemically synthesized entities and to determine if this is one of the contributing factors to its inability to inhibit HIV infected cells. If the compound in unable to enter the cell, it will not be able to elicit its response. The inhibitors that displayed the highest inhibitory potential against the pure enzyme reported in both studies were considered for this chapter. This included the cage derivative peptide, that mimicked the natural occurring HIV-1 protease substrate, the PCU-EAIS (IC_{50} = 0.078 ± 0.0035 μM) [3] and the sugar-based peptide that contained the D-gluco-Val-Ala-COOH sequence (IC_{50} = 1.09 ± 0.02 μM) [2].

4.3 Materials and methods

4.3.1 Cell line

Madin Darby canine kidney cells strain 1 (MDCK1) were purchased from the American Type Culture Collection (ATCC) at passage number 1. These cells were delivered as a cryopreserved culture.

4.3.2 Cell culture

4.3.2.1 Growth and maintenance of cell line

Tissue culture procedures were performed under sterile conditions in a class II bio-safety cabinet (*Esco* Airstream®, South Africa) .Cells were routinely maintained in a Dulbecco's modified eagle medium (DMEM) containing 4.5 g/L glucose and L-glutamine. Fully constituted media was prepared by supplementing DMEM with 25 mM4-(2-hydroxyethyl)-1-piperazineethanesulfonic acid (HEPES) (Merck, South Africa), 1 mM sodium pyruvate (Sigma Aldrich, Germany), 0.1 mg/ml penicillin (100 units/mL)/streptomycin (100 mg/mL) and 10 % (v/v) heat-inactivated fetal bovine serum (FBS) (Biochrom, South Africa). All media components, antibiotics and tissue culture reagents were purchased from Lonza (Switzerland) unless otherwise stated.

MDCK1 cells (passage 1) taken out of cryopreservation was thawed in a 37 °C water bath for four minutes with periodic agitation. Thereafter, the cell suspension was transferred to a sterile 12 ml tissue culture tube (Greiner bio-one, Netherlands), pelleted by centrifugation at 200 x g for 3 minutes and then re-suspended in 3 ml of fully constituted media. The cell suspension was then added to a sterile 25 cm^2 filtered flask and brought up to a total volume of 5 ml with fully constituted media.

Cells were initially cultured in 25 cm^2 flasks and then transferred to a 75 cm^2 flask upon reaching a rapid growth rate. Cell culture was thereafter performed using the bigger flasks with a total volume of 15 ml media. Cells were cultivated in the standard tissue culture environment of 5% CO_2 with 90% relative humidity at 37 °C via an IR water jacket CO_2 incubator (Nuaire, United Kingdom). At approximately 85-90% confluence, spent media was removed and the attached cells were washed with 10 ml of pre-warmed 1x phosphate buffered saline (PBS). Cells were exposed to 1.5 ml trypsin solution [0.25% (w/v) trypsin and 0.1% (w/v) ethylenediaminetetraacetic acid (EDTA)] for approximately 60 seconds and viewed under an Olympus CKX41 inverted microscope until cells had completely rounded off. The trypsin solution was then removed and trace amounts of trypsin was inactivated by aspirating 10 ml of fully supplemented DMEM into the flask. Cells were then evenly distributed to new flasks containing fresh media to yield a split ratio of 1:5. To aid attachment of the cells to the flask, 7.5 µL of poly-D-Lysine (Sigma Aldrich, Germany) was added. Subculturing was performed on a weekly basis to build working and stock cultures.

4.3.2.2 Cryopreservation of cell line

Stock cultures were prepared by washing confluent cells with 1x PBS, trypsinising and dislodging them as described above. Cells were re-suspended in Biofreeze (Biochrom, South Africa) or alternatively in 0.9 ml DMEM with 0.1 ml DMSO which was added as a cyroprotectant and transferred to 2 ml cryogenic vials (Greiner bio-one, Netherlands). Cryovials were then placed in a Nalgene® Mr Frosty freezing receptacle containing 250 ml isopropanol (Sigma Aldrich, Germany) and stored at -80 °C for a minimum of four hours to allow for slow freezing. Stock cultures were then stored in liquid nitrogen.

4.3.3. Mycoplasma detection and prevention

Although mycoplasma are known to be the smallest (0.3-0.8 µm) self-replicating bacteria, they are not harmless bystanders and cannot be ignored [5]. Fastidious in their nature, these bacterial infections in mammalian cell culture pose a serious and detrimental threat, having multiple effects on cell culture and having a significant influence on the results of scientific studies [6]. The significance of mycoplasma infection to this study is important because an infection could result in detrimental effects on monolayer formation. Thereby continuous testing for mycoplasma was vital.

4.3.3.1 Mycoplasma detection

Cell culture contamination with mycoplasma cannot be visibly detected and their effects on cell metabolism, morphology and growth are often only noticed when it is too late. Whilst there are several reported methods for the detection and subsequent elimination of these bacteria [7-10], a quick simple method is favoured in most tissue culture laboratories. The MycoAlert™ mycoplasma detection kit offers a convenient method for detection of viable mycoplasma in cell culture. This assay is a selective biochemical test that exploits the activity of certain mycoplasmal enzymes which are released once the viable mycoplasma cells are lysed. In a bioluminescent reaction the conversion of ADP to ATP is catalysed via the mixture of mycoplasma enzymes and the MycoAlert™ substrate. The resultant luminescence emitted, which measures the amount of ATP generated, is directly proportional to the quantity of mycoplasma present.

Mycoplasma detection was performed using the MycoAlert™ mycoplasma detection kit as per manufacturer's instructions and the MycoAlert™ assay control set was utilized to verify results. All luminescence readings were done via an automated microplate Reader (Synergy HT from BioTek Instruments) using sterile flat-bottomed white walled 96-well plates (Thermo Scientific, South Africa). All kit components, additives, antibiotics and reagents were purchased from Lonza (Switzerland) unless otherwise stated.

Results were analysed and interpreted as follows:

$$\text{Ratio} = \frac{\text{Reading B}}{\text{Reading A}}$$

Equation 2

Where Reading A is the measurement of ATP before substrate is added, and Reading B is the ATP measured after the substrate is added. The ratio obtained determines if the cell culture was contaminated by mycoplasma (Table 4.1).

Table 4.1: Interpretation of mycoplasma detection results

Ratio	Interpretation
<0.9	Negative for mycoplasma
0.9-1.2	Borderline: Quarantine cells and retest in 24 h
>1.2	Positive for mycoplasma

4.3.3.2 Mycoplasma prevention

As a precautious measure to ensure that mycoplasma infection did not occur cell lines were treated with a specialized dual purpose antibiotic MycoZAP^{TM} plus-CL which is designed to kill mycoplasma that are present and prevent contamination from occurring. Furthermore it is a broad spectrum antibiotic therefore it can be used in place of penicillin/streptomycin. Cells were subcultured with this antibiotic and if cell cultures were infected they were immediately discarded. Further prevention procedures included strict aseptic technique using 70% (v/v) ethanol and additional specialized disinfectant LookOut® mycoplasma erase (Sigma Aldrich, Germany) to ensure mycoplasma free cultures.

4.3.4 Cell-based trans-membrane assay to determine membrane permeability

As stated in chapter 2 section 2.7.1, specialized cell lines have a remarkable ability to grow as differentiated monolayers that are able to mimic the human intestinal epithelial membrane and are widely used for screening of the absorptive potential of lead candidates [11, 12]. Irvine *et al*. [13] has made the MDCK cell line a tool for this purpose as it provides a major advantage over the extensively used Caco-2 cell line in that a shorter monolayer cultivation time is required. Following this, the current study utilized the MDCK1 cell line.

4.3.4.1 Seeding of cells

Mycoplasma free MDCK1 cells were passaged 23 times and stored as stock cultures. Cells were then taken out of cryopreservation, subcultured and passage number 25 was used for all cell membrane assays to standardize the method. Cells were taken out of cryogenic vials and subcultured in DMEM supplemented with 20% (v/v) FBS, 25 mM HEPES (Merck, South Africa), 0.1% (v/v) sodium pyruvate (Sigma Aldrich, Germany), and with 0.08% (v/v) MycoZAP^{TM} as described above. At approximately 70-80% confluency, cells were counted to ascertain optimum seeding densities. This was done using a Countess^{TM} automated cell counter (Invitrogen^{TM}, USA). Equivalent amounts of cell suspension and 0.4% trypan blue stain were mixed (Invitrogen^{TM}, USA) before being transferred to a Countess^{TM} cell counting chamber slide (Invitrogen^{TM}, USA). Cells were then counted and various seeding densities were assessed by plating them on Costar® 12 well Transwell® plates (Corning Incorporated, USA).These polycarbonate coated inserts contain a 0.4 μm pore size, with a surface area of 1.12 cm^2. Poly-D-lysine at a concentration of 2 mM was added to each insert to aid in attachment.

Prior to seeding, the plates were pre-incubated with culture medium for 1 hour at 37 °C to improve initial attachment of cells. Once cells were plated, plates were incubated at 37 °C, at relative humidity of 95% and in 5% CO_2. Media was changed every 24 hours.

4.3.4.2 Determination of monolayer integrity

Although there are many ways to measure the integrity of cell monolayers on membrane support, the two most common means are trans-epithelial electrical resistance (TEER) and Lucifer yellow (LY) rejection.

4.3.4.2.1 Trans-epithelial electrical resistance (TEER)

It has been long standing that monolayer integrity can be determined by the measurement of the trans-epithelial electrical resistance (TEER) across the monolayer. This method measures the amount of resistance there is to the current that is passed across the cell monolayer. It is affected by the pore size and density of the membrane and it qualitatively measures cell monolayer health and quantitatively measures cell confluence [14]. The principle of this test is that the higher the TEER value obtained, the more intact the membrane is, because the membrane has a greater resistance to an electrical current. Electrical measurements across monolayers have been used by most studies that involve monolayer production to measure the integrity of the monolayer being studied [15-17] Integrity formed on trans-well membranes is determined using a special probe that is read by a volt meter.

For this study a Millicell®-ERS (Millipore, United Kingdom) volt-ohm meter with a MERSSTX01 electrode was used. The volt-ohm meter and electrodes were tested and equilibrated as per manufacturer's instructions before use. All TEER evaluation was done under sterile conditions.

Spent media was removed from each well and washed three times with sterile 1x Hank's balanced salt solution (HBSS) (Life Technologies, USA) supplemented with 10 mM HEPES at a pH of 7.4. Thereafter 500 µL and 1 ml HBSS (1x HBSS, 10 mM HEPES, pH7.4) were added to the apical and basolateral sides of the membrane respectively. Cells were then incubated for 30 minutes at 37 °C, at a relative humidity of 95% and in 5% CO_2 so that the monolayer can be equilibrated before TEER measurements. The electrodes were initially sterilized by submerging them in 70% ethanol for 15 minutes, followed by air drying for 15 seconds. Before every TEER measurement, electrodes were equilibrated for 15 minutes in HBSS. An average of six TEER readings was taken for each well.

TEER values were calculated as follows:

$$\mathrm{TEER} = (\mathrm{R} - \mathrm{R_{Blank}}) \times \mathrm{A}$$

Equation 3

Where R is equal to the resistance in ohms (Ω) of the insert that contains a cell membrane, R_{blank} is the resistance in ohms of an insert that is devoid of plated cells, and A is equivalent to the surface area of the insert, which in this study is 1.12 cm^2. Final TEER values are expressed as $\Omega \cdot cm^2$.

4.3.5 Parallel Artificial Membrane Permeability Assay (PAMPA)

Since its discovery in 1998, PAMPA has emerged as the superior method in terms of useful tools for assessing permeability of NCEs. Over the years, many researchers have demonstrated correlation of PAMPA to the intestinal permeability of drugs, thus this assay is currently used by many pharmaceutical companies as well as research institutes to predict the passive transport capability of new chemical entities [18-22]. Permeability is expressed as Log P_e which represents the effective permeability of a compound.

4.3.5.1 Preparation of reference drugs

Four controls as listed in Table 4.2 were used for this study. All controls are commercially available drugs and were procured from Sigma Aldrich (Germany). Based on literature, three of the four drugs are easily absorbed by the human intestine, and are commonly used as efficient positive controls for drug passive transcellular permeation studies [13]. The fourth compound, Saquinavir, was chosen since it is a commercially available HIV-1 protease inhibitor, and it would thus be interesting to compare its permeability to the two novel inhibitors.

Table 4.2: The absorption properties of reference drugs

Drug	Fa (%)	Reported Log P_e values
Antipyrine	100	-4.90
Metoprolol	95	-6.47
Caffeine	100	-6.55
Saquinavir	30	NA

[Fa] is the fraction absorbed obtained from literature [13, 18, 23]. Data for Saquinavir is obtained from Hoffmann LaRoche [24].

Lucifer yellow was used both as a negative control as well as a membrane integrity marker. All controls were prepared immediately prior to use by dilution in 1 x PBS. Three different pH levels (pH 5.5, 6.8, and 7.4) were used for each compound because they represent the varying pH of the small intestine which is the major site of absorption. The assay was performed using each compound at a final concentration of 100 µM.

4.3.5.2. Generation of standard curves

Before performing the PAMPA, generation of a standard curve was necessary so that the assay could be analysed. All drugs were freshly diluted with transport buffer (1 x PBS, pH 5.5, 6.8 and 7.4) to concentrations of 20, 40, 60, 80, 120 and 150 µM. Saquinavir, was first dissolved in 100 % (v/v) DMSO before dilutions were prepared since it is not soluble in aqueous solution. The final dilution of Saquinavir was in 1 x PBS (pH 7.4) containing 8% (v/v) DMSO. Each compound at the different concentrations were plated (100 µL) into 96-well flat bottomed micro-titre plates (Costar®, USA) and analysed using the microplate reader. First the optimal UV absorption wavelength of each drug was ascertained by scanning using a broad range of the electromagnetic spectrum (200-500 nm). Thereafter standard curves were generated using the optimum single wavelength, λ_{max}.

The Lucifer yellow standard curve was generated in a similar manner using the same dilutions, except that analysis was performed via fluorescence at an excitation wavelength of 480 nm and emission wavelength of 530 nm. Fluorescence is measured in relative fluorescence units (RFU) and analysis was done using solid black-walled 96-well flat bottomed micro-titre plates. For the Saquinavir experiment Lucifer yellow was also dissolved in 8% DMSO so as to keep assay conditions standard.

4.3.5.3 Preparation of test compounds

The two test compounds used were the chemically synthesized HIV-1 protease inhibitors that either contained a glycopeptide (Inhibitor 1) or a cage moiety (Inhibitor 2). These compounds were a kind gift from Dr S. Pawar and Dr M. Makatini respectively, from the Department of Chemistry, University of KwaZulu-Natal, South Africa. These two inhibitors were chosen as they portrayed the best inhibitory potential in *in vitro* enzymatic assays using purified HIV-1 protease.

Both these inhibitors are completely soluble in an aqueous solution, therefore they were prepared by dilution in 1 x PBS at different pH values (pH 5.5, 6.8 and 7.4). Inhibitors were subjected to optimum UV wavelength analysis and standard curves were generated as described above PAMPA was performed using each compound at a final concentration of 100 µM.

4.3.5.4 PAMPA analysis

PAMPA was performed using the Millipore multiscreen assay. PAMPA components were purchased from Millipore (United Kingdom) and included the multiscreen filter plates (MAIPN4550, Millipore) and the multiscreen 96-well acceptor plate (MSSACCEPTOR, Millipore). The artificial membrane solution used in this study was PAMPA lipid blend 1 which was purchased from Avanti® Polar Lipids, Inc. (USA). These lipids were stored at -20 °C when not in use. The transport buffer utilized was PBS which was purchased from Lonza, Switzerland. All PAMPA procedures were done in a sterile environment using a class II bio-safety cabinet. PAMPA was performed using the lipid-PAMPA with the multiscreen® filter plates protocol from Millipore [25].

The artificial membrane solution, PAMPA lipid blend 1was transferred to glass containers with Teflon caps using filtered polypropylene tips (Axygen, USA) and stored in 50 µL aliquots. On the day of use, an aliquot was brought up to room temperature from -20 °C storage without the aid of artificial heat. This lipid mixture was pre-treated by sonication with a bath sonicator for 5 minutes until the lipid mixture approached the clarity of water.

To each well of the donor plate, 5 µL of PAMPA lipid blend 1 was added carefully making sure that the membrane was not pierced. This was left to stand for 5 minutes. After the application of the artificial membrane, 150 µL of drug-containing donor solution (drugs dissolved in PBS) was added to each well of the donor plate. The acceptor plate contained 300 µL of aqueous PBS in each well. The donor plate was then placed onto the acceptor plate to form a “sandwich” making sure that the underside of the membrane was in contact with the buffer in all wells. The plate was then incubated in a humidity controlled environment at room temperature for 16 hours. This was achieved using a sealed container with wet towels which also avoided evaporation.

After the incubation period, buffer in the acceptor plate was transferred to sterile 96-well flat bottomed micro-titre plates (Costar®, USA) and analysed for the presence of sample via UV spectrophotometric means using a microplate reader. Thereafter drug solutions were made up to their respective theoretical equilibrium concentrations, i.e. the resulting concentration obtained from combining the donor and acceptor solutions, and similarly analysed. The permeability rates were calculated from the below equation as reported by Faller *et al.* [26]:

$$\mathrm{LogPe} = \mathrm{Log}\left\{C \cdot - \ln\left(1 - \frac{[\mathrm{drug}]_{\mathrm{Acceptor}}}{[\mathrm{drug}]_{\mathrm{Equlibrium}}}\right)\right\} \text{ where } C = \left(\frac{V_D \cdot V_A}{(V_D + V_A)\mathrm{Area} \cdot \mathrm{time}}\right)$$

Equation 4

Table 4.3: Variables used to calculate $LogP_e$

Term	Definition	Notes
V_D	Volume of donor compartment	Expressed in cm^3, 150 µL = 0.15 cm^3
V_A	Volume of acceptor compartment	Expressed in cm^3, 300µL = 0.30 cm^3
Area	Active surface area of membrane	Defined as membrane area × porosity. For the membrane in the MultiScreen Permeability Filter Plate, area = 0.24cm^2 × 100%; or 0.24 cm^2
Time	Incubation time for the assay	Expressed in seconds, 1 h = 3600 seconds
$[drug]_{acceptor}$	Concentration of compound in the acceptor compartment at the completion of the assay	The absorbance of the sample as recorded by the microplate reader
$[drug]_{equilibrium}$	Concentration of compound at theoretical equilibrium	The absorbance of the equilibrium sample as recorded by microplate reader

PAMPA is able to determine if a compound has high, low or moderate permeability; depending on the effective permeability ($LogP_e$) obtained. The standard analogy is that if a compound has a $LogP_e$ value less than -5.00 it is considered as a highly permeable drug, conversely a value that is greater than -5.00 is indicative of a low permeable drug [27].

Statistical analysis was performed using the One-way Analysis of Variance (ANOVA) and Tukey-Kramer Multiple comparisons test (GraphPad InStat version 3 for Windows XP, U.S.A) and results were considered significantly different if p values were less than 0.05.

Percentage transport across the artificial membrane was calculated as follows:

$$\%\,\mathrm{T} = 100 \times {\mathrm{ABS}_{\mathrm{Acceptor}}}/{\mathrm{ABS}_{\mathrm{Equilibrium}}}$$

Equation 5

Where $\mathrm{ABS}_{\mathrm{Acceptor}}$ and $\mathrm{ABS}_{\mathrm{Equilibrium}}$ are the absorbance obtained from the acceptor wells and theoretical equilibrium respectively. Permeation was ranked as low, medium or high based on the %T values of <2%, 2–5% and >5%, respectively. The calculated value for %T was subsequently used to project the percent fraction absorbed (Fa) in humans, based on an established correlation model:

$$\mathrm{Fa} = 100 \times [1 - \mathrm{EXP} \times (-\mathrm{R} \times \%\mathrm{T})]$$

Equation 6

Where Fa is fraction absorbed, %T is PAMPA percentage transport and R is the regression coefficient (R=0.85) [25].

4.3.6 Determination of the integrity of PAMPA membrane

4.3.6.1 TEER measurements

As stated previously, trans-epithelial electrical resistance (TEER) is one of the most common means of determining the integrity of a membrane. PAMPA membrane integrity was evaluated using the TEER procedure as described in section 4.3.4.2.1, however, for this analysis the surface area was 0.24 cm^2 and the buffer used was PBS instead of HBSS. A TEER reading of over 300 $\Omega \cdot cm^2$ for PAMPA membranes is indicative of an intact membrane.

4.3.6.2 Lucifer yellow (LY) rejection

The other means of determining if a membrane is intact is by Lucifer yellow rejection. Lucifer yellow is a florescent dye used for a wide variety of applications in many cell research areas. Its key property is that it is easily visible in many cell based experiments. It was engineered in 1978 by Walter W. Stewart [28] and it changed the dynamics of drug permeability testing immensely. Lucifer yellow passes through cell monolayers by means of passive paracellular diffusion (through the spaces of the cell) and is not readily permeable. Thus it cannot pass through monolayers where tight junctions between cells are maintained, such as the MDCK1 cell line. In membrane permeability studies, LY is used as a membrane integrity marker with a higher percentage being retained indicative of a more intact membrane.

LY passage was done via the method described by Millipore [29]. For quantification of LY transport, it is important to create standard curves and this was done as described in section 4.3.6.3. Lucifer yellow was treated as a control drug and retention was tested in the same manner as that of the other drugs in the assay. Lucifer yellow passage was calculated as follows:

$$\%\text{LY passage} = \left[\frac{\text{RFU}_{\text{Test}} - \text{RFU}_{\text{Blank}}}{\text{RFU}_{\text{Equilibrium}} - \text{RFU}_{\text{Blank}}}\right] \times 100$$

Equation 5

Where $RFU_{(test)}$ is the fluorescence measured in the acceptor plate, $RFU_{(blank)}$ is the fluorescence measured in a blank well and $RFU_{(equilibrium)}$ is the theoretical equilibrium calculated which is the combination of both acceptor and donor wells.

Lucifer yellow passage of 5% and below is a good indication of an intact membrane.

4.4 Results

4.4.1 Cell growth and maintenance

It was established that the MDCK1 cell line grows at an exponential rate therefore a high split ratio was required. Cells were subcultured routinely as described above, however, in studies regarding cell culture a major cause for concern in mycoplasma infection. Thereby cultivation of initial passages included routine testing for the presence of mycoplasma.

4.4.2 Mycoplasma detection assay

Cell lines were tested for mycoplasma using the MycoAlert™ mycoplasma detection kit. The results indicated that initial passages of cells were negative for mycoplasma (Table 4.4). The validity of the test was confirmed using the MycoAlert™ control set, where the MycoAlert™ positive control and assay buffer served as the positive and negative control respectively. In addition, a sample of mycoplasma-free cells from a neighbouring laboratory was tested to validate test reagent viability.

Table 4.4: Mycoplasma detection results of initial cultures

Sample	Ratio*
Negative Control	0.3586
Positive Control	14.154
Passage 1	0.1269
Passage 2	0.6350
Passage 3	0.145
Cells from neighbouring lab	0.4253

* <0.9 = mycoplasma free, 0.9-1.2 = Borderline contamination with mycoplasma, >1.2 = mycoplasma contamination

The initial mycoplasma detection analysis revealed that cultures tested at early passage numbers were mycoplasma-free (Table 4.4). To maintain this environment routine monitoring for mycoplasma was employed and the exposure to the strong antibiotic, MycoZap™, aided in the maintenance of mycoplasma-free cultures (Figure 4.1).

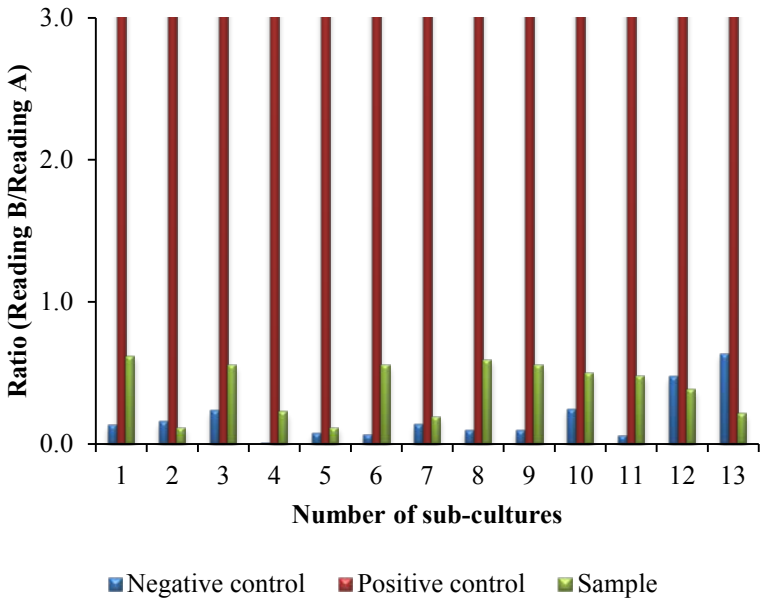

Figure 4.1 The ratio obtained from the MycoAlert™ assay after each subculture of MDCK1 cells in DMEM containing MycoZAP™ plus-CL antibiotic. Assay buffer was used for the negative control and the MycoAlert™ positive control was employed to validate the test. A ratio over three was obtained for all positive controls used for each test at each subculture, the use of three as minimum was depicted so a clear indication of a negative result for mycoplasma is noticed.

4.4.3 Cell based assay to determine permeability of novel inhibitors

4.4.3.1 TEER

According to literature, an intact membrane is represented by optimum TEER value above 200 Ω·cm^2 when using the MDCK cell line. These values correlate to studies using this cell line for permeability testing [30, 31]. However it should also be noted that Irvine *et al*.[13] reported TEER values of 173 (±51) Ω·cm^2 for intact membranes. The theoretical time for monolayer formation is between 5-7 days from seeding of cells [11, 31].

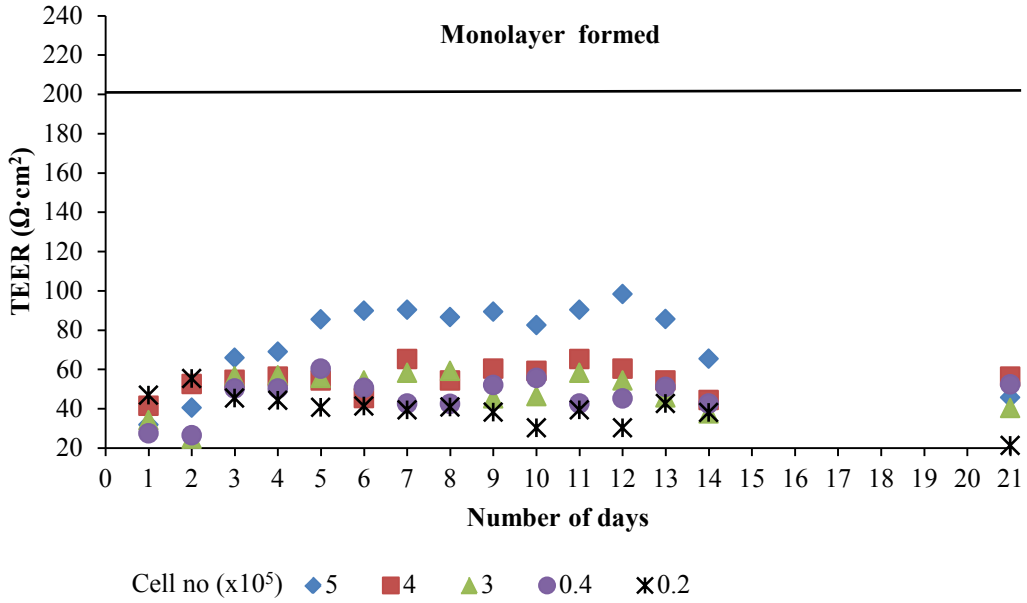

Figure 4.2 TEER values of low cell numbers 2 x 10^4, 4 x 10^4, 3 x 10^5, 4 x 10^5 and 5 x 10^5 cells/cm^2 was used in order to determine the optimal cell seeding density. TEER was observed over 21 days. Results are depicted as an average of three independent determinations and six resistance values were taken into account for each well. Each experiment was done with two cell-free wells that served as the control well (blank).

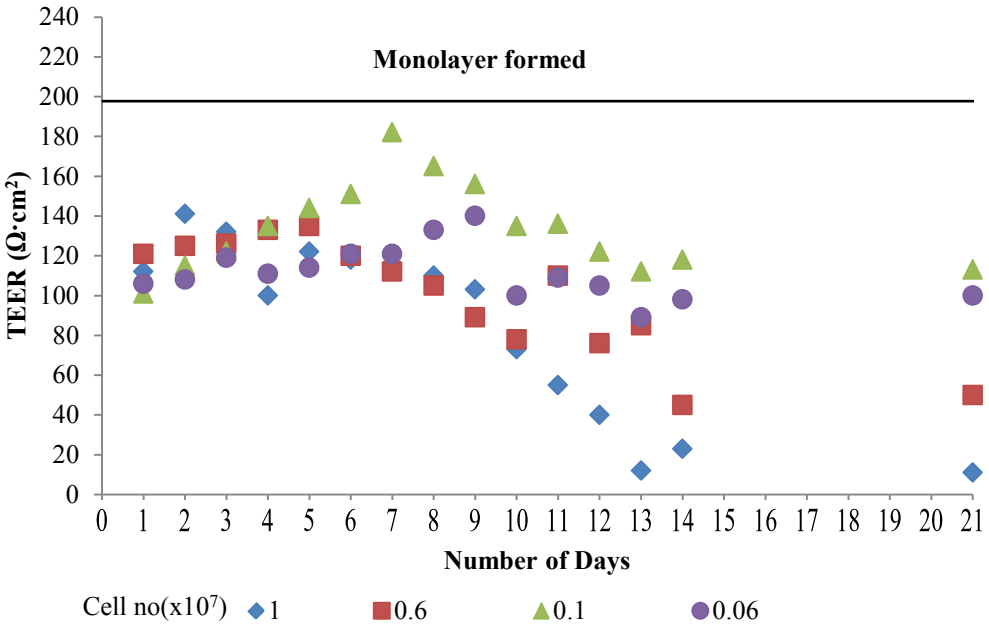

Figure 4.3 TEER values of high cell numbers 6 x 10^5, 1 x 10^6, 6 x 10^6 and 1 x 10^7 cells/cm^2 was used in order to determine the optimal cell seeding density. TEER was observed over 21 days. Results are depicted as an average of three independent determinations and six resistance values were taken into account for each well. Each experiment was done with two cell-free wells that served as the control well (blank).

Theoretically a maximum of 7 days should be sufficient to observe monolayer formation. TEER readings were recorded on a daily basis for 7 consecutive days, but an intact monolayer was not evident. Taking into consideration that laboratory culture conditions differ in different environments and that cell monolayer formation is dependent on the culture conditions, cells were incubated and monitored for a further 7 days to establish if our laboratory conditions required an extended growth period. However, this did not result in expected TEER values. It was however, observed, that using higher cell densities yielded values closer to the expected TEER value but intact monolayers did not develop, even after an extended growth period for all cell densities (Figure 4.2 and 4.3). Data obtained from the cell density experiments showed that the most suited cell number was 1 x 10^6 cells/cm^2 (Figure 4.3) because at this density the highest TEER value of 180 ± 45 was obtained. According to a study by Irvine *et al.* this TEER value would have been sufficient for an intact monolayer [13], however, this value was not reproducible.

Figure 4.4 Partial monolayer formations of MDCK1 cells after 21 days when using various cell densities. Wells 1- 3 contained 1 x 10^7 cells/cm^2, wells 4- 6 contained 6 x 10^6 cells/cm^2, wells 7- 10 contained 1 x 10^6 cells/cm^2. Wells 11 and 12 served as blanks as they did not contain cells.

As seen in Figure 4.4, cells were not consistent in their growth patterns and formation of the membrane was not achieved. Some wells (wells 5, 8, 9 and 10) contained a partial monolayer of cells which did not cover the entire surface area therefore could not progress to form a uniform and intact monolayer. In some cases the cells would clump and eventually be removed during changing of media. Despite various optimization approaches an intact membrane could not be resolved. Due to the inability to culture intact MDCK cell monolayers that could mimic the human intestinal barrier, the trans-membrane assay could not be performed in its entirety.

4.4.4 Parallel Artificial Membrane Permeability Assay (PAMPA)

4.4.4.1 Generation of standard curves

The absorption potential of these compounds were evaluated at the different pH levels that are present in the small intestine (the main site of absorption of orally administered drugs) [25]. All control drugs as well as the chemically synthesised inhibitors were evaluated at pH 5.5, 6.8 and 7.4. The optimal wavelength (λ_{max}) was determined for all control drugs and inhibitors as shown in Table 4.5.

Table 4.5: Optimum UV absorbance wavelengths of all drugs

Drug	Wavelength of maximum UV absorbance (λ_{max}) (nm)
Antipyrine	260
Metoprolol	230
Caffeine	270
Saquinavir	229
HIV protease Inhibitor 1	200
HIV protease Inhibitor 2	200

A linear relationship existed between drug concentration and absorbance detected at concentrations ranging between 20-150 µM (Figures 4.5 and 4.7). This was also true for LY concentration and fluorescence readings (Figure 4.6). These results signify that the Beer-Lambert law applied at these concentrations and that the concentration of drugs and inhibitors in the incubation buffer could be interpolated from the detected absorbance or florescence. Standard curves were generated at pH 5.5, 6.8 and 7.4 (data not shown). Interestingly, it was found that pH made no difference to the R^2 value obtained.

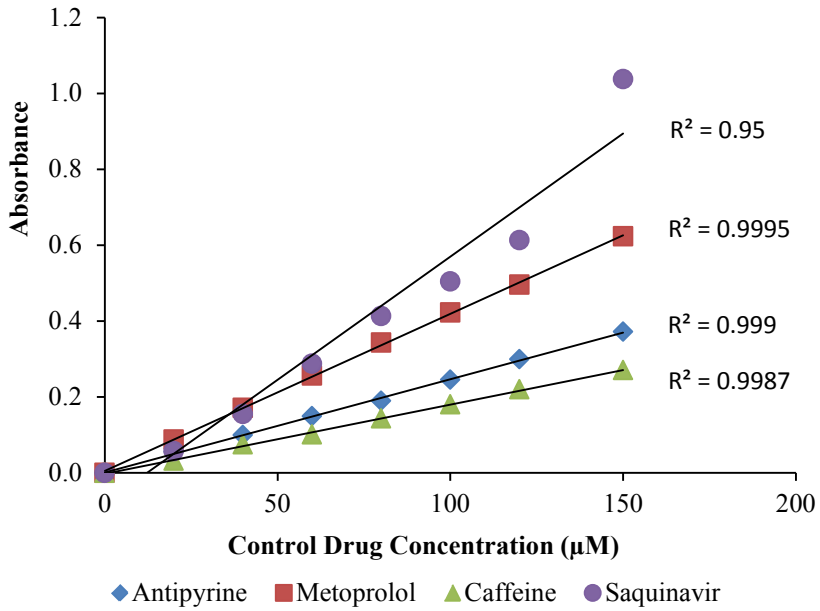

Figure 4.5 Standard curves depicting concentration of the control drugs and absorbance at λ_{max}. The maximum wavelength of antipyrine, metoprolol and caffeine were 260, 230 and 270 nm respectively. Results are an average of three independent experiments and R^2 values of 0.95 and over were taken into consideration.

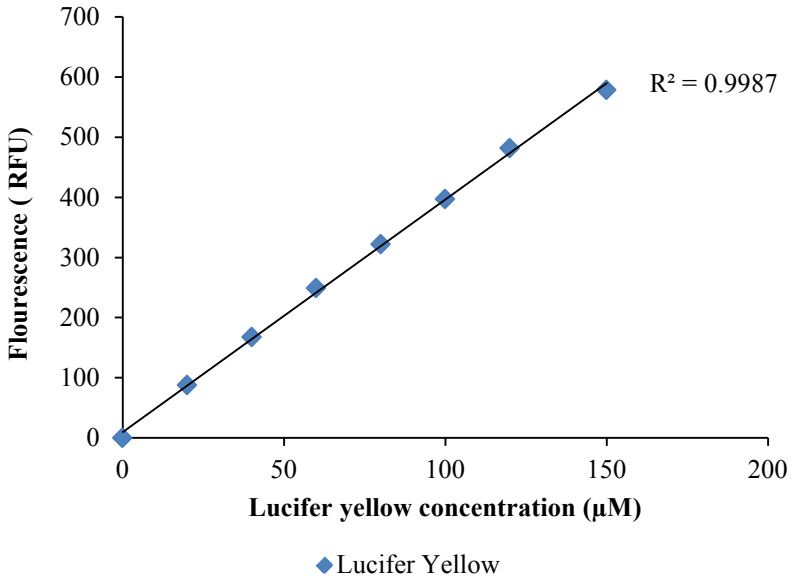

Figure 4.6 Standard curve showing the relationship between Lucifer yellow concentration and fluorescence detected. Results displayed are an average of three independent experiments and R^2 values of 0.95 and over were considered.

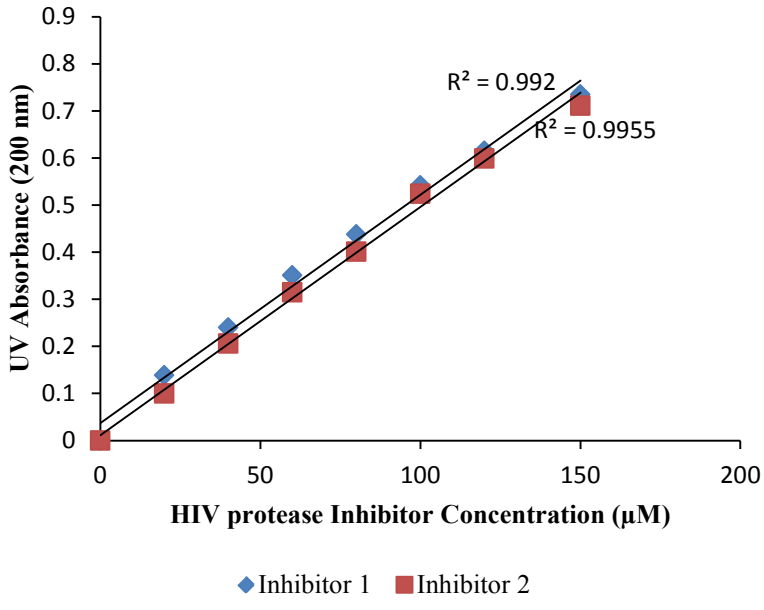

Figure 4.7 Standard curves showing the relationship between concentration of HIV protease inhibitors and UV absorbance at λ_{max}. Results are an average of three independent experiments and R^2 values of 0.95 and over were considered.

4.4.4.2 Verification of integrity of artificial membrane

To ascertain if the PAMPA membrane was intact, the same methods (materials and methods) employed for the cell based assay were used, i.e. TEER evaluation and LY rejection.

Table 4.6: Verification of membrane integrity using TEER values and LY rejection

Well*	TEER values ($\Omega \cdot cm^2$)	LY Passage (%)
1	374.5±47	0
2	381±40	0
3	402±35	0

*Area of PAMPA = 0.24 cm^2

As ascertained from the TEER readings (Table 4.6), an intact artificial membrane was generated which was suitable for subsequent experiments. In addition, TEER values correlated to that obtained in literature using PAMPA [19]. Lucifer yellow passage was 0% in all experiments, once again confirming presence of an intact artificial membrane.

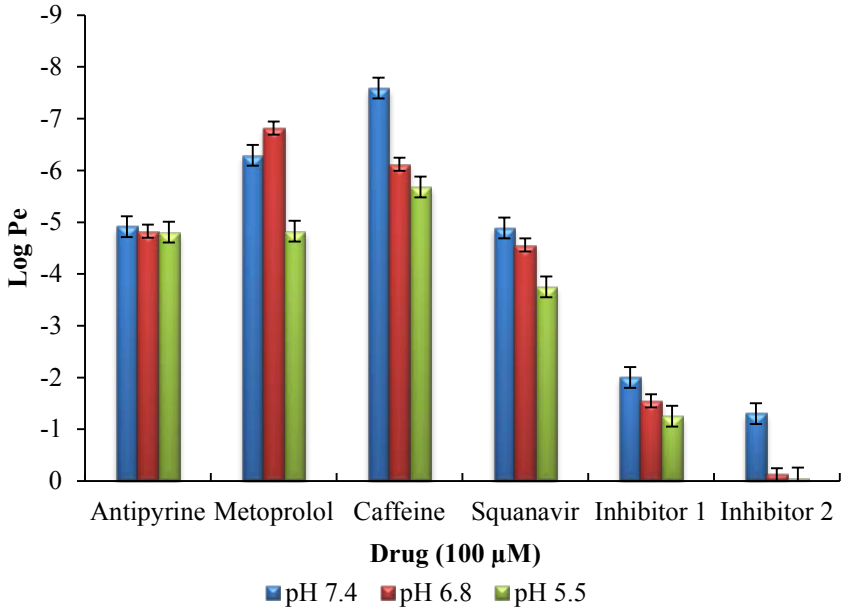

Figure 4.8 The effective permeability ($LogP_e$) of control drugs and inhibitors at different pH levels and at a concentration of 100 µM Results show an average of three independent experiments and the error bars represent standard deviations.

The positive controls antipyrine, metoprolol and caffeine demonstrated expected $LogP_e$ values (Table 4.2). For these controls pH did play a role in its passive permeability. It appears that at a lower pH (more acidic), the permeability was poor when compared to the higher pH levels. However, this is not a cause for concern as the small intestine generally has a basic to neutral pH. Saquinavir, which is a commercially available HIV protease inhibitor, portrayed a medium permeation ranking. The HIV-1 protease inhibitor 1 and 2 produced a low permeation ranking. All three protease inhibitors displayed very poor permeation at pH 5.5 thus reiterating the critical role that pH plays in permeability [32].

Table 4.7 displays the fraction absorbed generated from results of the PAMPA experiments. These results correlate with previous research studies displayed in Table 4.2. All controls displayed a high percentage of fraction absorbed. Saquinavir did not display similar results to that obtained from literature (Table 4.2) as the reported Fa is 30% and this study revealed a value of 50%. The negative control displayed expected results as 0% of LY was absorbed thereby confirming the integrity of the membrane as well as serving as the negative control.

Table 4.7: Fraction absorbed of all control drugs and inhibitors

Compound	PAMPA %T	Fa (%)
Antipyrine	7.65	80
Metoprolol	10.99	90
Caffeine	15.10	100
Saquinavir	3.89	50
Inhibitor 1	1.99	15
Inhibitor 2	0.42	0
LY passage*	0	0

* LY represents the negative control and was calculated by a different equation from the other drugs (Section 4.2)

4.5 Discussion

The presence of mycoplasma in mammalian cell cultures is one of the most dangerous threats to healthy cell lines. Not only can they kill the cells, but more often than not they cohabit with the cells, rising to high titres, before producing noticeable effects (granule formation occurring in cultures, quick trypsinisation times and detachment of cells). Mycoplasma produce a myriad of effects on contaminated cell lines and are known to produce severe cytopathic effects. In a comprehensive review by Drexler and Uphoff [5], it was stated that mycoplasma interfere primarily with nucleic acid synthesis, alters cellular metabolism, induces chromosomal aberrations, changes cell membrane composition and cellular morphology, interferes with biochemical processes in the cell, and alters proliferation characteristics such as growth and viability. The damage inflicted is dependent on a number of parameters such as the intensity and duration of infection, the type of infected cell, culture conditions and infecting mycoplasma species.

The effects of mycoplasma infection specifically to the complex nature of monolayer formation would be a significant contribution to its failure. Monolayer development requires the cell line to differentiate into an intact membrane that represents the human GIT. This is achieved once the cell reaches confluency. Once confluent, the MDCK1 cell line differentiates into cells that represent columnar-epithelial cells. This process includes the expression of specific proteins that consists of the tight junctions that occur between cells, the characteristic apical brush border of microvilli and villi expression [30, 31]. Thus advance differentiation cannot be achieved if the cells are compromised by the effects of mycoplasma contamination. Visually cells may appear healthy, and even be able to grow to confluency; however, chromosomal abnormalities could be detrimental for differentiation to an intact monolayer that represents the enterocytes of the human intestine. Therefore measures were implemented to detect and prevent mycoplasma infection (Figure 4.1) which could compromise complete MDCK1 monolayer formation which is central to the success of this study.

One of the key advantages for the utilization of the MDCK cell line as an alternative to the Caco-2 cell line is its ability to differentiate into intact monolayers with tight junctions that mimic the gastrointestinal barrier within a short period of time (7 days as opposed to 21 days) [13]. This advantage reduces cost implications and allows for a higher throughput of results in a defined period. After 21 days of maintenance and observation, expected TEER values were not obtained (Figures 4.2 and 4.3). Furthermore, upon visual inspection, it seemed that uniform layers were not formed (Figure 4.4). Although numerous possible strategies were attempted in this study, an intact monolayer could not be resolved.

It should be noted that there are reports which pertain to the reproducibility and in house validity of this model for permeability studies [33, 34]. In a detailed review, Volpe *et al*. [35] reported many variables that could account for the irreproducibility of this method. It was mentioned that variances in TEER values seems to be a common issue with the cell-based method and there can be numerous cases of erratic TEER values being obtained. This was also confirmed by Hidalgo [36]. Volpe also stated that factors such as cell passage number, initial seeding densities, media composition, monolayer age and confluency could account for poor monolayer formation [35]. Furthermore heterogeneity (properties of the cells may change with time in culture) of the cell line can have an immense effect on cell proliferation [35]. A report by Wunderli-Allenspach indicated that in order to get this system to work optimally, standardization of the cultivation method (cell density, passage number, media composition etc.) is the most critical factor [37]. Similarly Braun *et al.* stated that there are a culmination of factors (cell culture origin, medium and serum, cell growth supports, seeding densities) that if not standardized efficiently could lead to unsatisfactory monolayer formation [38].

These studies reiterate the difficulty in reproducing reliable permeability data using this cell based assay. Approximately 21 attempts were made to grow the cell monolayer, standardization efforts included use of an exact passage number cultured from one parent line, utilization of materials, such as media and serum from the same lot, the time of culturing was kept consistent and a wide range of seeding densities were tested. Furthermore techniques such as continuous shaking, whilst seeding of cells, for better dispersion as well as the addition of cells after initial attachment were used to improve the uniformity of cell growth over the entire surface. The frequency of media change was altered to every 12, instead of 24 hours to ensure that cells were always replenished with nutrients to prevent premature death. Although strict efforts were employed to standardize the cultivation protocol, expected results could not be obtained in our laboratory. The variety of factors discussed above could have contributed to a less than satisfactory monolayer being formed

The cell-based method was difficult to implement therefore, evaluation of the inhibitors permeability characteristics were obtained from the parallel artificial membrane permeability assay (PAMPA). Control drugs used in this study were antipyrine, metoprolol and caffeine. These drugs fall into the category of the 20 model drugs suggested by the FDA for use in establishing suitability of permeability methods [39] and have been used in several permeability studies as positive controls to validate the permeability system. All three drugs

are commercially available and are used extensively due to their excellent passive paracellular and transcellular permeability characteristics. As mentioned previously, Saquinavir was also used in this study since it is a commercially available HIV-1 protease inhibitor, and would thus serve a comparative purpose given that the permeability of HIV protease inhibitors are in question.

All controls displayed expected behaviour thereby validating the PAMPA system. Saquinavir has a low human fraction absorbed percentage because it is a prime target to the P-gp protein that plays a significant role in bioavailability and which cannot be ignored [40]. Additionally its bioavailability has been enhanced via different dosage regimes such as using hard and soft gelatin capsules, liquid filled capsules as well as incorporation with other anti-retroviral inhibitors [41, 42] Absorption is also enhanced by incorporating this capsule with a high-fat content meal [43]. In this study, the result obtained from PAMPA ranked this inhibitor in the medium range. From literature of Saquinavir is ranked in the low range however, this was obtained from a cell-based method using Caco-2 cell line [24, 44]. The difference in ranking could be attributed to biological systems consisting of a complex membrane compared to the PAMPA artificial membrane which is a lipid composition. However, Saquinavir displayed greater permeability characteristics when compared to the permeability of novel inhibitors assessed in this study which were ranked low.

The novel HIV-1 protease inhibitors did not produce high permeability attributes. Although both compounds have exceptional solubility in an aqueous solution they do not display attractive permeability characteristics. As Saquinavir requires enhancement for its bioavailability, it can be tentatively suggested that similar regimes may improve the bioavailability if these novel inhibitors. From the result both inhibitors displayed a low permeability ranking. According to the findings of Inhibitor 2, the addition of the cage moiety to the inhibitory peptide is supposed to enhance the bioavailability properties of the compound [1]. However, the results obtained suggested minimal permeability through the artificial membrane of the PAMPA, and 0% fraction absorbed (Figure 4.9 and Table 4.7). Identical permeability properties as the negative control were obtained and thus Inhibitor 2 does not enter the cell by transcellular passive diffusion. The fraction absorbed for Inhibitor 1 was 15% (Table 4.7) which is impractical because that implies that only 15% is entering the system. It should be noted that these extremely limited amounts has still to be processed via metabolism, elimination and excretion processes of the human body. The bioavailability index as such of both these newly designed drugs can be deemed insufficient to elicit the

desired response. It was reported that the IC_{50} value of the cage peptide (0.078 μM) was lower than the sugar moiety (1.09 μM) thus representing a more potent inhibitor of the two. However the sugar derived peptide was more passively permeable than the cage derived peptide and since the only difference in structure was the addition of these moieties it can be concluded that glycosylation provides better bioavailable characteristics.

During whole cell evaluation of the inhibitors, the pH was maintained at 7.4, as the incubation medium used was constituted RPMI with physiological pH [2, 3]. Literature states that pH can play a critical role in the bioavailability of a compound [32] therefore in this study the PAMPA system was employed at different pH levels to determine if a change in pH would enhance the permeability of these compounds. It was founded that different pH levels does not significantly improve the permeability properties of these inhibitors.

Taking the findings of this study into consideration, it must be noted that PAMPA is used to solely determine a single permeability mechanism (transcellular passive diffusion) of compounds and confers the degree of permeation [45]. It does not allow for in-depth analysis, such as the quantification of the inhibitor's ability to permeate the membrane, as the cell-based assay would have. Furthermore the MDCK trans-membrane assay allows for the prediction of most transport pathways practiced by the GI tract whereas PAMPA allows for the establishment of only a basic insight into the permeation capability of the inhibitors. However, since the majority of commercially available drugs are absorbed primarily by passive diffusion [46], the rate of permeation through a simple artificial membrane, which mimics passive transcellular transport, is likely to provide a good indication of a drug's absorption potential [18] and has adequately answered the questions posed in this study.

Further investigation regarding the absorption potential of these compounds is imperative if these are to be developed further as anti-retroviral agents. Although not commonly used for oral absorption, the paracellular route of transport should also be investigated. Ultimately, it would seem that a re-design of these inhibitors that incorporates chemical moieties that aid in or facilitate passive diffusion of these inhibitors, is necessary. Possibly this can be achieved by the addition of functional groups or structural modifications to the scaffold that improve permeability. These modifications, must be carefully considered so that it does not interfere with the inhibitory activity against HIV-1 protease. It must be highlighted that even with these considerations the outcome of a compound which displays adequate permeability is not guaranteed.

4.6 Conclusion

The cell-based assay employed in this study generated inconclusive data; therefore evaluation of the HIV-1 protease inhibitor's permeability was established via PAMPA analysis. The data seems to suggest a limitation with regards to cell membrane permeation could have resulted in inactivity of the inhibitors during whole T-cell testing of HIV-1 infected MT4 cells. It can be concluded that active mechanisms of transport does not exist for these inhibitors since inhibition of the HIV-1 infected MT4 cells did not occur. Transport across the membranes can possibly be achieved, passively or actively, via structural modifications to provide better bioavailability properties that these inhibitors can be presented as promising anti-retroviral agents. Once these modifications are implemented then it will be of interest to evaluate further experimentation that looks at all modes of transport across membranes (paracellular, receptor mediated etc.)

4.7 Acknowledgements

This study was made possible through financial support from the National Research Foundation and the research facilities were provided by the University of KwaZulu-Natal.

4.8 References

1. Makatini, M.M., et al., Pentacycloundecane-based inhibitors of wild-type C-South African HIV-protease. *Bioorganic & medicinal chemistry letters*, 2011. **21**(8): p. 2274-2277.
2. Pawar, S.A., et al., Synthesis and molecular modelling studies of novel carbapeptide analogs for inhibition of HIV-1 protease. *European journal of medicinal chemistry*, 2012. **53**: p. 13-21.
3. Makatini, M.M., *Design, Synthesis and Screening of Novel PCU-peptide/peptoid Derived HIV Protease Inhibitors*, 2011, University of KwaZulu-Natal, Westville.
4. Scudiero, D.A., et al., Evaluation of a soluble tetrazolium/formazan assay for cell growth and drug sensitivity in culture using human and other tumor cell lines. *Cancer Research*, 1988. **48**(17): p. 4827-4833.
5. Drexler, H.G. and C.C. Uphoff, Mycoplasma contamination of cell cultures: incidence, sources, effects, detection, elimination, prevention. *Cytotechnology*, 2002. **39**(2): p. 75-90.
6. Ogawa, M., et al., Decontamination of mycoplasma-contaminated Orientia tsutsugamushi strains by repeating passages through cell cultures with antibiotics. *BMC microbiology*, 2013. **13**(1): p. 32.
7. Uphoff, C.C., S.M. Gignac, and H.G. Drexler, Mycoplasma contamination in human leukemia cell lines: I. Comparison of various detection methods. *Journal of immunological methods*, 1992. **149**(1): p. 43-53.
8. Levine, E., Mycoplasma contamination of animal cell cultures: a simple, rapid detection method. *Experimental cell research*, 1972. **74**(1): p. 99-109.
9. Johansson, K.-E., I. Johansson, and U.B. Göbel, Evaluation of different hybridization procedures for the detection of mycoplasma contamination in cell cultures. *Molecular and cellular probes*, 1990. **4**(1): p. 33-42.
10. Hessling, J.J., S.E. Miller, and N.L. Levy, A direct comparison of procedures for the detection of mycoplasma in tissue culture. *Journal of immunological methods*, 1980. **38**(3): p. 315-324.
11. Cho, M.J., et al., The Madin Darby canine kidney (MDCK) epithelial-cell monolayer as a model cellular-transport barrier. *Pharmaceutical research*, 1989. **6**(1): p. 71-77.
12. Laitinen, L., Caco-2 cell cultures in the assessment of intestinal absorption: Effects of some co-administered drugs and natural compounds in biological matrices. 2006.
13. Irvine, J.D., et al., MDCK (Madin-Darby canine kidney) cells: A tool for membrane permeability screening. *Journal of pharmaceutical sciences*, 1999. **88**(1): p. 28-33.
14. Corning. Corning HTS Transwell-96 permeable support protocols for drug transport. Accessed on 6 June 2012. Available from: http://www.level.com.tw/html/ezcatfiles/vipweb20/img/img/34961/2-10t_HTS_Transwell_96_Protocols_Drug_Transport_CLS-AN-058.pdf.
15. Artursson, P., Epithelial transport of drugs in cell culture. I: A model for studying the passive diffusion of drugs over intestinal absorptive (Caco-2) cells. *Journal of pharmaceutical sciences*, 1990. **79**(6): p. 476-82.
16. Artursson, P., K. Palm, and K. Luthman, Caco-2 monolayers in experimental and theoretical predictions of drug transport. *Advanced Drug Delivery Reviews*, 2001. **46**(1–3): p. 27-43.
17. Schwerdt, G., et al., Apical-to-basolateral transepithelial transport of ochratoxin A by two subtypes of Madin-Darby canine kidney cells. *Biochimica Et Biophysica Acta-Biomembranes*, 1997. **1324**(2): p. 191-199.
18. Zhu, C.Y., et al., A comparative study of artificial membrane permeability assay for high throughput profiling of drug absorption potential. *European Journal of Medicinal Chemistry*, 2002. **37**(5): p. 399-407.
19. Kerns, E.H., High throughput physicochemical profiling for drug discovery. *Journal of pharmaceutical sciences*, 2001. **90**(11): p. 1838-1858.
20. Wohnsland, F. and B. Faller, High-throughput permeability pH profile and high-throughput alkane/water log P with artificial membranes. *Journal of medicinal chemistry*, 2001. **44**(6): p. 923-930.
21. Galinis-Luciani, D., L. Nguyen, and M. Yazdanian, Is PAMPA a useful tool for discovery? *Journal of pharmaceutical sciences*, 2007. **96**(11): p. 2886-2892.
22. Masungi, C., et al., Parallel artificial membrane permeability assay (PAMPA) combined with a 10-day multiscreen Caco-2 cell culture as a tool for assessing new drug candidates. *Pharmazie*, 2008. **63**(3): p. 194-9.
23. Kansy, M., F. Senner, and K. Gubernator, Physicochemical high throughput screening: parallel artificial membrane permeation assay in the description of passive absorption processes. *Journal of medicinal chemistry*, 1998. **41**(7): p. 1007-10.
24. Parrott, N. and T. Lavé, Prediction of intestinal absorption: comparative assessment of gastroplus™ and idea™. *European journal of pharmaceutical sciences*, 2002. **17**(1): p. 51-61.
25. Millipore. Lipid-PAMPA with the MultiScreen® Filer Plates. Accessed on 18 August 2013. Available from: http://www.millipore.com/userguides.nsf/a73664f9f981af8c852569b9005b4eee/8ab981483eea7aab852577a000513d9e/$FILE/PC040EN00.pdf.
26. Faller, B., Artificial Membrane Assays to Assess Permeability. *Current Drug Metabolism*, 2008. **9**(9): p. 886-892.

27. Di, L., et al., Parallel artificial membrane permeability assay (PAMPA).
28. Stewart, W.W., Functional connections between cells as revealed by dye-coupling with a highly fluorescent naphthalimide tracer. *Cell*, 1978. **14**(3): p. 741-759.
29. Millipore. MultiScreen Filter Plates for PAMPA, Evaluation of the reproducibility of Parallel Artificial Membrane Permeation Assays (PAMPA). Accessed on 20 May 2013. Available from: http://www.millipore.com/publications.nsf/a73664f9f981af8c852569b9005b4eee/9aab870dfd5881df85256d0a0062c62a/$FILE/AN1728EN00.pdf.
30. Ungell, A.-L. and P. Artursson, *An Overview of Caco-2 and Alternatives for Prediction of Intestinal Drug Transport and Absorption*, in *Drug Bioavailability*. 2009, Wiley-VCH Verlag GmbH & Co. KGaA. p. 133-159.
31. Richardson, J.C.W., V. Scalera, and N.L. Simmons, Identification of 2 strains of MDCK cells which resemble separate nephron tubule segments. *Biochimica Et Biophysica Acta*, 1981. **673**(1): p. 26-36.
32. Kerns, E.H. and L. Di, *pK(a)*. Drug-Like Properties: Concepts, Structure Design and Methods: From ADME to toxicity optimization. 2008. 48-55.
33. Le Ferrec, E., et al., In vitro models of the intestinal barrier - The report and recommendations of ECVAM Workshop 46. *Atla-Alternatives to Laboratory Animals*, 2001. **29**(6): p. 649-668.
34. Artursson, P. and J. Karlsson, Correlation between oral drug absorption in humans and apparent drug permeability coefficients in human intestinal epithelial (Caco-2) cells. *Biochemical and biophysical research communications*, 1991. **175**(3): p. 880-885.
35. Volpe, D.A., Variability in Caco-2 and MDCK cell-based intestinal permeability assays. *Journal of pharmaceutical sciences*, 2008. **97**(2): p. 712-25.
36. Hidalgo, I.J., T.J. Raub, and R.T. Borchardt, Characterization of the human colon carcinoma cell line (Caco-2) as a model system for intestinal epithelial permeability. *Gastroenterology*, 1989. **96**(3): p. 736-49.
37. Wunderli-Allenspach, H., Methodologies in cell culture. *Pharmacokinetic optimization in drug research: biological, physicochemical and computational strategies. Zurich: Wiley-VHCA*, 2001: p. 99-116.
38. Braun, A., et al., Cell cultures as tools in biopharmacy. *European Journal of Pharmaceutical Sciences*, 2000. **11**: p. S51-S60.
39. Benet, L.Z., et al., The use of BDDCS in classifying the permeability of marketed drugs. *Pharmaceutical research*, 2008. **25**(3): p. 483-488.
40. Varma, M.V.S., et al., P-glycoprotein inhibitors and their screening: a perspective from bioavailability enhancement. *Pharmacological Research*, 2003. **48**(4): p. 347-359.
41. Figgitt, D.P. and G.L. Plosker, Saquinavir Soft-Gel Capsule. *Drugs*, 2000. **60**(2): p. 481-516.
42. Merry, C., et al., Saquinavir pharmacokinetics alone and in combination with nelfinavir in HIV-infected patients. *Aids*, 1997. **11**(15): p. F117-F120.
43. Albano, A.A., et al., *Saquinavir Mesylate Oral Dosage Form*, 2008, Google Patents.
44. Usansky, H.H. and P.J. Sinko, Estimating human drug oral absorption kinetics from Caco-2 permeability using an absorption-disposition model: model development and evaluation and derivation of analytical solutions for ka and Fa. *Journal of pharmacology and experimental therapeutics*, 2005. **314**(1): p. 391-399.
45. Kerns, E.H., et al., Combined application of parallel artificial membrane permeability assay and Caco-2 permeability assays in drug discovery. *Journal of Pharmaceutical Sciences*, 2004. **93**(6): p. 1440-1453.
46. Artursson, P. and R.T. Borchardt, Intestinal drug absorption and metabolism in cell cultures: Caco-2 and beyond. *Pharmaceutical research*, 1997. **14**(12): p. 1655-8.

Chapter 5

GENERAL DISCUSSION AND CONCLUSION

5.1 General Discussion and Conclusions

From as early as the 1980's, various methods for the isolation of HIV protease have been reported. The HIV-1 protease enzyme in its entirety was previously chemically synthesized [1], however, the preferred method for its production is by expression using recombinant DNA technology in various heterologous systems. The use of transgenic *E. coli* that expresses the protease as inclusion bodies has become the gold standard for the isolation and purification of this enzyme. The primary motivation for adoption of the latter strategy is placed on obtaining higher yields of enzyme, and genetic engineering using different strategies have been employed to this end [2].

In this study, it was proposed that instead of altering the genetic makeup of a transgenic bacterial strain to increase protease yields, it was decided that a change in culture media composition could increase the yield of desired enzyme. Using the proposed strategy it was clearly demonstrated that HIV-1 protease subtype C was isolated and its yield substantially increased. It was observed that the use of chemically defined medium promoted a greater bio-mass yield of the transgenic *E. coli* strain. Isolation from this biomass generated from chemically defined medium doubled the yield of enzyme when compared to use of previously preferred nutrient rich LB medium.

The Bradford assay is a suggested method to detect the protease eluted from anion exchange column chromatography whilst UV-based (280nm) spectrophotometric analysis of protein content resulted in the collection of fractions that displayed multiple band formation. Sufficient amounts of HIV protease was purified and used for the testing of the inhibitory potential of chemically synthesized novel HIV protease inhibitors.

The second aspect of this study was designed to ascertain if the inactivity of the two novel chemically synthesized HIV protease inhibitors in whole T-cell based assays was due to their inherent incapacity to successfully permeate the cell membrane. Despite numerous attempts and although reported as a tenable method [3, 4], the present study demonstrated that it was indeed difficult to cultivate a MDCK cell monolayer to assess the cell membrane permeability indexes of the newly designed drugs. The study revealed that higher cell numbers were more acceptable as it resulted in closer TEER values that were indicative of intact monolayer formation (above 200 $\Omega \cdot cm^2$). Permeability assessment studies in which an MDCK intact monolayer was achieved generally used lower cell numbers, however, it should

be noted that the trans-well inserts employed in these studies were of a smaller surface area [3, 5, 6]. High cell densities are not always advisable as it leads to limitations such as competition for nutrients and CO_2, cell crowding, quick confluency times that can lead to premature lifting of cells. Thereby utilization of plates that contain smaller trans-well insert sizes to accommodate for a smaller surface area, resulting in smaller cell densities could be a means to improve the protocol.

Transcellular passive diffusion is the most commonly used pathway for orally administered commercial drugs [7, 8]. The PAMPA technology has proven to be a valuable tool that is able to predict the transcellular passive diffusion of compounds which in drug discovery which should ideally be established early in the drug development process [9]. In this study, the results obtained from PAMPA indicated that both inhibitors did not exhibit promising transcellular passive diffusion properties. The $LogP_e$ values calculated for both inhibitors were below the threshold (-5.00), which is associated with compounds with very poor permeability characteristics. Although Inhibitor 1 which was a glycosylated peptide possessed more attractive permeable characteristics than the cage-derived peptide (Inhibitor 2) both were shown to not be passively permeable compounds. Interestingly it must be noted that the cage derived peptide exhibited greater potency against the enzyme in *in vitro* HIV-1 protease analysis compared to the sugar derived peptide [10, 11]. The peptide moiety of both inhibitors are identical with the critical difference residing in either glycosylation or cage derivitisation. Therefore it can be stated that although having lower inhibitory potential, the sugar moiety seems to promote a 15-fold increase in passive permeability over their cage derived counterparts. To improve the bioavailability of these compounds, an alteration of their chemical structure that incorporates moieties that promote passive diffusion seems necessary logical developmental strategy. This will however, imply returning to the initial chemical synthetic protocol and it must be noted that alteration of the structure of these putative HIV-1 protease inhibitors may retard their inhibitory activity.

The dynamics of drug design needs to be approached from a different perspective in order to circumvent reverting to the design stages of the process. Resources, time and cost are being continuously wasted in attempting to develop drugs that are not bioavailable. The key to efficient drug development is if chemical synthesis of compounds in a combinatorial approach were to be effected in tandem with their bioavailability characteristics. This knowledge is not unfamiliar; however, it is barely being practiced in many drug developing

research environments. However, high throughput screening (HTS) methods are being developed and improved as research has advanced to quickly identify potential drug candidates. Interestingly readily made databases such as the comprehensive medicinal chemistry (CMC) [12] that consists of medical agents in humans, MARCCS-II drug data report (MDDR) [13] and the world drug index (WDI) [14] that consists of marketed drugs and compounds that are under development, are available to the industry to minimize the time and the cost spent on designing and assessing a new entity [15]. These databases provide criteria that must be thoroughly evaluated to implement more effective drug design strategies.

The new era, however, is leading towards a more computational approach to alter this major limitation of drug discovery. In a process referred to computer aided drug design (CADD) which represents computational tools and sources for the storage, management, analysis and modeling of compounds [16]. This avenue of research is classified into structure-based and ligand-based methods that cover aspects of drug discovery that incorporates the chemical synthesis of drug design as well as ascertains certain biological considerations [17-20]. These include chemical aspects such as accurate "hit" targets as well as biological aspects such as predicting the permeability coefficients. Both of which, will be extremely beneficial at the onset of the drug design process.

Computational tools can be applied to most aspects of drug discovery and development process, from target validation to lead discovery and optimization, these tools can even be applied to pre-clinical trials, which greatly alters the pipeline for drug discovery and development and could reduce the cost of drug development by up to 50% [21]. There are many databases and systems in research that are available to make this approach more frequently implemented in industry and most importantly in academia [18, 22]. Future outlooks that will have a major impact in the scientific research community would be the integration of computational chemistry and biology together with chemoinformatics and bioinformatics, which will result in a new field known as pharmacoinformatics [16].

In conclusion, it is imperative that 21st century drug development strategies implement computational means for assessing drug design before actual bench top experiments are employed. This would save tremendous time, effort and most importantly costly resources that are used in conventional approaches that utilize target validation then assessing the bioavailability requirements. These software programs can determine if the particular

compound in question does meet the requirements of a successful candidate such as appropriate permeability indexes. Only after this has been achieved, attempts at whole T-cell systems should be done. If this next level of testing results in failure, further in depth permeability, metabolic and toxicity testing should be employed to find out if these attributes are indeed a cause for concern. With regards to HIV specifically, it must be highlighted that time is a critical factor and therefore a quicker discovery process is essential given the nature of the disease, the release of an effective drug would be ground breaking due to the need for preventing a higher motility rate.

5.2 References

1. Nutt, R.F., et al., Chemical synthesis and enzymatic activity of a 99-residue peptide with a sequence proposed for the human immunodeficiency virus protease. *Proceedings of the National Academy of Sciences*, 1988. **85**(19): p. 7129-7133.
2. Volontè, F., L. Piubelli, and L. Pollegioni, Optimizing HIV-1 protease production in Escherichia coli as fusion protein. *Microb Cell Fact*, 2011. **10**: p. 53.
3. Irvine, J.D., et al., MDCK (Madin-Darby canine kidney) cells: A tool for membrane permeability screening. *Journal of pharmaceutical sciences*, 1999. **88**(1): p. 28-33.
4. Rothen-Rutishauser, B., et al., MDCK cell cultures as an epithelial in vitro model: Cytoskeleton and tight junctions as indicators for the definition of age-related stages by confocal microscopy. *Pharmaceutical research*, 1998. **15**(7): p. 964-971.
5. Taub, M.E., L. Kristensen, and S. Frokjaer, Optimized conditions for MDCK permeability and turbidimetric solubility studies using compounds representative of BCS classes I-IV. *European journal of pharmaceutical sciences : official journal of the European Federation for Pharmaceutical Sciences*, 2002. **15**(4): p. 331-40.
6. Pabla, D., F. Akhlaghi, and H. Zia, Intestinal permeability enhancement of levothyroxine sodium by straight chain fatty acids studied in MDCK epithelial cell line. *European Journal of Pharmaceutical Sciences*, 2010. **40**(5): p. 466-472.
7. Pappenheimer, J.R. and K.Z. Reiss, Contribution of solvent drag through intercellular junctions to absorption of nutrients by the small intestine of the rat. *J Membr Biol*, 1987. **100**(2): p. 123-36.
8. Grass, G.M., Simulation models to predict oral drug absorption from in vitro data. *Advanced Drug Delivery Reviews*, 1997. **23**(1-3): p. 199-219.
9. Galinis-Luciani, D., L. Nguyen, and M. Yazdanian, Is PAMPA a useful tool for discovery? *Journal of pharmaceutical sciences*, 2007. **96**(11): p. 2886-2892.
10. Makatini, M.M., *Design, Synthesis and Screening of Novel PCU-peptide/peptoid Derived HIV Protease Inhibitors*, 2011, University of KwaZulu-Natal, Westville.
11. Pawar, S.A., et al., Synthesis and molecular modelling studies of novel carbapeptide analogs for inhibition of HIV-1 protease. *European journal of medicinal chemistry*, 2012. **53**: p. 13-21.
12. CMC. . Accessed on 16/01/2013. Available from: http: / /www.mdli.com.
13. MDDR. Accessed on 14/01/2013. Available from: http: / /www.mdli.com.
14. WDI. Accessed on 14/01/2013. Available from: http: / /www.derwent.com.
15. Walters, W.P. and M.A. Murcko, Prediction of 'drug-likeness'. *Advanced Drug Delivery Reviews*, 2002. **54**(3): p. 255-271.
16. Ou-Yang, S.-s., et al., Computational drug discovery. *Acta Pharmacologica Sinica*, 2012.
17. Sun, X., S. Vilar, and N.P. Tatonetti, High-Throughput Methods for Combinatorial Drug Discovery. *Science Translational Medicine*, 2013. **5**(205): p. 205rv1.
18. Materi, W. and D.S. Wishart, Computational systems biology in drug discovery and development: methods and applications. *Drug Discov Today*, 2007. **12**(7-8): p. 295-303.
19. Song, C.M., S.J. Lim, and J.C. Tong, Recent advances in computer-aided drug design. *Briefings in bioinformatics*, 2009. **10**(5): p. 579-591.
20. Shekhar, C., In silico pharmacology: computer-aided methods could transform drug development. *Chemistry & biology*, 2008. **15**(5): p. 413-414.
21. Tan, J.J., et al., Therapeutic strategies underpinning the development of novel techniques for the treatment of HIV infection. *Drug discovery today*, 2010. **15**(5): p. 186-197.
22. Gupta, R.R., et al., Using open source computational tools for predicting human metabolic stability and additional absorption, distribution, metabolism, excretion, and toxicity properties. *Drug Metabolism and Disposition*, 2010. **38**(11): p. 2083-2090.

6. 1 Appendix

6.1.1 Additional standard curves from section 4.4.4.1

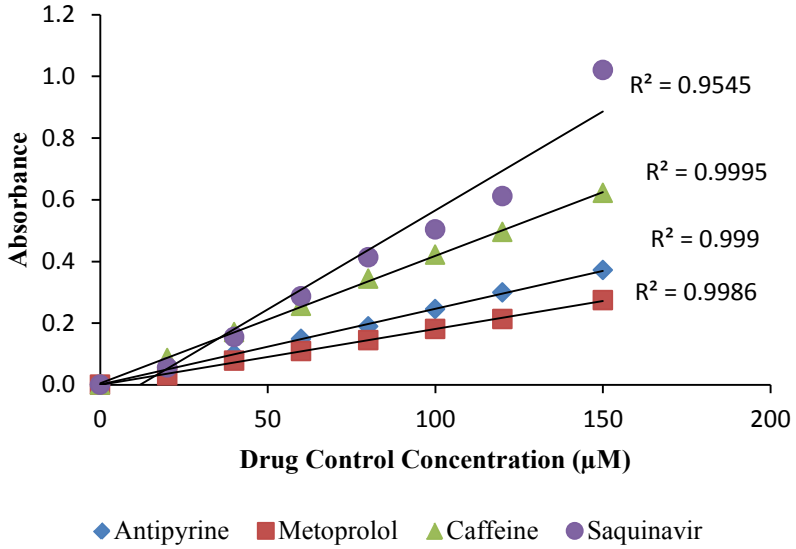

Figure 6.1 Standard curves depicting concentration of the control drugs and absorbance at λ_{max} at pH 5.5. The maximum wavelength of antipyrine, metoprolol and caffeine were 260, 230 and 270 nm respectively. Results are an average of three independent experiments and R^2 values of 0.95 and over were taken into consideration.

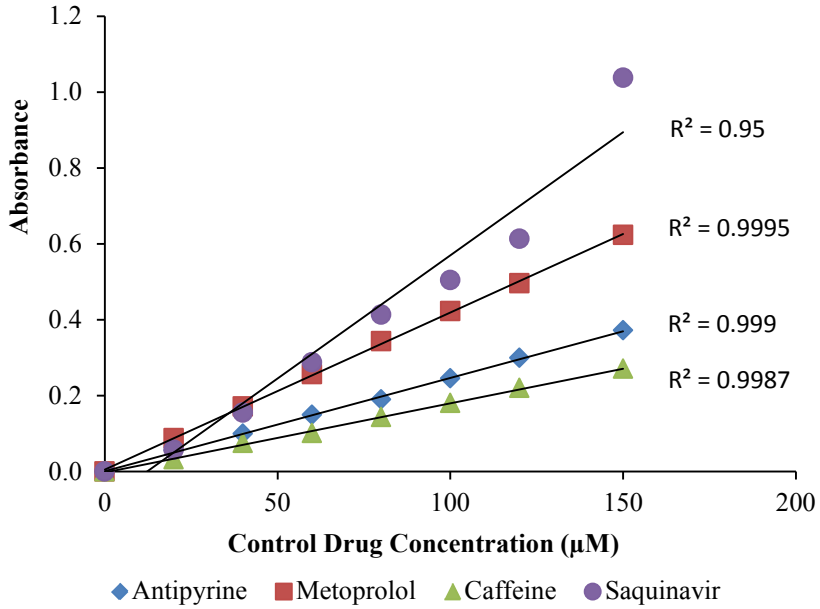

Figure 6.2 Standard curves depicting concentration of the control drugs and absorbance at λ_{max} at pH 6.8. The maximum wavelength of antipyrine, metoprolol and caffeine were 260, 230 and 270 nm respectively. Results are an average of three independent experiments and R^2 values of 0.95 and over were taken into consideration.